LIST OF PUBLISHED AND COMMUNICATED PAPERS

The subject matter of the thesis presented in several chapters has been published and communicated to different indian and foreign journals of international repute.

1. Structural and associational aspects of binary and single polar liquids in nonpolar solvent under high frequency electric field : S.K. Sit, N. Ghosh, U. Saha and S. Acharyya *Indian J Phys* **71B** (1997) 533.

2. Double relaxations of some isomeric octyl alcohols by high frequency absorption in nonpolar solvent : S.K. Sit, N.Ghosh and S. Acharyya *Indian J. Pure & Appl. Phys* **35** (1997) 329.

3. Dielectric relaxation of para polar liquids under high frequency electric field : N. Ghosh, R.C. Basak, S.K. Sit and S. Acharyya, *J. Mol. Liquids* (Germany) **85** (2000) 375.

4. Structural and associational aspects of dielectropolar straight chain alcohols from relaxation phenomena : N. Ghosh, A. Karmakar, S.K. Sit and S. Acharyya, *Indian J. Pure & Appl. Phys.* **38** (2000) 574.

5. Structural and associational aspects of isomers of anisidine and toluidine under a gigahertz electric field : N. Ghosh, S.K. Sit, A.K. Bothra and S. Acharyya. *J. Phys. D : Appl Phys* (U.K) **34** (2001) 379.

6. Double relaxation phenomena of monosubstituted anilines in benzene under high frequency electric field : N. Ghosh, S.K. Sit and S. Acharyya, *J. Mol. Liquids* (Germany) Accepted for publication 2001.

7. Structural conformation and associational aspects of some normal alcohols in benzene and their mixtures under rf electric field at single and different temperatures : N. Ghosh, R. Ghosh, R.C. Basak, K. Dutta and S. Acharyya *Pramana J Phys* communicated 2002.

8. Relaxation phenomena of aprotic polar liquid molecules under a kilohertz electric field : N. Ghosh, R. Ghosh and S. Acharyya *Indian J Pure & Appl. Phys.* Communicated 2001.

Indian J. Phys. **71B** (4), 533–539 (1997)

NOTE

IJP B
— an international journal

Structural and associational aspects of binary and single polar liquids in non polar solvent under high frequency electric field

S K Sit, N Ghosh, U Saha and S Acharyya
Department of Physics, Raiganj College, Raiganj, Uttar Dinajpur-733 134, West Bengal, India

Received 17 April 1996, accepted 19 December 1996

Abstract : The structural and associational aspects of binary (jk) polar mixtures of N,N dimethyl formamide (DMF) and dimethyl sulphoxide (DMSO) together with a single (j or k) N, N diethyl formamide (DEF) and DMSO in nonpolar solvents (i) are studied in terms of their high frequency (hf) conductivities. The relaxation times τ's and dipole moments μ's of the solutes under Giga hertz electric field at various temperatures are estimated from the measured real and imaginary parts of hf dielectric constants at different weight fractions of polar solutes. The variation of τ_{jk}'s with mole fractions x_k's of DMSO in DMF and C_6H_6 reveals the probable solute-solute molecular association around $x_k = 0.5$ of DMSO. The solute-solvent molecular association begins at and around 50 mole% DMSO in DMF and continues upto 100 mole% DMSO. The concentration and temperature variations of τ_{jk} of these protic liquids are in accord with the information of variation of τ_{jk} of jk polar mixtures with x_k's of DMSO. Thermodynamic energy parameters are also obtained from Eyring's rate process equation with the estimated τ's to support the molecular associations. The slight disagreement between the theoretical dipole moments μ_{theo}'s from the bond angles and bond moments is noticed with the measured μ's in terms of slopes of concentration variation of hf conductivity curves at infinite dilutions and τ's. This indicates the temperature dependence of mesomeric and inductive moments of different substituent groups of the molecules.

Keywords : Dipole moment, relaxation time, associational aspects.

PACS Nos. : 31.70.Dk, 33.15.Kr

The dielectric relaxation mechanism of a polar-nonpolar liquid mixture under the microwave electric field is of special interest [1,2] for its inherent ability to predict the associational aspects of polar solutes in nonpolar solvents. An investigation was, however, made on ternary solution of binary polar liquids in which both or even one of them are aprolic [2,3] to study various types of weak molecular associations by polar liquids in

nonpolar solvents. We are, therefore, tempted further to consider more mixtures of binary aprotic polar liquids like N,N dimethyl formamide (DMF) and dimethyl sulphoxide (DMSO) together with a single aprotic polar liquid like N,N diethyl formamide (DEF) and DMSO in C_6H_6 and CCl_4 [4–6] respectively. DMSO, DMF and DEF are very interesting liquids for their wide application in medicine and industry. They also act as building blocks of proteins and enzymes. The concentration variation of the measured real ε'_{ijk}, ε'_{ij} or ε'_{ik} and imaginary ε''_{ijk}, ε''_{ij} or ε''_{ik} parts of *hf* complex dielectric constants ε^*_{ijk}, ε^*_{ij} or ε^*_{ik} of jk, j or k polar solutes in nonpolar solvents are used to detect the weak molecular interactions among the molecules [7] at a single or different temperatures under nearly 3 cm wavelength electric field. The τ_{jk} of jk polar mixtures as well as τ_j's or τ_k's of j or k polar solutes in a nonpolar solvent were estimated from :

$$K''_{ijk} = K_{\infty ijk} + \frac{1}{\omega\tau_{jk}} K'_{ijk}, \tag{1}$$

where $K''_{ijk} = \frac{\omega}{4\pi}\varepsilon'_{ijk}$ and $K'_{ijk} = \frac{\omega}{4\pi}\varepsilon''_{ijk}$ are the imaginary and real parts of complex *hf* conductivity K^*_{ijk} [8]. The other terms carry usual significance as presented elsewhere [2]. The τ_{jk}'s are estimated from the slopes of the linear variations of K''_{ijk} against K'_{ijk} of eq. (1). The linearity of eq. (1) is tested by the correlation coefficients and the errors involved in the measurement of τ's are within 5%. τ_{jk}'s are then plotted with different mole fractions x_k's of DMSO at various experimental temperatures as shown in Figure 1.

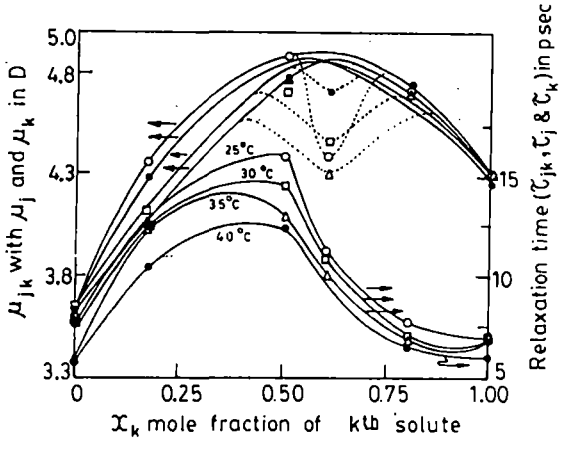

Figure 1. Variation of τ_{jk} and μ_{jk} of DMF–DMSO mixture in C_6H_6 against mole fraction x_k of DMSO with τ_j and τ_k and μ_j and μ_k of DMF and DMSO respectively at different temperatures : (○) at 25°C, (□) at 30°C, (Δ) at 35°C and (●) at 40°C.

The formation of dimer is responsible for the gradual rise of τ_{jk} from τ_j of DMF at $x_k = 0$ to $x_k = 0.5$ and then its rapid fall to τ_k due to rupture of dimerisation and self association [4]. The estimated τ's are slightly larger than those of Gopalakrishna's method [9]. But τ's from conductivity measurement are much more reliable as they provide microscopic relaxation times [10].

The energy parameters due to dielectric relaxation process were then obtained in terms of measured τ from the rate process equation of Eyring *et al* [11] :

$$\tau_S = \frac{A}{T} e^{\Delta F_\tau / RT},$$

$$\text{or} \quad \ln(\tau_S T) = \ln A' + \frac{\Delta H_\tau}{RT}, \tag{2}$$

where $A' = Ae^{-\Delta S_\tau / R}$.

Eq. (2) is a straight line of $\ln(\tau_s T)$ against $\frac{1}{T}$ as seen in Figure 2 having intercepts and slopes to yield the entropy of activation ΔS_τ, enthalpy of activation ΔH_τ and free energy of activation ΔF_τ due to dielectric relaxation. The values of $\gamma\left(= \frac{\Delta H_\tau}{\Delta H_\eta}\right)$ for all the liquids

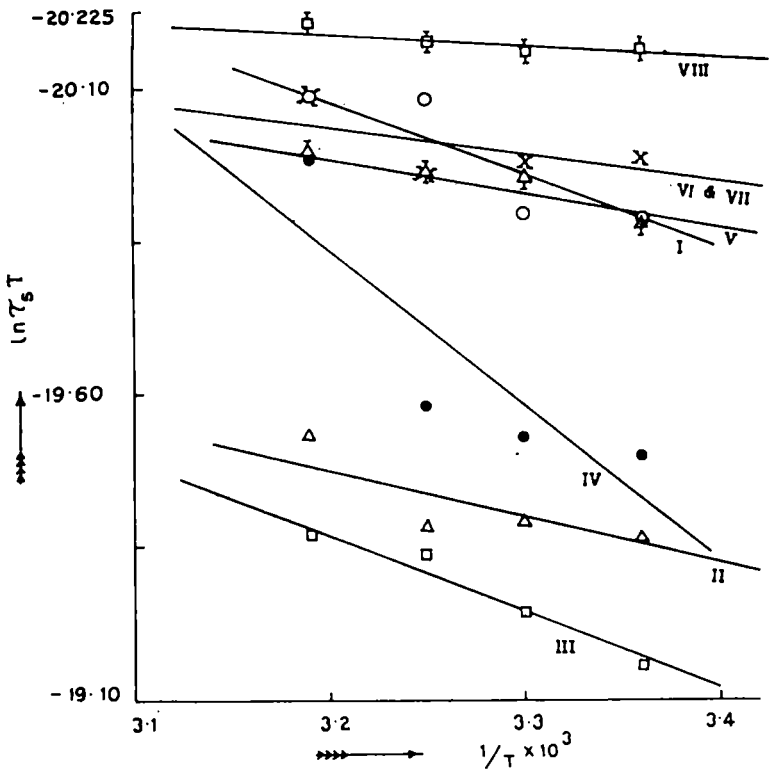

Figure 2. Variation of $\ln(\tau_s T)$ against $\frac{1}{T}$ of binary and single polar solutes in nonpolar solvent. I–DMF + 0 mole% DMSO in C_6H_6 (O), II–DMF + 17 mole% DMSO in C_6H_6 (Δ), III–DMF + 50 mole% DMSO in C_6H_6 (□), IV–DMF + 60 mole% DMSO in C_6H_6 (•), V–DMF + 80 mole% DMSO in C_6H_6 (Δ), VI–DMF + 100 mole% DMSO in C_6H_6 (X), VII–DMSO in C_6H_6, (X), VIII–DMSO in CCl_4 (Δ).

xcept DMSO in CCl_4 are greater than 0.55, as obtained from the slope of the linear relation f $\ln(\tau_s T)$ with $\ln\eta$ indicating them as solid phase rotators in solvent environment. η is the

coefficient of viscosity of solvent. ΔH_η due to viscous flow of the solvent is obtained from slope of $\ln(\tau_s T)$ against $\frac{1}{T}$ and known γ. Again, ΔH_η are greater than ΔH_τ for all the mixtures except 0, 50 and 60 mole% DMSO in DMF and C_6H_6. The difference in ΔH_τ and ΔH_η is due to the involvement of various types of bondings which are either formed or broken to some extent, depending on the temperature and concentration of the system. The negative values of ΔS_τ's for all the systems except 0 and 60 mole% DMSO in DMF and C_6H_6 indicate the existence of cooperative orientation of the molecules arising out of steric forces to yield more ordered states while the reverse is true for positive ΔS_τ's. Although, ΔF_τ's in all cases are almost constant at all temperatures, they increase with x_k of DMSO from $x_k = 0.0$ to $x_k = 0.5$ and then decrease gradually to $x_k = 1.0$ signifying the maximum dimerisation of DMF–DMSO mixture around $x_k = 0.5$. The formation of dimer causes larger molecular size and hence, the energy needed for rotation in the relaxation process is higher.

The *hf* conductivity K_{ijk} as a function of weight fraction W_{jk} is given by

$$K_{ijk} = \frac{\omega}{4\pi}\left(\varepsilon'^2_{ijk} + \varepsilon''^2_{ijk}\right)^{\frac{1}{2}}. \tag{3}$$

Since $\varepsilon'_{ijk} \gg \varepsilon''_{ijk}$ eq. (1) can be written as

$$K_{ijk} = K_{\infty ijk} + \frac{1}{\omega\tau_{jk}} K'_{ijk},$$

or
$$\left(\frac{dK'_{ijk}}{dW_{jk}}\right)_{W_{jk}\to 0} = \omega\tau_{jk}\beta. \tag{4}$$

Here, β 's are the slopes of $K_{ijk} - W_{jk}$, $K_{ij} - W_j$ or $K_{ik} - W_k$ curves respectively, which are linear with almost identical intercepts probably due to same polarity of the molecules [2]. The real part of *hf* conductivity, K'_{ijk} is again related to W_{jk} of *jk* polar solute dissolved in a nonpolar solvent (i) at temperature T°K [12] as

$$K'_{ijk} = \frac{\mu^2_{jk} N \rho_{ijk} F_{ijk}}{3 M_{jk} kT}\left(\frac{\omega^2\tau_{jk}}{1+\omega^2\tau^2_{jk}}\right) W_{jk}. \tag{5}$$

Differentiating eq. (5) with respect to W_{jk} and comparing the result at $W_{jk} \to 0$ to eq. (4), one obtains the following relation

$$\mu_{jk} = \left[\frac{27 M_{jk} kT}{N\rho_i(\varepsilon_i+2)^2}\cdot\frac{\beta}{\omega b}\right]^{1/2} \tag{6}$$

to estimate μ_{jk}, μ_j or μ_k of the respective solutes. b is a dimensionless parameter in terms of estimated τ_{jk}, τ_j or τ_k given by :

$$b = \frac{1}{1+\omega^2\tau^2_{jk}}. \tag{7}$$

The other terms in eq. (6) carry usual significance [2]. All the μ's are then plotted against different x_k's of DMSO at each temperature as shown in Figure 1. It shows the gradual rise of μ_{jk} in the range $0 < x_k \leq 0.5$. It then decreases slowly in order to exhibit the convex nature of each curve with an abnormally low value of μ_{jk} around $x_k = 0.6$. This sort of behaviours of $\mu_{jk} - x_k$ curves (Figure 1) is explained by the fact that dimers are being formed from $x_k \geq 0$ to $x_k = 0.6$ causing increase of μ. The rupture of dimerisation *i.e.* self association occurs in higher concentrations in the range $0.6 \leq x_k < 1.0$ to yield lower values of μ's. But around $x_k = 0.6$, all μ_{jk}'s are minimum indicating the possible occurrence of double relaxation phenomena in such mixtures to be studied later on. μ_{jk} together with μ_j and μ_k for each mixture of a fixed concentration are shown graphically only to observe their temperature dependence like $\mu_{jk} = a + bt + ct^2$ with coefficients a, b and c as seen in Figure 3. The variation is concave with maximum depression at 17 mole% DMSO in DMF mixture. The depression gradually decreases upto $x_k = 0.6$ of DMSO in DMF and C_6H_6 probably due to solute-solute molecular association in the range $0 < x_k < 0.6$. The maximum

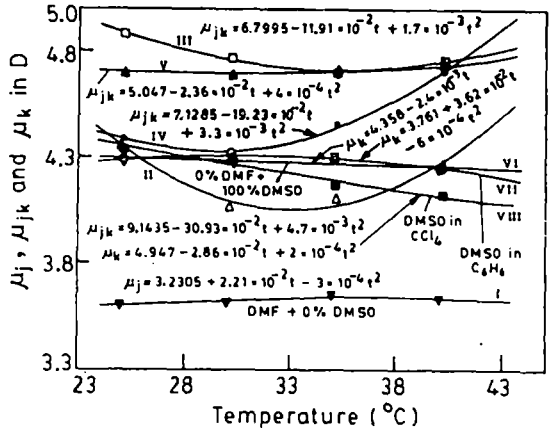

Figure 3. Variation of μ_j, μ_{jk} and μ_k of binary and single polar solutes in nonpolar solvent with temperature t in °C.

I–DMF + 0 mole% DMSO in C_6H_6 (▼), II–DMF + 17 mole% DMSO in C_6H_6 (Δ), III–DMF + 50 mole% DMSO in C_6H_6 (□), IV–DMF + 60 mole% DMSO in C_6H_6 (●), V–DMF + 80 mole% DMSO in C_6H_6 (▲), VI–DMF + 100 mole% DMSO in C_6H_6 (∇), VII–DMSO in C_6H_6, (O), VIII–DMSO in CCl_4 (■).

dimerisation is, however, inferred from low μ's because of the larger molecular sizes as confirmed by high values of $\tau_s T/\eta^\gamma$ (being proportional to volume of the rotating unit) for 60 mole% DMSO in DMF and C_6H_6. As temperature increases the dipole-dipole nteraction is weakened and the absorption of *hf* electric energy increases resulting in he rupture of dimer to yield high μ's for smaller molecular species [10]. The slight :onvex nature of curves for 0 mole% DMSO in DMF and C_6H_6 and DMSO in C_6H_6, long with almost straight line variation of 100 mole% DMSO in DMF and C_6H_6 and)MSO in CCl_4 (Figure 3) is probably due to solute-solvent molecular interaction of either)MF with C_6H_6 or DMSO with C_6H_6 and CCl_4 respectively as illustrated in Figure 4. he associations of DMF, DEF and DMSO in C_6H_6 can arise due to interactions of actional positive charges of N and S atoms of the molecules with the π delocalised ectron cloud of C_6H_6 ring as seen in Figure 4(i), (iii) and (iia) respectively. Again, one C–Cl dipoles of CCl_4, owing to more –ve charge on Cl atom, interacts with the fractional

+ve charge of S-atom of DMSO (Figure 4 (iib)). The μ_{theo} = 4.55 D of DMSO is, however, computed from available bond moments of 2.35 D and 1.55 D for S ← CH_3 and 0 = S respectively, assuming the molecule to be planar one. The major contributions to μ_{theo} for DMF and DEF are due to 0.64 D and 0.78 D for N ← CH_3 and N ← C_2H_5 since the other common bond moments in them are the same with values of 0.3 D, 0.45 D and 3.10 D for C ← H, C ← N and C = 0 respectively. Figure 4 (iv), however, shows a certain angle ϕ (= 106°) between monomeric μ's of DMF and DMSO to have μ_{theo} = 4.77 D of dimer below $x_k = 0.6$.

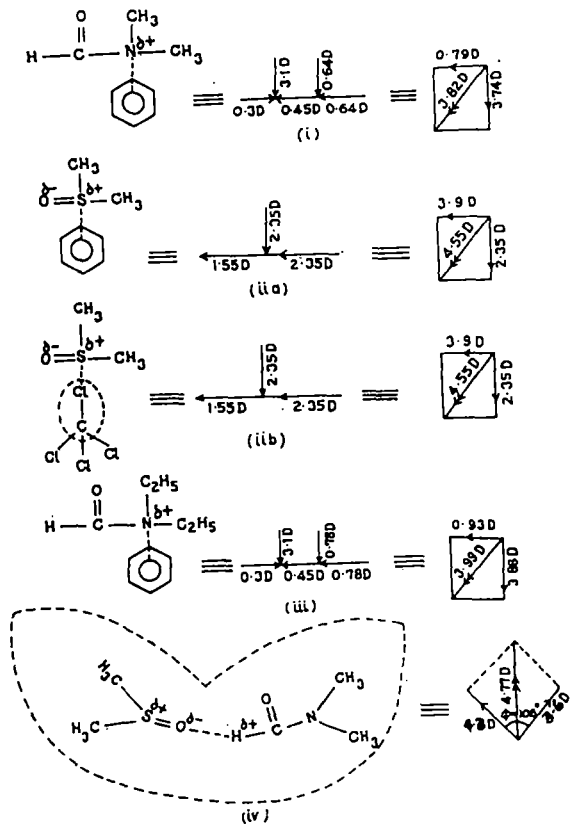

Figure 4. Conformational structures along with solute-solvent and solute-solute interaction of molecules. (i) DMF in C_6H_6, (iia) DMSO in C_6H_6, (iib) DMSO in CCl_4 (iii) DEF in C_6H_6. (iv) DMSO–DMF dimer.

The slight deviations of the μ's from the μ_{theo}'s occur probably due to the presence of inductive and mesomeric moments of such molecules. This is also observed elsewhere [13]. The corrected μ's obtained from the reduced bond moments of the substituent groups by factors μ_{cal}/μ_{theo} establish the above facts at different temperatures, too. Thus the dielectric relaxation parameters from *hf* conductivity measurements offer a useful tool to arrive at the structural and associational aspects of the non-spherical polar liquids.

Acknowledgment

The authors are thankful to Sri R C Basak for his interest in this work.

References

[1] C R Acharyya, A K Chatterjee, P K Sanyal and S Acharyya *Indian J. Pure Appl. Phys.* **24** 234 (1986)

[2] A K Chatterjee, U Saha, N Nandi, R C Basak and S Acharyya *Indian J. Phys.* **66B** 291 (1992)

[3] U Saha and S Acharyya *Indian J. Pure Appl. Phys.* **31** 181 (1993)

[4] A Sharma, D R Sharma and M S Chauhan *Indian J. Pure Appl. Phys.* **31** 841 (1993)

[5] A Sharma and D R Sharma *J. Phys. Soc. Jpn.* **61** 1049 (1992)

[6] A R Saksena *Indian J. Pure Appl. Phys.* **16** 1079 (1978)

[7] U Saha and S Acharyya *Indian J. Pure Appl. Phys.* **32** 346 (1994)

[8] F J Murphy and S O Morgan *Bull. Syst. Tech. J.* **18** 502 (1939)

[9] K V Gopalakrishna *Trans. Faraday Soc.* **53** 767 (1957)

[10] S K Sit and S Acharyya *Indian J. Phys.* **70B** 19 (1996)

[11] H Eyring, S Glasstone and K J Laidler *The Theory of Rate Process* (New York : McGraw-Hill) (1941)

[12] C P Smyth *Dielectric Behaviour and Structure* (New York : McGraw Hill) (1955)

[13] R C Basak, S K Sit, N Nandi and S Acharyya *Indian J. Phys.* **70B** 37 (1996)

Indian Journal of Pure & Applied Physics
Vol. 35, May 1997, pp. 329-337

Double relaxations of some isomeric octyl alcohols by high frequency absorption in non-polar solvent

S K Sit, N Ghosh & S Acharyya
Department of Physics, University College, P O Raiganj, Dist Uttar Dinajpur, 733 134, W Bengal

Received 29 March 1996; revised 18 June 1996; accepted 7 November 1996

The double relaxation behaviour of some isomeric octyl alcohols in n-heptane at 25°C under the electric field frequencies of 24.33, 9.25 and 3.00 GHz is studied to get the relaxation times τ_1 and τ_2 for their flexible parts and whole molecules by a method of single frequency measurements of dielectric relaxation parameters. The isomers are long, straight chain, hydrogen bonded, polymer type molecules having methyl and hydroxyl groups attached to their C-atoms which may bend, twist or rotate internally under *hf* electric field each with a characteristic τ. The relative contributions, c_1 and c_2 towards dielectric relaxations due to τ_1 and τ_2 are also estimated by using Fröhlich's equations and the graphical technique. The dipole moments μ_1 and μ_2 in terms of τ_1 and τ_2 of flexible part and the whole molecules are again found out from slope β of the total *hf* conductivity K_{ij} as a function of weight fractions ω_j's of the solute indicating μ_1 for the rotation of their $-OH$ groups about $C-C$ bonds only. μ_1 and μ_2 are finally compared with the theoretical dipole moments μ_{theo} arising out of the structures with bond-angles and bond-moments of their substitutent groups to establish the conformations of these isomers are justified like normal alcohols observed earlier..

1 Introduction

The dielectric relaxation mechanism of a polar-non-polar liquid mixture is a very convenient and useful tool in ascertaining the shape, size and structure of a polar molecule[1]. The process is generally involved with the estimation of dipole moment μ in terms of the relaxation time τ for a polar molecule in a non-polar solvent under different high frequency (*hf*) electric field of giga hertz (GHz) range at a fixed or different temperatures. There exist several methods[2] to estimate τ of a polar liquid in a non-polar solvent. They offer a deep insight into the intrinsic properties of a polar molecule because of the absence of dipole-dipole interactions in polar-non-polar liquid mixtures.

Highly non-spherical polar molecules, on the other hand, possess more than one τ in the electric field of GHz range for the rotations of different substituent groups attached to the parent molecule and the whole molecule itself. Budo[3], however, proposed that complex dielectric constant ε^* of a polar liquid may be represented as the sum of a number of non-interacting Debye type dispersions each with a characteristic τ. The method was then made simpler by Bergmann *et al.*[4] by assuming that the dielectric relaxation is the sum of two Debye type dispersions characterised by the intramolecular and molecular τ_1 and τ_2 respectively. The corresponding relative contributions c_1 and c_2 towards dielectric relaxations could then be estimated. They used a graphical analysis which consists of plotting normalised values of $(\varepsilon' - \varepsilon_\infty)/(\varepsilon_0 - \varepsilon_\infty)$ against $\varepsilon''/(\varepsilon_0 - \varepsilon_\infty)$ on a complex plane in terms of the measured real ε', imaginary ε'' parts of ε^*, static dielectric constant ε_0 and high frequency dielectric constant ε_∞ of a polar liquid for different frequencies of the electric field. A number of chords were then drawn through the points on the curve unitil a set of parameters was found out in consistency with all the experimental points. Bhattacharyya *et al.*[5] subsequently modified the above procedure to get τ_1, τ_2 and c_1, c_2 for a polar liquid from the relaxation data measured at least at two different frequencies of the electric fields.

A procedure was devised[6] to get τ_1 and τ_2 from the slope and intercept of a derived straight line equation involved with the single frequency mesurements of the dielectric relexation parameters like ε_{oij}, $\varepsilon_{\beta ij}$, ε'_{ij} and ε''_{ij} for different weight fractions ω_j's of a polar solute (j) in a non-polar solvent (i) at a given temperature. The technique had already been applied on disubstituted benzenes and anilines[6] at 9.945 GHz electric field as well as mono-substituted anilines[7] at 22.06, 3.86,

2.02 GHz electric fields respectively. All these investigations reveal that they often showed the double relaxation behaviour at certain frequency of the electric field.

The aliphatic alcohols are long straight chain, hydrogen bonded polymer type molecules having possibility of their bending, twisting and rotation under *hf* electric field each with a characteristic τ, besides the average macroscopic distribution of τ. The alcohols have high dipole moments owing to their strong intermolecular forces exerted by them like polymers in solution. Onsager's equation may be a better choice for such associative liquids, but it is not so simple like Debye's equation because of the presence of quadratic term ε^*_{ij}. The relaxation behaviour of aliphatic alcohols is very interesting because they show more than two τ's in pure state, but for a polar-non-polar liquid mixture *hf* process becomes increasingly important on dilution[8,9]. An extensive study to detect the frequency dependence of double relaxation behaviour of four long chain normal aliphatic alcohols like 1-butanol, 1-hexanol, 1-heptenol, 1-decanol in solvent n-heptane[10] including methanol and ethanol at 9.84 GHz in benzene[11,12] at 25°C was already made[13]. All the alcohols showed τ_1 and τ_2 at all frequencies of the electric field except methanol which is a simple molecule to possess the expected τ_2 only.

The method[6] was applied on six isomeric octyl alcohols like 2-methyl-3-heptanol, 3-methyl-3-heptanol, 4-methyl-3-heptanol, 5-methyl-3-heptanol, 4-octanol and 2-octanol at 24.33, 9.25 and 3.00 GHz electric fields, as reported in Tables 1-3 respectively, because of the availability of ε'_{ij}, ε''_{ij}, ε_{0ij} and $\varepsilon_{\infty ij}$ measured by Crossley *et al.*[14] in n-heptane at 25°C. The straight line equations between $(\varepsilon_{0ij}-\varepsilon'_{ij})/(\varepsilon'_{ij}-\varepsilon_{\infty ij})$ and $\varepsilon''_{ij}/c\ \varepsilon'_{ij}-\varepsilon_{\infty ij})$ for all the octyl alcohols at different ω_j's are linear as shown in Fig. 1 only to establish the applicability of Debye model in such isomeric alcohols like normal alcohols[13] once again. Moreover, all the long chain octyl alcohols are structural isomers with the molecular formula $C_8H_{18}O$ having greater

Table 1—The estimated relaxation times τ_2 and τ_1 from the slopes and the intercept of straight line Eq. (8) with errors and correlations (r) together with measured τ_s from $K''_{ij}-K'_{ij}$ curve and most probable relaxation time $\tau_0=\sqrt{\tau_1\tau_2}$ for six isomeric octyl alcohols at 25°C under different frequencies of electric fields

System with Sl. No. & Mol. wt M_j	Frequency in GHz	Intercept & slope of Eq.(8)		Correlation coefficient (r)	% Error in regression technique	Estimated values of τ_2 & τ_1 in p Sec.		Measured τ_s in p Sec.	Most probable relaxation time $\tau_0=\sqrt{\tau_1\tau_2}$
I 2-methyl-3-heptanol	(a) 24.33	2.3718	5.0952	0.9011	6.34	29.96	3.39	1.84	10.08
in n-heptane	(b) 9.25	0.6871	3.1205	0.9700	1.90	49.61	4.10	3.58	14.26
M_j = 130 gm	(c) 3.00	0.1408	1.4830	0.9771	1.50	73.31	5.41	6.74	19.91
II 3-methyl-3-heptanol	(a) 24.33	0.9087	2.6282	0.9294	4.59	14.52	2.68	2.19	6.24
in n-heptane	(b) 9.25	0.6389	2.7714	0.9709	1.93	43.34	4.37	3.70	13.76
M_j = 130 gm	(c) 3.00	0.1611	1.5018	0.9985	0.10	73.55	6.17	5.58	21.30
III 4-methyl-3-heptanol	(a) 24.33	1.9653	4.3873	0.8851	7.30	25.40	3.31	1.90	9.17
in n-heptane	(b) 9.25	0.6411	2.8636	0.9682	2.11	45.08	4.21	4.13	13.78
M_j = 130 gm	(c) 3.00	0.2008	1.7153	0.9206	5.14	84.34	6.71	11.98	23.79
IV 5-methyl-3-heptanol	(a) 24.33	0.6929	2.9788	0.5684	26.36	17.83	1.66	1.71	5.44
in n-heptane	(b) 9.25	0.7445	3.2866	0.9846	1.19	52.36	4.21	5.39	14.85
M_j = 130 gm	(c) 3.00	0.2362	2.0308	0.9371	4.74	101.22	6.58	13.11	25.81
V 4-octanol in	(a) 24.33	0.9572	3.4750	0.8569	10.34	20.77	1.97	1.83	5.40
n-heptane	(b) 9.25	0.3810	2.6361	0.9470	4.02	42.74	2.64	5.46	10.62
M_j = 130 gm	(c) 3.00	0.1428	1.6929	0.9846	1.18	85.13	4.72	12.76	20.05
VI 2-octanol in	(a) 24.33	1.3664	5.0208	0.6336	23.30	30.97	1.89	1.83	7.65
n-heptane	(b) 9.25	1.5853	5.6407	0.9888	0.86	92.00	5.11	6.26	21.68
M_j = 130 gm	(c) 3.00	0.4458	3.1697	0.9780	1.69	160.41	7.83	18.70	35.44

Table 2—Fröhlich parameter A, relative contributions c_1 and c_2 due to τ_1 and τ_2, theoretical values of x and y from Fröhlich's Eqs (9)and (10) and from graphical extrapolation technique at $\omega_j \to 0$

System with Sl. No.	Frequency, GHz	Fröhlich parameter $\Delta = \ln(\tau_2/\tau_1)$	Theoretical values of x & y from Eqs (9) and (10)		Theoretical values of c_1 & c_2		Estimated values of x & y at $\omega_j \to 0$		Estimated values of c_1 and c_2	
I 2-methyl-3-heptanol in	(a) 24.33	2.1790	0.3457	0.4028	0.3686	1.2101	0.795	0.366	1.0226	−0.2476
n-heptane	(b) 9.25	2.4932	0.5637	0.4023	0.4886	0.9434	1.075	0.19	1.1624	−0.2324
	(c) 3.00	2.6063	0.7973	0.3232	0.6144	0.5500	1.075	0.074	1.1143	−0.0808
II 3-methyl-3-heptanol in	(a) 24.33	1.6997	0.5195	0.4490	0.4542	0.7733	0.865	0.32	1.0321	−0.1120
n-heptane	(b) 9.25	2.2943	0.5792	0.4115	0.4922	0.8573	0.91	0.256	0.9569	0.0810
	(c) 3.00	2.4781	0.7865	0.3349	0.6028	0.5600	1.025	0.094	1.0589	−0.0579
III 4-methyl-3-heptanol	(a) 24.33	2.0378	0.3747	0.4173	0.3857	1.0842	0.78	0.35	0.9961	−0.2117
n-heptane	(b) 9.25	2.3710	0.5775	0.4075	0.4932	0.8812	0.95	0.208	1.0177	−0.0805
	(c) 3.00	2.5313	0.7543	0.3490	0.5902	0.6112	1.015	0.094	1.0551	−0.0827
VI 5-methyl-3-heptanol	(a) 24.33	2.3741	0.5644	0.4088	0.4862	0.9057	0.645	0.274	0.6389	0.3763
n-heptane	(b) 9.25	7.5207	0.5499	0.4020	0.4814	0.9805	0.95	0.172	1.0297	−0.2211
	(c) 3.00	2.7332	0.7222	0.3529	0.5833	0.6848	1.065	0.042	1.1326	−0.2341
V 4-octanol in n-heptane	(a) 24.33	2.3555	0.5080	0.4131	0.4553	1.0030	0.72	0.22	0.7840	0.0126
	(b) 9.25	2.7833	0.6506	0.8720	0.5463	0.8372	0.895	0.116	0.9254	−0.0654
	(c) 3.00	2.8924	0.7813	0.3197	0.6210	0.5900	0.99	0.052	1.0218	−0.0850
VI 2-octanol in n-heptane	(a) 24.33	2.7964	0.4507	0.3867	0.4257	1.3507	0.67	0.208	0.7223	0.0764
	(b) 9.25	2.3925	0.4292	0.3795	0.4124	1.4780	0.895	0.214	0.9850	−0.3026
	(c) 3.00	3.0198	0.6201	0.3658	0.5361	0.9672	1.04	0.102	1.0810	−0.1813

Table3—Estimated intercept and slope of $K_{ij} - \omega_j$ equation, dimensionless parameters b_2, b_1 (eq. (16)), estimated dipole moments μ_2, μ_1 (eq.(15)), μ_{theo} from bond angles and bond moments together with μ_1 from $\mu_1 = \mu_2(c_1/c_2)^{1/2}$ in Debye

System with Sl. No. Mol wt.	Frequency GHz	Intercept & slope or of $K_{ij} = \omega_j$ equation		Dimensionless parameter		Estimated dipole moments (in Deybe)		μ_{theo} in D	Estimated μ_1 in D from $\mu_1 = \mu_2(c_1/c_2)^{1/2}$
		$\alpha \times 10^{-10}$	$\beta \times 10^{-10}$	b_1	b_2	μ_2	μ_1		
I 2-methyl-3-heptanol	(a) 24.33	2.3632	0.6974	0.0455	0.7885	4.80	1.15		2.65
in n-heptane	(b) 9.25	0.8998	0.3126	0.1075	0.9463	3.39	1.14	1.76	2.44
$M_j = 130$ gm	(c) 3.00	0.2911	0.1224	0.3439	0.9897	2.08	1.23		2.20
II 3-methyl-3-heptanol	(a) 24.33	2.3630	0.7490	0.1689	0.8564	2.58	1.15		1.98
in n-heptane	(b) 9.25	0.8959	0.3554	0.1363	0.9395	3.21	1.22	1.76	2.43
$M = 130$ gm	(c) 3.00	0.2910	0.1330	0.3425	0.2867	2.18	1.29		2.26
III 4-methyl-3-heptanol	(a) 24.33	2.3635	0.7213	0.623	0.7963	4.17	1.17		2.49
in n-heptane	(b) 9.25	0.8984	0.3278	0.1273	0.9436	3.19	1.17	1.76	2.39
$M_j = 130$ gm	(c) 3.00	0.2911	0.1283	0.2837	0.9843	2.35	1.26		2.31
IV 5-methyl-3-heptanol	(a) 24.33	2.3646	0.6415	0.1187	0.9396	2.85	1.01		2.09
in n-hetpane	(b) 9.25	0.9021	0.2771	0.0975	0.9436	3.35	1.08	1.76	2.35
$M_j = 130$ gm	(c) 3.00	0.2922	0.1138	0.2157	0.9849	2.54	1.19		2.34
V 4-octanol in	(a) 24.33	2.3561	0.6492	0.0903	0.9169	3.29	1.03		2.22
n-heptane	(b) 9.25	0.8965	0.2618	0.1396	0.9770	2.72	1.03	1.08	2.20
$M_j = 130$ gm	(c) 3.00	0.2919	0.1044	0.2799	0.9922	2.13	1.13		2.19
VI 2-octanol in heptane	(a) 24.33	2.3533	0.6572	0.9428	0.9230	4.80	1.03		2.69
$M_j = 130$ gm	(b) 9.25	0.8980	0.2753	0.0338	0.9190	5.67	1.09	1.08	3.00
	(c) 3.00	0.2897	0.1221	0.0887	0.9787	3.88	1.23		2.89

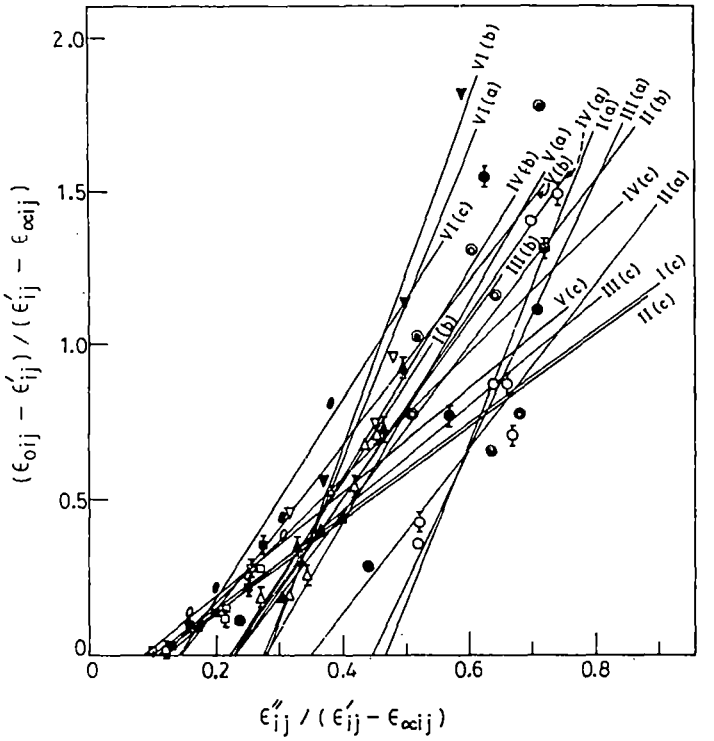

Fig. 1—Plot of $(\varepsilon_{0ij} - \varepsilon'_{ij})/(\varepsilon'_{ij} - \varepsilon_{\infty ij})$ against $\varepsilon''_{ij}/(\varepsilon'_{ij} - \varepsilon_{\infty ij})$ of some isomeric octyl alcohols in n-heptane at 25°C. Curves of I (a), I (b), I (c) for 2-methyl-3-heptanol at 24.33, 9.25 and 3.00 GHz. (○, ⅄, ⏃). Curves of II (a), II (b), II (c) for 3-methyl-3-heptanol at 24.33, 9.25 and 3.00 GHz (●, ▲, ■). Curves of III (a), III (b), III (c) for 4-methy-3-heptanol at 24.33, 9.25 and 3.00 GHz (○, △, □). Curves of IV(a), IV (b), IV (c) for 5-methyl-3-heptanol at 24.33, 9.25, 3.00 GHz (◐, ⅄, ⏃). Curves of V (a), V (b), V (c) for 4-octanol at 24.33, 9.25 and 3.00 GHz (○, ▽, ◇). Curves of VI (a), VI (b), VI (c) for 2-octanol at 24.33, 9.25 and 3.00 GHz (◐, ▼, ◆).

number of C-atoms in their structures. They are, therefore, expected to possess two relaxation processes at audio and radio frequencies of electric field at low temperature in pure state[14].

The paper presents the frequency dependence of τ_1 and τ_2 at all frequencies of 24.33, 9.25 and 3.00 GHz electric field for all the octyl alcohols like normal alcohols too. The measured τ_s from the slope of the linear equation of imaginary K''_{ij} and real K'_{ij} parts of the total complex hf conductivity K^*_{ij} and the most probable relaxation time τ_0 from $\tau_0 = \sqrt{\tau_1 \tau_2}$ are placed in Table 1 together with the estimated τ_1 and τ_2 in order to see their trends with frequency of the applied electric field. The relative contributions c_1 abd c_2 towards dielectric relaxations in terms of intramolecular relaxation time τ_1 and molecular relaxation time τ_2 are then estimated from Fröhlich's equations[15] as well as the graphical method of Figs 2 and 3. The estimated c_1 and c_2 are placed in Table 2.

The dipole moments μ_1 and μ_2 due to flexible parts as well as the whole molecules in terms of the estimated τ_1 and τ_2 and the slopes β of the linear variation of hf conductivity K_{ij} with ω_j are shown in Table 3. The slopes β and the intercepts α of the linear variation of K_{ij} with ω_j, as placed in Table 3, at each frequency for all the isomers in n-heptane are almost the same probably due to their same polarity[16]. This fact is also supported by their conformations as shown in Fig. 4. It was, therefore, very difficult to plot K_{ij} against ω_j. The computed μ_2's for most of the isomeric alcohols show larger values at 24.33 GHz and gradually decrease with lower frequencies unlike μ_1. In order to compare μ_2 and μ_1 with theoretical dipole moments μ_{theo}, a special attention is to be paid on the conformational structure of each isomer from the available bond angles and bond moment. They are shown in Fig. 4. Using the usual C−C bond moment of 0.09 D from methanol and ethanol[13] μ_{theo} for four methyl substituted octanols are found to show slightly larger values (see Fig. 4 and Table 3) than 1-heptanol[13] except the desired values for 2-octanol and 4-octanol perhaps due to

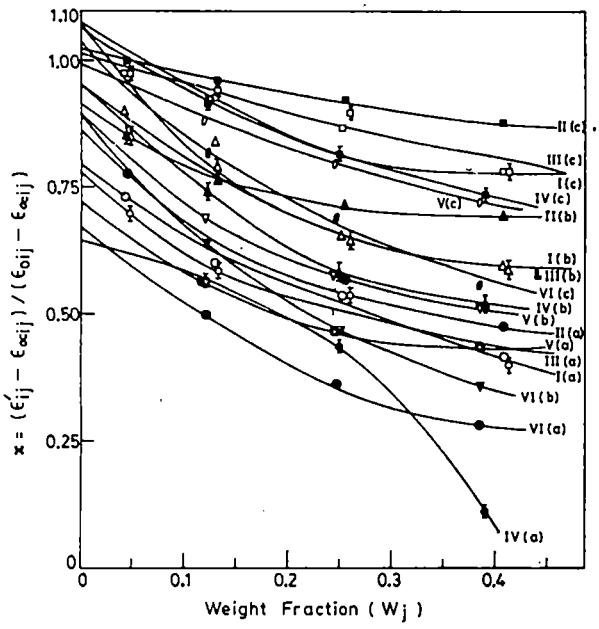

Fig. 2—Plot of $(\varepsilon_{0ij}-\varepsilon'_{ij})/(\varepsilon'_{ij}-\varepsilon_{\infty ij})$ against weight fraction ω_j of some isomeric octyl alcohols in n-heptane at 25°C. Curves of I (a), I (b), I (c) for 2-methyl-3-heptanol at 24.33, 9.25 and 3.00 GHz. (○, △, □). Curves of II (a), II (b), II (c) for 3-methyl-3-heptanol at 24.33, 9.25 and 3.00 GHz (●, ▲, ■). Curves of III (a), III (b), III (c) for 4-methy-3-heptanol at 24.33, 9.25 and 3.00 GHz (⊙, ⏃, ⊡). Curves of IV(a), IV (b), IV (c) for 5-methyl-3-heptanol at 24.33, 9.25, 3.00 GHz (◐, ◭, ◨). Curves of V (a), V (b), V (c) for 4-octanol at 24.33, 9.25 and 3.00 GHz (○, ▽, ◇). Curves of VI (a), VI (b), VI (c) for 2-octanol at 24.33, 9.25 and 3.00 GHz (◓, ▼, ●).

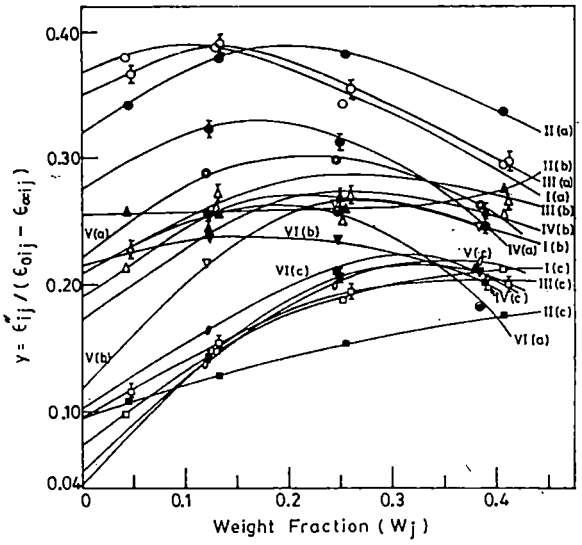

Fig. 3—Plot of $\varepsilon''_{ij}/(\varepsilon_{0ij}-\varepsilon_{\infty ij})$ against weight fraction ω_j of some isomeric octyl alcohols in n-heptane at 25°C. Curves of I (a), I (b), I (c) for 2-methyl-3-heptanol at 24.33, 9.25 and 3.00 GHz. (○, △, □). Curves of II (a), II (b), II (c) for 3-methyl-3-heptanol at 24.33, 9.25 and 3.00 GHz (●, ▲, ■). Curves of III (a), III (b), III (c) for 4-methy-3-heptanol at 24.33, 9.25 and 3.00 GHz (⊙, ⏃, ⊡). Curves of IV(a), IV (b), IV (c) for 5-methyl-3-heptanol at 24.33, 9.25, 3.00 GHz (◐, ◭, ◨). Curves of V (a), V (b), V (c) for 4-octanol at 24.33, 9.25 and 3.00 GHz (○, ▽, ◇). Curves of VI (a), VI (b), VI (c) for 2-octanol at 24.33, 9.25 and 3.00 GHz (◓, ▼, ●).

bond moments of C—H_3 and —O—H groups in their structures. The calculated value of μ_1 from $\mu_1=\mu_2(c_1/c_2)^{1/2}$ assuming two relaxation processes are equally probable, are also placed in the last column of Table 3 with all the estimated μ's for comparison.

2 Theoretical Formulations to Estimate Relaxation Parameters

The complex dielectric constant ε^*_{ij} of a polar-non-polar liquid mixture can be represented as the sum of a number of non-interacting Debye type dispersions in accordance with Budo's[3] relation.

$$\frac{\varepsilon^*_{ij}-\varepsilon_{\infty ij}}{\varepsilon_{0ij}-\varepsilon_{\infty ij}}=\sum\frac{c_k}{1+j\omega\tau_k} \qquad \ldots(1)$$

where $j=\sqrt{-1}$ is a complex number and $\Sigma c_k=1$. The term c_k is the relative contribution for the kth type of relaxation processes. When ε^*_{ij} consists of two Debye type dispersions, Budo's relation reduces to Bergmann's equations[4]:

$$\frac{\varepsilon'_{ij}-\varepsilon_{\infty ij}}{\varepsilon_{0ij}-\varepsilon_{\infty ij}}=\frac{c_1}{1+\omega^2\tau_1^2}+\frac{c_2}{1+\omega^2\tau_2^2} \qquad \ldots(2)$$

and

$$\frac{\varepsilon''_{ij}}{\varepsilon_{0ij}-\varepsilon_{\infty ij}}=c_1\frac{\omega\tau_1}{1+\omega^2\tau_1^2}+c_2\frac{\omega\tau_2}{1+\omega^2\tau_2^2} \qquad \ldots(3)$$

such that $c_1+c_2=1$. Now with

$$\frac{\varepsilon'_{ij}-\varepsilon_{\infty ij}}{\varepsilon_{0ij}-\varepsilon_{\infty ij}}=x, \quad \frac{\varepsilon''_{ij}}{\varepsilon_{0ij}\varepsilon_{\infty ij}}=y$$

$\omega\tau=\alpha$ and using $a=(1/1+\alpha^2)$ and $b=\alpha/(1+\alpha^2)$ the Eqs (2) and (3) can be written as;

$$x=c_1a_1+c_2a_2 \qquad \ldots(4)$$

$$y=c_1b_1+c_2b_2 \qquad \ldots(5)$$

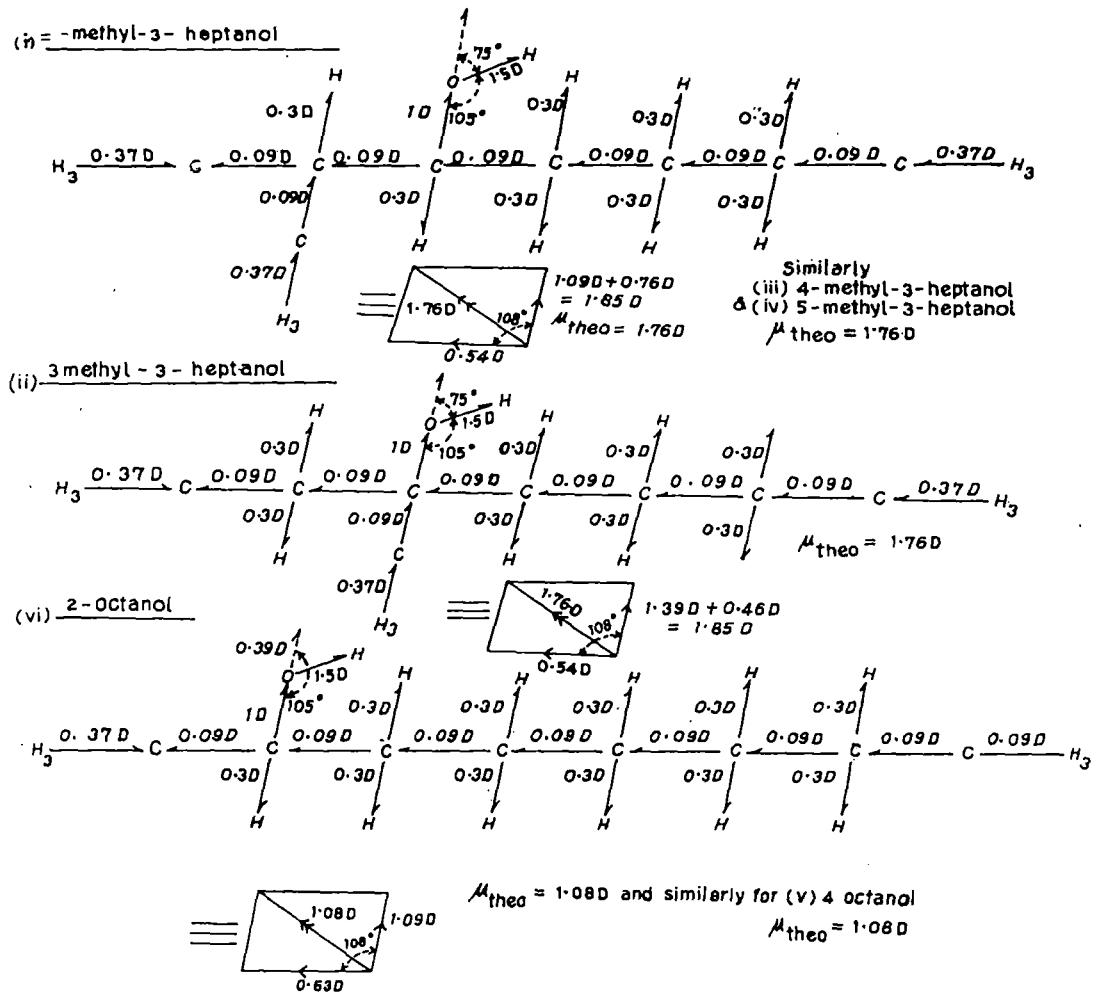

Fig. 4—Conformations of some isomeric octyl alcohols

where suffixes 1 and 2 with a and b are related to τ_1 and τ_2 respectively. From Eqs (4) and (5), since $\alpha_2 - \alpha_1 \neq 0$ and $\alpha_2 > \alpha_1$ we have

$$c_1 = \frac{(x\alpha_2 - y)(1+\alpha_1^2)}{\alpha_2 - \alpha_1} \qquad \ldots (6)$$

$$c_2 = \frac{(y - x\alpha_1)(1+\alpha_2^2)}{\alpha_2 - \alpha_1} \qquad \ldots (7)$$

Since $c_1 + c_2 = 1$, we get the following equation with the help of Eqs (6) and (7):

$$\frac{1-x}{y} = (\alpha_1 + \alpha_2) - \frac{x}{y}\alpha_1\alpha_2$$

which on substitution of the values x, y and α yields:

$$\frac{\varepsilon_{0ij} - \varepsilon'_{ij}}{\varepsilon'_{ij} - \varepsilon_{\infty ij}} = \omega(\tau_1 + \tau_2)\frac{\varepsilon''_{ij}}{\varepsilon'_{ij} - \varepsilon_{\infty ij}} - \omega^2\tau_1\tau_2 \qquad \ldots (8)$$

Eq. (8) is thus a straight line equation between $(\varepsilon_{0ij} - \varepsilon'_{ij})/(\varepsilon'_{ij} - \varepsilon_{\infty ij})$ and $\varepsilon''_{ij}/(\varepsilon'_{ij} - \varepsilon_{\infty ij})$ with slope $\omega(\tau_1 + \tau_2)$ and intercept $-\omega^2\tau_1\tau_2$ respectively, where ω is the angular frequency of the applied electric field of frequency f in GHz. With the measured dielectric relaxation data of ε'_{ij}, ε''_{ij}, ε_{0ij} and $\varepsilon_{\infty ij}$ for different weight fractions ω_j's of each octyl alcohol in n-heptane at 25°C under 24.33, 9.25 and 3.00 GHz electric fields[14] we get slope and intercept of Eq. (8) to yield τ_1 and τ_2 as shown in Talble 1.

The relative contributions, c_1 and c_2 towards the dielectric relaxations in terms of x, y and τ_1, τ_2 for each octyl alcohol are found out and placed in Table 2. The theoretical values[15] of x and y are, however, calculated from Fröhlich's Eqs:

$$x=\frac{\varepsilon'_{ij}-\varepsilon_{\infty ij}}{\varepsilon_{0ij}-\varepsilon_{\infty ij}}=1-\frac{1}{2A}\ln\left(\frac{e^{2A}\omega^2\tau_1^2+1}{1+\omega^2\tau_1^2}\right) \quad \ldots(9)$$

$$y=\frac{\varepsilon''_{ij}}{\varepsilon_{0ij}-\varepsilon_{\infty ij}}=\frac{1}{A}[\tan^{-1}(e^A\omega\varepsilon_1)-\tan^{-1}(\omega\tau_1)\ldots(10)$$

where A= Fröhlich parameter $=\ln(\tau_2/\tau_1)$ and τ_1 is called the small limiting relaxation time as obtained from the double relaxation method. A simple graphical extrapolation technique, on the other hand, was considered to get the values of x and y at $\omega_j \to 0$ from Figs 2 and 3 respectively. This is really in accordance with Bergmann's Eqs (2) and (3) when the once estimated τ_1 and τ_2 from Eq. (8) are substituted in the right hand sides of above Eqs (2) and (3).

The values of μ_1 and μ_2 of octyl alcohols in terms of τ_1, τ_2 and slope β of the concentration variation of the experimental *hf* conductivity K_{ij} were then estimated. The *hf* conductivity K_{ij} is, however, given by Murphy and Morgan[17]:

$$K_{ij}=\frac{\omega}{4\pi}(\varepsilon''^2_{ij}+\varepsilon'^2_{ij})^{1/2} \quad \ldots(11)$$

as a function of ω_j of polar solute. Since $\varepsilon''_{ij} \ll \varepsilon'_{ij}$ in the *hf* electric field, the term ε''_{ij} offers resistance of polarisation. Thus the real part K'_{ij} of the *hf* K^*_{ij} of a polar-non-polar liquid mixture at TK can be written according to Smyth[18] as:

$$K'_{ij}=\frac{\mu_j^2 N\rho_{ij}F_{ij}}{3M_j kT}\left(\frac{\omega^2\tau}{1+\omega^2\tau^2}\right)\omega_j \quad \ldots(12)$$

which on differentiation with respect to ω_j and for $\omega_j \to 0$ yields that:

$$\left(\frac{dK'_{ij}}{d\omega_j}\right)_{\omega_j\to 0}=\frac{\mu_j^2 N\rho_i F_i}{3M_j kT}\left(\frac{\omega^2\tau}{1+\omega^2\tau^2}\right) \quad \ldots(13)$$

where M_j is the molecular weight of a polar solute, N the Avogadro number, k the Boltzmann constant, the local field $F_{ij}=1/9\ (\varepsilon_{ij}+2)^2$ between $F_i=1/9\ (\varepsilon_i+2)^2$ and the density $\rho_{ij} \to \rho_i$ the density of solvent at $\omega_j \to 0$.

Again, the total *hf* conductivity $K_{ij}=\omega/4\pi\ \varepsilon_{ij}$ can be written as:

$$K_{ij}=K_{ij\infty}+\frac{1}{\omega\tau}K'_{ij}$$

or

$$\left(\frac{dK'_{ij}}{d\omega_j}\right)_{\omega_j\to 0}=\omega\tau\left(\frac{dK_{ij}}{d\omega_j}\right)_{\omega_j\to 0}=\omega\tau\beta \quad \ldots(14)$$

where β is the slope of $K_{ij}-\omega_j$ curve at infinite dilution. From Eqs (13) and (14) we get:

$$\mu_j=\left[\frac{27M_j kT}{N\rho_i(\varepsilon_i+2)^2}\cdot\frac{\beta}{\omega b}\right]^{1/2} \quad \ldots(15)$$

as the dipole moment of each octyl alcohol in terms of b, where b is a dimensionless parameter given by:

$$b=\frac{1}{1+\omega^2\tau^2} \quad \ldots(16)$$

The computed μ_1 and μ_2 together with b, b_2 and β of $K_{ij}-\omega_j$ equations for all the octyl alcohols are placed in Table 3.

3 Results and Discussion

The least square fitted straight line equations of $(\varepsilon_{0ij}-\varepsilon'_{ij})/(\varepsilon'_{ij}-\varepsilon_{\infty ij})$ against $\varepsilon''_{ij}/(\varepsilon'_{ij}-\varepsilon_{\infty ij})$ for six isomeric octyl alcohols like 2-methyl-3-heptanol, 3-methyl-3-heptanol, 4-methyl-3-heptanol, 5-methyl-1,3-heptanol, 4-octanol and 2-octanol in solvent n-heptane at 25°C under 24.33, 9.25 and 3.00 GHz electric field at different ω_j's of polar solutes are shown in Fig. 1 together with the experimental points on them. ω_j's are, however, calculated from the mole fractions x_i and x_j of solvent and solute with molecular weights M_i and M_j respectively according to the relation[19]:

$$\omega_j=\frac{x_j M_j}{x_i M_i+x_j M_j}$$

All the straight line equations are almost perfectly linear as evident from the correlation coefficients r lying in the range 0.9985-0.5684. The corresponding % of errors in terms of r in getting the slopes and intercepts of all the straight lines are placed in the 6th and 5th columns of Table 1. The errors are, however, large at 24.33 GHz indicating departure from the linear behaviour as evi-

dent from low values of r perhaps due to inherent uncertainty in measured data for such higher frequency[13].

The estimated values of τ_2 and τ_1 for all the isomeric octyl alcohols from the slopes and the intercepts of straight line equations are of smaller magnitude at 24.33 GHz and increase gradually to attain maximum value at 3.00 GHz under the present investigation. This may be due to the fact that at higher frequency the rate of hydrogen bond rupture in long chain alcohols is the maximum thereby reducing τ for each rotating unit[13]. τ_2 and τ_1 are then compared with the measured τ_s from the relation:

$$K''_{ij} = K_{ij\infty} + \frac{1}{\omega \tau_s} K'_{ij}$$

and τ_0 where $\tau_0 = \sqrt{\tau_1 \tau_2}$. As evident from Table 1 although $\tau_0 > \tau_1$; τ_s agrees well with τ_1 for most of the solutes except slight disagreement at 3.00 GHz for 4-methyl-3-heptanol, 5-methyl-3-heptanol, 4-octanol and 2-octanol. This is explained on the basis of the fact that conductivity measurement may be applicable in higher frequency in yielding microscopic τ only whereas the double relaxation method offers a better understanding of molecular relaxation phenomena showing microscopic as well as macroscopic τ as observed earlier[13]. Unlike normal aliphatic alcohols, $-OH$ groups are screened by the substituted $-CH_3$ group, broad dispersion characterised by relatively short relaxation times were thus observed[14]. The respective positions of $-CH_3$ and $-OH$ groups also greatly affect the static dielectric constant, correlation factor, their temperature dependence and type of hydrogen bonding in them.

The relative contributions c_1 and c_2 towards dielectric relaxations are also estimated in terms of $(\varepsilon'_{ij} - \varepsilon_{\infty ij})/(\varepsilon_{0ij} - \varepsilon_{\infty ij})$, $\varepsilon''_{ij}/(\varepsilon_{0ij} - \varepsilon_{\infty ij})$ with the estimated, τ_1, τ_2 as shown in Table 2 by Fröhlich and graphical methods. $x = (\varepsilon'_{ij} - \varepsilon_{\infty ij})/(\varepsilon_{0ij} - \varepsilon_{\infty ij})$ and $y = \varepsilon''_{ij}/(\varepsilon_{0ij} - \varepsilon_{\infty ij})$ were, however, evaluated from Fröhlich's Eqs (9) and (10) in the first case. The usual variations of $(\varepsilon'_{ij} - \varepsilon_{\infty ij})/(\varepsilon_{0ij} - \varepsilon_{\infty ij})$ and $\varepsilon''_{ij}/(\varepsilon_{0ij} - \varepsilon_{\infty ij})$ with ω_j are concave and convex as found in Figs 2 and 3 in accordance with Bergmann Eqs (2) and (3), except 5-methyl-3-heptanol at 24.33 GHz whose $[(\varepsilon'_{ij} - \varepsilon_{\infty ij})/(\varepsilon_{0ij} - \varepsilon_{\infty ij})]$ curves is convex in nature due to its non-accurate ε_{0ij} and $\varepsilon_{\infty ij}$ values like ethanol as observed earlier[13]. x and y were also obtained graphically from Figs (2) and (3) in the limit $\omega_j = 0$.

In Fröhlich-method c_1 and c_2 are all positive as evident from 6th and 7th columns of Table 2 with $c_2 > c_1$. In graphical method $c_1 > c_2$ with negative c_2 for most of the systems probably due to inertia of the flexible parts under *hf* electric field, as shown in 10th and 11th columns of same Table 2. c_2 are, however, positive for the systems 5-methyl-3-heptanol, 4-octanol and 2-octanol at 24.33 GHz as well as 3-methyl-3-heptanol at 9.25 GHz. Both the methods in most cases, yield $|c_1 + c_2| \geq 1$, signifying thus the possibility of occurrence of more than two relaxation processes in them[13].

The dipole moments μ_1 and μ_2 of all the isomeric alcohols due to their flexible parts and the whole molecules are estimated in terms of dimensionless parameters b_1, b_2 and slope β of K_{ij}-ω_j curves by using Eq. (15). The variations of K_{ij} with ω_j are all linear having almost the same intercepts α and slopes β at each frequency of electric field. It was, therefore, difficult to plot them as they almost coincide. The values of α and β of K_{ij}'s are little different and comparatively large at 24.33 GHz (Table 3). This sort of behaviour is perhaps due to same dipole moments[16] possessed by the polar molecules under investigation as evident from μ_2 and μ_1 placed in 7th and 8th columns of Table 3. μ_2 for most of the polar molecules shows high values at 24.33 GHz and decrease gradually with lower frequencies except 3-methyl-3-heptanol, 5-methyl-3-heptanol and 2-octanol whose μ_2's are found greater at 9.25 GHz electric field. This type of behaviour may be explained on the basis of the fact that such alcohols behaving almost like the polymer molecules have long chain of C-atoms and tend to break up in a non-polar solvent in order to reduce or even eliminate the absorption under *hf* electric field. The proportion of smaller molecular species having comparatively small number of C-atoms and their corresponding absorption will increase thereby[10]. The values of μ_1's on the other hand, are almost constant exhibiting a trend to increase a little towards low frequency. They are finally compared with bond moments of 1.5 D of $-O-H$ group maing an angle 105° with the $-C-O-$ bond axis according to the preferred conformations of all the isomers as sketched in Fig. 4. This confirms that μ_1 arises due to the rotation of $-OH$ group around $C-O$ bond in the long chain alcohols studied so far[13]. The slight difference is due to difference in steric hindrances as a result of structural configurations at different frequencies. μ_1 also estimated from $\mu_1 = \mu_2 (c_1/c_2)^{1/2}$ assuming two relaxation processes are equally probable as shown in the last column of Table 3. The other bond moments 0.47, 0.3, 1.0 and 0.09 D for

$C-H_3$, C—H, C—O and C—C bonds are also involved to justify their conformations. The resultant of all these bonds by vector addition method yields μ_{theo} of 1.76 D and 1.08 D for four methyl substituted heptanols and two octanols respectively. The derived result should decrease with increase in the number of C-atoms and μ_{theo} for them should be less than that for 1-heptanol[13]. But for μ_{theo} in Fig. 4 three isomers are only displayed due to typical positions of $-CH_3$ and $-OH$ groups. This may probably be the reason of having slightly larger values of μ_{theo} from 1-heptanol as observed earlier[13].

4 Conclusion

The methodology so far advanced for the double broad dispersions of the polar-non-polar liquid mixtures based on Debye's model seems to be much simpler, straightforward and significant one to detect the very existence of τ_1 and τ_2 of a polar liquid in a non-polar solvent. The correlation coefficients between the desired dielectric relaxation parameters involved in the derived equations of Eq. (8) could, however, be estimated to find out % of errors entered in the estimated τ_1 and τ_2 of a polar liquid, because τ is claimed to be accurate within $\pm 10\%$. The isomeric octyl alcohols like normal aliphatic alcohols are found to yield both τ_1 and τ_2 at all frequencies of the electric field of GHz range. The corresponding μ_1 and μ_2 can then be estimated from Eq. (15) in terms of b_1 and b_2 which are, however, involved with τ_1 and τ_2 as estimated, to arrive at their preferred conformations as shown in Fig. 4.

Acknowledgement

The authors are thankful to Mr A R Sit, BE (Electrical) for his interest in this work.

References

1 Saha U & Acharyya S, *Indian J Pure & Appl Phys*, 32(1994) 346.
2 Gopalakrishna KV, *Trans Faraday Soc*, 53 (1957) 767.
3 Budo A, *Phys Z*, 39 (1938) 706.
4 Bergmann K, Roberti D M & Smyth C P, *J Phys Chem*, 64 (1960) 665.
5 Bhattacharyya J, Hasan A, Roy S B & Kastha G S, *J Phys Soc Japan*, 28 (1970) 204.
6 Saha U, Sit S K, Basak R C & Acharyya S, *J Phys D Appl Phys*, 27 (1994) 596.
7 Sit S K, Basak R C, Saha U & Acharyya S, *J Phys D: Appl Phys*, 27 (1994) 2194.
8 Denney D J & Ring J W, *J Chem Phys*, 39 (1963) 1268.
9 Moriamez M & Lebrun A, *Arch Soi (Geneva)*, 13 (1960) 40.
10 Glasser L, Crossley J & Smyth C P, *J Chem Phys*, 57 (1972) 3977.
11 Purohit H D & Sharma H S, *Indian J Pure& Appl Phys*, 8 (1970) 10.
12 Ghosh A K, PhD Dissertation (NBU), 1981.
13 Sit S K & Acharyya S, *Indian J Phys B*, 70 (1996) 19.
14 Crossley J, Glasser L & Smyth C P, *J Chem Phys*, 55 (1971) 2197.
15 Fröhlich H, *Theory of dielectrics* (Oxford University Press, Oxford) 1949.
16 Chatterjee A K, Saha U, Nandi N, Basak R C & Acharyya S, *Indian J Phys*, 668 (1992) 291.
17 Murphy F J & Morgan S D, *Bull Syst Techn J*, 18 (1939) 502.
18 Smyth C P, *Dielectric behaviour and structure*, (McGraw-Hill, New York) 1955.
19 Ghosh A K & Acharyya S, *Indian J Phys*, 528 (1978) 129.

Reprinted from

journal of
MOLECULAR
LIQUIDS

Journal of Molecular Liquids 85 (2000) 375–385

Dielectric relaxation of para polar liquids under high frequency electric field

N Ghosh, RC Basak, SK Sit, S Acharyya

Department of Physics, Raiganj College (University College) P.O. Raiganj, Dist. Uttar Dinajpur. Pin-733134 (W.B), India.

ELSEVIER

ELSEVIER

Journal of Molecular Liquids 85 (2000) 375–385

journal of MOLECULAR LIQUIDS

www.elsevier.nl/locate/molliq

Dielectric relaxation of para polar liquids under high frequency electric field

N Ghosh, RC Basak, SK Sit, S Acharyya

Department of Physics, Raiganj College (University College) P.O. Raiganj, Dist. Uttar Dinajpur, Pin-733134 (W.B), India.

Abstract

The structural and associational aspects of nonspherical para polar liquids (j) in nonpolar solvents (i) are studied through high frequency conductivities σ_{ij}'s of solutions. The relaxation time τ of the respective liquids under 3cm. wavelength electric field at various experimental temperatures in °C are estimated from the slope of individual variations of real σ'_{ij} and imaginary σ''_{ij} parts of hf complex conductivity σ^*_{ij} with weight fractions w_j's of polar liquid. The temperature variation of τ for comparatively larger nonspherical para molecules in dioxane are not strictly obeyed by the Debye model unlike other simpler para di- or tri-substituted benzene in benzene. Thermodynamic energy parameters ΔH_τ, ΔS_τ and ΔF_τ are obtained from Eyring's rate process equation with the estimated τ's in order to get information on the solvent environment around them. The higher values of γ obtained from $\ln\tau_j T$ against $\ln\eta$ equation indicate the solid phase rotators for the liquids. The estimated Kalman and Debye factors $\tau_j T/\eta^\gamma$ and $\tau_j T/\eta$ establish the Debye relaxation mechanism for almost all the para-molecules. The obtained dipole moments μ_j's in terms of slope β of σ_{ij}-w_j curve and dimensionless parameter 'b' involved with estimated τ are then compared with the reported μ and μ_{theo} obtained from bond angles and bond moments. The μ_j's of para liquids are often zero but at other temperatures they show net moments. The slight disagreement between the measured and theoretical μ's reveals the presence of the inductive and mesomeric moments of substituted polar groups in molecules at different temperatures.

1. INTRODUCTION

The dielectric relaxation phenomena of a polar liquid in nonpolar solvent have already gained much attention from a large number of workers [1–3]. The process is thought to be a sensitive tool to investigate the molecular size, shape and structure of a polar liquid. The structural and associational aspects of the polar liquid can thus be inferred in terms of their measured relaxation time τ and hence dipole moment μ at different experimental temperatures in °C. The subsequent use of the temperature dependence of τ's usually yields different thermodynamic energy parameters of a polar unit. The polar liquids having substituted polar groups in their para positions deserve to be specially investigated. The μ's of such para liquids are usually found to be zero [4] due to symmetrical distribution of bond moments of the substituted polar groups in a plane. Sometimes they show a resultant μ when the dipolar and free groups are out of plane with the parent ring.

Earlier investigations [5] were made on substituted hydroxy and methoxybenzaldehydes in

0167-7322/00/$ - see front matter
PII S0167-7322(99)00105-7

benzene, to reveal that τ is generally governed by both molecular and intra-molecular rotations. However, no such study on the long chain substituted parabenzaldehydes and phenones have been made so far. Dhar et al [6] and Somevanshi et al [7] have recently measured real ε'_{ij} and imaginary ε''_{ij} parts of complex dielectric constant ε^*_{ij} of p-hydroxypropiophenone, p-chloropropiophenone, p-acetamidobenzaldehyde, p-benzyloxybenzaldehyde in dioxane and p-anisidine, p-phenitidine, o-chloroparanitroaniline and p-bromonitrobenzene in benzene respectively under 3 cm. wavelength electric field at different experimental temperatures. The purpose of their study was only to observe the molecular and intra-molecular group rotations in the molecules. Nonspherical molecular liquids of such type also are known to be strongly non-Debye in their relaxation behaviour. We, therefore, concentrate our attention to these molecules [6,7] to study dielectric relaxation phenomena by conductivity measurement technique [8] based on the internationally accepted symbols of dielectric terminology and parameters. The phenones together with other di- or tri-substituted benzenes having rigid and free dipolar groups at their para positions are included in the present investigation to compare the dielectric relaxation properties with the benzaldehyde groups. Moreover, our aim is to observe how τ's and μ's vary with respect to sizes, shapes and structures of the molecules and to get an idea of molecular environment of such polar liquids too, in solvents. For most of the polar liquids the imaginary part σ''_{ij} varies linearly [8] with the real part σ'_{ij} of hf complex conductivity σ^*_{ij} for different w_j's of a solute. But in the present polar-nonpolar liquid mixtures the variation of σ''_{ij} with σ'_{ij} was not linear [9] to yield τ_j. The ratio of the individual slopes of σ''_{ij} and σ'_{ij} against w_j's curves at $w_j \to 0$, on the other hand, is used to get τ_j's of these p-polar liquids in order to report them in Table 1.

The intercepts and slopes of linear relationship of ln $(\tau_j T)$ against $1/T$ as shown in Table 2, could, however, be used to obtain thermodynamic energy parameters like enthalpy of activation ΔH_τ, entropy of activation ΔS_τ and free energy of activation ΔF_τ of dielectric

Table 1

The ratio of slopes of concentration variation of imaginary σ''_{ij} and real σ'_{ij} parts of high frequency complex conductivity σ^*_{ij} at $w_j \to 0$ estimated and reported τ_j in pico second, dimensionless parameter b [$= 1/(1 + \omega^2\tau_j^2)$], coefficients α, β, γ, of equation : $\sigma_{ij} = \alpha + \beta w_j + \gamma w_j^2$, estimated and reported dipole moment μ_j in Coulomb-metre at different experimental temperatures in °C and the theoretical dipole moment μ_{theo} in Coulomb-metre from bond angles and bond moments for different para compounds.[a]

System with Sl. No. and Molecular weight M_j	Temp. in °C	Ratio of slopes of σ''_{ij} & σ'_{ij} with w_j $x/y = \frac{(d\sigma''_{ij}/dw_j)}{(d\sigma'_{ij}/dw_j)}$	Estimated τ_j in p.sec	Reported τ_j in p.sec	Dimensionless parameter $b = 1/(1+\omega^2\tau^2)$	Coefficients in the equation $\sigma_{ij} = \alpha + \beta w_j + \gamma w_j^2$ $\alpha \times 10^{-10}$	$\beta \times 10^{-11}$	$\gamma \times 10^{-12}$		Estimated $\mu_j \times 10^{30}$ in Coulomb metre	Reported $\mu_j \times 10^{30}$ in Coulomb metre	Dipole moments $\mu_{theo} \times 10^{30}$ from bond angles and bond moments
1. Para hydroxy- propiophenone	17	0.8287	19.86	-	0.4070	12.8647	− 5.0205	42.5270	0.00			
	23	0.7451	22.08	25.40	0.3571	12.8887	0.0919	15.2643	2.36	10.20		8.27
M_j = 0.150kg	30	0.7028	23.41	24.20	0.3307	13.5236	− 2.4503	− 24.4312	0.00			
	37	1.1073	14.86	23.10	0.5508	12.9387	− 19.8001	5.2591	15.03			
2. Para - chloropro	19	0.7427	22.15	20.80	0.3556	12.7486	1.3145	6.8967	9.43			
piophenone	25	0.8261	19.92	19.70	0.4056	12.9382	− 1.5409	16.8094	0.00	9.84		9.73
M_j = 0.1685kg	31	0.7272	22.63	18.20	0.3458	12.8983	1.4290	0.2140	10.31			
	37	2.1799	7.55	17.10	0.8261	12.5003	13.8819	− 64.5742	21.14			
3. Para acetamido-	17	0.5756	28.58	21.80	0.2490	13.0577	0.7906	6.5180	8.55			
benzaldehyde	23	0.7736	21.27	20.80	0.3744	13.0602	2.5550	− 7.2309	12.75	10.37		13.12
M_j = 0.163kg	30	0.7260	22.66	19.00	0.3453	12.9053	5.8673	17.9855	20.51			
	37	1.0111	16.27	18.60	0.5056	12.6908	13.9352	− 50.5510	26.62			
4. Para benzyloxy	20	0.5865	28.06	20.00	0.2259	12.9919	1.3256	− 3.8704	12.56			
benzaldehyde	25	0.6247	26.34	19.40	0.2807	13.1236	1.0601	-	10.87	10.63		6.23
M_j = 0.212kg	30	0.8358	19.69	18.00	0.4112	13.2032	1.3264	-	10.19			
	35	1.2238	13.44	16.90	0.5998	13.3518	0.8984	-	7.04			

System with Sl. No. and Molecular weight M_j	Temp. in °C	Ratio of slopes of σ'_{ij} & σ'_{ij} with w_j $x/y = \frac{(d\sigma'_{ij}/dw_j)}{(d\sigma'_{ik}/dw_j)}$	Estimated τ_j in p.sec	Reported τ_j in p sec	Dimensionless parameter $b = 1/(1+\omega^2\tau^2)$ $\omega \times 10^{-10}$	Coefficients in the equation $\sigma_{ij} = \alpha + \beta w_j + \gamma w_j^2$ $\beta \times 10^{-11}$	$\gamma \times 10^{-12}$		Estimated $\mu_j \times 10^{30}$ in Coulomb metre	Reported $\mu_j \times 10^{30}$ In Coulomb metre	Dipole moments $\mu_{theo} \times 10^{30}$ from bond angles and bond moments
5. Paraanisidine	20	2.2120	7.43	3.89	0.8306	12.8499	6.1740	− 16.7410	12.23	5.20	
M_j = 0.123 kg	30	2.4152	6.81	3.67	0.8537	13.1252	1.8955	−	6.87	10.33	6.28
	40	3.4952	4.71	3.17	0.9243	13.1862	1.9022	−	6.79	8.87	
6. Paraphenitidine	20	1.5288	10.76	11.08	0.7005	13.3177	5.4487	−	13.21	7.47	15.04
M_j = 0.137 kg	30	1.9049	8.64	10.63	0.7839	12.7717	14.0691	− 24.4860	20.61	9.27	
	40	2.1036	7.32	9.95	0.8158	13.6273	3.9487	2.2744	10.98	10.47	
7. Ortho-chloro-	20	1.5124	10.88	10.57	0.6958	12.3443	1.2822	− 0.9397	7.21	8.13	
paranitroaniline	30	1.9522	8.43	9.89	0.7921	12.7291	0.1756	−	2.57	10.93	15.93
Mj = 0.1725	40	2.2126	7.44	9.18	0.8302	12.8787	0.0908	−	1.85	13.10	
8. Para-bromo-	20	1.6446	10.01	−	0.7299	13.3533	0.6908	0.2145	5.59	−	
nitrobenzene	30	1.7818	9.24	−	0.7603	13.7402	− 0.6908	2.5184	0.00	−	8.40
M_j = 0.202 kg	40	1.9503	8.44	− 0.7917	13.8959	− 0.5847	2.5301	0.00	−		

relaxation process of the rate theory of Eyring et al [10]. The enthalpy of activation ΔH_η due to viscous flow was, however, obtained from the slope γ of the linear relationship in $\ln(\tau_j T)$ against $\ln\eta$, where η is the coefficient of viscosity of the solvent to test the behaviour of solutes in solvents.

The value of ΔS_τ, and ΔH_τ and ΔF_τ, of Table 2 give an insight into the molecular dynamics of the systems. The estimated Debye factor $\tau_j T/\eta$ and Kalman factor $\tau_j T/\eta^\gamma$ in Table 2 signify the applicability of the required relaxation model for such p-liquids.

Table 2
The intercepts and slopes of $\ln \tau_j T$ against $1/T$ curves, energy parameters like enthalpy of activation ΔH_τ in Kilo Joule mole^{-1}, the entropy of activation ΔS_τ in Joule mole^{-1} K^{-1}, free energy of activation ΔF_τ in Kilo-Joule-mole^{-1} for dielectric relaxation process, enthalpy of activation ΔH_η in Kilo Joule mole^{-1} due to viscous flow, γ as the ratio of ΔH_τ and ΔH_η, Kalman factor $(\tau_j T/\eta^\gamma)$, Debye factor $(\tau_j T/\eta)$ at different experimental temperatures in °C and the coefficients of μ_j-t equations $\mu_j = a + bt + ct^2$ of different para compounds

System with Sl. No.	Temp. in °C	Intercept & slope of $\ln \tau_j T$ Vs $1/T$ Curve Intercept	slope	ΔH_τ KJ mole^{-1} in	ΔS_τ in J mole^{-1} K^{-1}	ΔF_τ in KJ mole^{-1}	$\gamma = (\Delta H_\tau/\Delta H_\eta)$	ΔH_η in KJ mole^{-1}	Kalman Factor $\tau_j T/\eta^\gamma$	Debye Factor $(\tau_j T/\eta) \times 10^5$	Coefficients in the equation $\mu_j \times 10^{30} = a + bt + ct^2$ a	b	c
1. Para hydroxy	17				− 19.02	11.53			19.75×10^{-8}	4.0135	35.4250	− 3.2286	0.0716
propiophenone	23	− 21.36	− 724.41	6.02	− 20.49	12.08	0.54	11.15	23.64×10^{-8}	5.0274			
	30				− 21.64	12.58			27.55×10^{-8}	6.2221			
	37				− 18.51	11.76			19.36×10^{-8}	4.6767			
2. Para chloro-	19				79.57	11.90			0.2112	4.6531			
propiophenone	25	− 33.17	4227.52	35.13	77.86	11.93	2.63	13.36	0.2535	4.7300	92.9880	− 7.1216	0.1407
	31				74.30	12.54			0.2938	6.1424			
	37				81.03	10.01			0.1890	2.3761			
3. Para acetamido	17				7.92								
benzaldehye	23	− 24.76	1770.09	14.71	9.17	12.41			11.12×10^{-6}	5.7757			
	30				7.31	11.99	1.10	13.37	9.41×10^{-6}	4.8430	− 4.2996	0.6554	0.0050
	37				8.77	12.49			11.86×10^{-6}	6.0228			
						11.99			10.23×10^{-6}	5.1205			
4. Para benzyloxy	20				71.34	12.52			19.57×10^{-4}	5.7293	9.0620	0.4582	0.0146
benzaldahyde	25	− 32.27	4022.34	33.43	69.81	12.62	1.89	17.68	22.42×10^{-4}	6.0379			
	30				70.24	12.14			22.09×10^{-4}	5.2333			
	35				71.49	11.41			20.70×10^{-4}	4.2025			

System with Sl. No.	Temp- in °C	Intercept & slope of $\ln \tau_j T$ Vs $1/T$ Curve Intercept slope	ΔH_τ KJ $mole^{-1}$ in	ΔS_τ in J $mole^{-1}$ K^{-1}	ΔF_τ in KJ $mole^{-1}$	$\gamma = (\Delta H_\tau / \Delta H_\eta)$	ΔH_η in KJ $mole^{-1}$	Kalman Factor $\tau_j T/\eta^\gamma$	Debye Factor $(\tau_j T/\eta) \times 10^6$	Coefficients in the equation $\mu_j \times 10^{30} = a + bt + ct^2$ a	b	c
5. Paraanisidine	20			18.54	9.29			3.20×10^{-4}	3.3647			
	30	−25.94 1771.20	14.71	17.33	9.47	1.62	9.08	3.82×10^{-4}	3.6781	38.7900	−1.8560	0.0264
	40			18.57	8.91			3.07×10^{-4}	2.8188			
6. Paraaphentidine	20	−23.58 1167.25	9.70	−1.67	10.19			22.87×10^{-6}	4.8728			
	30			−1.22	10.07	1.21	8.02	22.49×10^{-6}	4.6665	−52.6800	4.9975	−0.0851
	40			−1.68	10.22			22.87×10^{-6}	4.6800			
7. Ortho chloro-	20			6.19	10.22			17.99×10^{-5}	4.9271			
para nitroaniline	30	−24.52 1447.51	12.03	6.88	10.00	1.49	8.07	17.86×10^{-5}	4.5531	28.2500	−1.4440	0.0196
	40			6.18	10.09			18.05×10^{-5}	4.4526			
8. Para bromo-	20			−20.58	10.01			9.25×10^{-8}	4.5331			
nitrobenzene	30	−21.28 479.23	3.98	−20.64	10.24	0.47	8.47	9.44×10^{-8}	4.9906	33.5400	−1.9565	0.0280
	40			−20.58	10.42			9.21×10^{-8}	5.0511			

The dipole moments μ_j's of all the liquids were finally worked out from the slopes β's of hf conductivities σ_{ij}'s with w_j's and dimensionless parameters b's with the estimated τ_j at all the temperatures. All the μ_j's placed in Table 1 are found to be temperature dependent quantities. The coefficients a, b and c of μ_j–t curves of Figure 2, are, however, placed in Table 2, in order to compare with the reported μ's as well as theoretical μ_{theo}'s, obtained from bond angles and bond moments of substituent polar groups attached with the parent ones of Figure 3. The disagreement of the measured μ's with μ_{theo}'s as obtained from Figure 3, for these compounds establishes the fact that the inductive moments combined with the mesomeric moments of the substituent polar groups with the parent molecules is a function of temperature.

2. THEORETICAL FORMULATIONS

Under the hf electric field the dimensionless complex dielectric constant k^*_{ij} is:

$$k^*_{ij} = k'_{ij} - jk''_{ij} \tag{1}$$

where $k'_{ij} = \varepsilon'_{ij}/\varepsilon_0$ = real part of dielectric constant and $k''_{ij} = \varepsilon''_{ij}/\varepsilon_0$ = dielectric loss factor, respectively. ε'_{ij} and ε''_{ij} are real and imaginary parts of complex permittivity ε^*_{ij} having dimension of Farad $meter^{-1}$ ($F.m^{-1}$) and ε_0 = permittivity of free space = 8.854×10^{-12} $F.m^{-1}$. Hence Murphy–Morgan relation for the complex hf conductivity σ^*_{ij} of a solution of a polar–nonpolar liquid mixture of weight fraction w_j is:

$$\sigma^*_{ij} = \omega\varepsilon_0 k''_{ij} + j\omega\varepsilon_0 k'_{ij} \tag{2}$$

where $\sigma'_{ij}(= \omega\varepsilon_0 k''_{ij})$ and $\sigma''_{ij}(= \omega\varepsilon_0 k'_{ij})$ are the real and imaginary parts of complex conductivity and j is a complex number = $\sqrt{-1}$.

The hf conductivity σ_{ij} is however obtained from:

$$\sigma_{ij} = \omega\varepsilon_0\sqrt{k''^2_{ij} + k'^2_{ij}} \tag{3}$$

The imaginary part of hf conductivity σ''_{ij} is related to the real part of hf conductivity σ'_{ij} by

$$\sigma''_{ij} = \sigma_{\alpha ij} + (1/\omega\tau)\sigma'_{ij} \tag{4}$$

where $\sigma_{\alpha ij}$ is the constant conductivity at $w_j = 0$ and τ is the relaxation time of a polar unit = τ_j. Equation (4) on differentiation with respect to σ'_{ij} becomes.

$$(d\sigma''_{ij}/d\sigma'_{ij}) = (1/\omega\tau_j) \tag{5}$$

to yield τ_j of a polar solute. It is often better to use the ratio of the individual slopes of variations of σ''_{ij} and σ'_{ij} with w_j at $w_j \to 0$ to avoid the effect of polar–polar interactions in a liquid mixture to get τ_j from:

$$(d\sigma''_{ij}/dw_j)w_{j\to 0}/(d\sigma'_{ij}/dw_j)w_{j\to 0} = 1/\omega\tau_j$$

$$\text{or, } x/y = 1/\omega\tau_j \tag{6}$$

Again, it is observed experimentally that σ''_{ij} is nearly equal to σ_{ij} of equation (3) under hf alternating electric field, hence equation (4) becomes :

$$\sigma_{ij} = \sigma_{\alpha ij} + (1/\omega\tau_j)\sigma'_{ij}$$

$$\text{or } (d\sigma'_{ij}/dw_j) = \omega\tau_j\beta \tag{7}$$

where $\beta = (d\sigma_{ij}/dw_j)$ = the slope of σ_{ij}–w_j curve at $w_j \to 0$.

All the β's are however, presented in Table 1 for all the liquids. The real part of hf conductivity [9–12], σ'_{ij} at T K of a given solution of w_j is :

$$\sigma'_{ij} = \left(N\rho_{ij}\mu_j^2/27\varepsilon_0 k_B M_j T\right)(\omega^2\tau/1 + \omega^2\tau^2)(\varepsilon_0 k_{oij} + 2)(\varepsilon_0 k_{\alpha ij} + 2)w_j. \tag{8}$$

which on differentiation with respect to w_j and at $w_j \to 0$ yields :

$$(d\sigma'_{ij}/dw_j)_{wj\to 0} = \left(N\rho_i\mu_j^2/3\varepsilon_0 k_B T M_j\right)\left(\frac{\varepsilon_i + 2}{3}\right)^2(\omega^2\tau/1 + \omega^2\tau^2) \tag{9}$$

where N = Avogadro's Number, ρ_i = density of solvent, ε_i = dielectric permittivity of the solvent, M_j = molecular weight of solute and k_B = Boltzmann constant. All the symbols stated above are expressed in SI units. From equations (7) and (9) one gets μ_j in Coulomb meter under hf electric field as

$$\mu_j = \left[\frac{27\varepsilon_0 k_B T M_j}{N\rho_i(\varepsilon_i + 2)^2}\frac{\beta}{\omega b}\right]^{1/2} \tag{10}$$

in terms of a dimensionless parameter 'b'

$$b = 1/\left(1 + \omega^2\tau_j^2\right) \tag{11}$$

with the measured τ_j of the liquid.

All the measured τ_j's in terms of β's and b's of equations (10) and (11) are, however, placed in Table 1 and compared with the reported μ's and μ_{theo}'s the latter ones are obtained from bond angles and bond moments of the substituted groups of the molecules as shown in Figure 3.

3. RESULTS AND DISCUSSIONS

The relaxation time τ_j's of the para polar liquids as reported in Table 1 in dioxane and benzene respectively were estimated from the ratio of the individual slopes of both the imaginary σ''_{ij} and real σ'_{ij} parts of high frequency conductivity σ^*_{ij} with weight fraction w_j of polar solutes at different experimental temperatures in °C under 3 cm. wavelength electric field. τ_js of these liquids could not be obtained directly from the slope of equation (5) of σ''_{ij} with σ'_{ij} because of the non-linear character [8]. Thus the ratio of the individual slopes of σ''_{ij}–w_j and σ'_{ij}–w_j curves at $w_j \to 0$ was used to get τ's of these para polar liquids

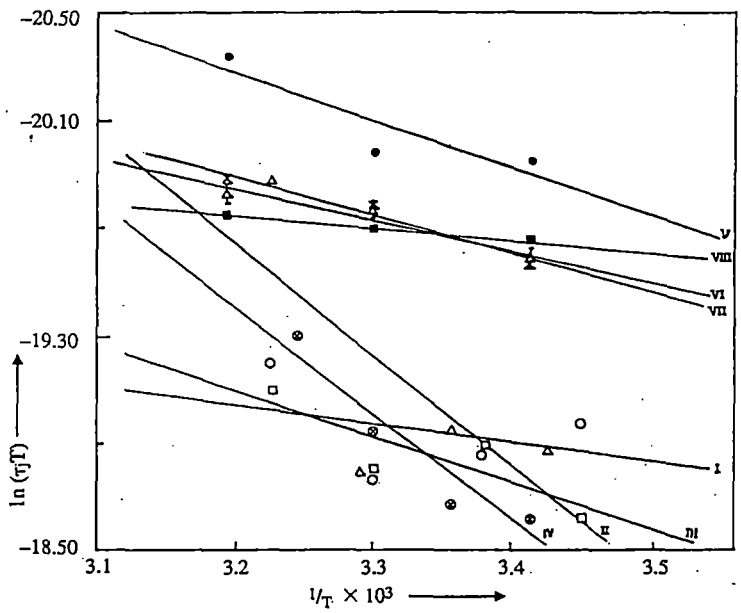

Figure 1. Straight line plots of ln (τ_jT) against 1/T. (I) parahydroxypropiophenone (—○—), (II) parachloropropiophenone (— △ —), (III) paraacetamidobenzaldehyde (— □ —), (IV) parabenzyloxybenzaldehyde (— ⊗ —), (V) paraanisidine (—●—) (VI) paraphenitidine (— ⊼ —), (VII) orthochloroparanitroaniline (—x—) and (VIII) parabromonitrobenzene (— ■ —)

from equation (6) in order to minimize the effects of dipole–dipole interactions, macroscopic viscosity, internal field etc.

The estimated ratio of the individual slopes of σ''_{ij} and σ'_{ij} curves with w_i's together with estimated and reported τ's are placed in the 3rd, 4th and 5th columns of Table 1. The τ_j's thus obtained agree well with the reported τ_j's where such are available [6,7] based on Gopalakrishna's method [13]. As observed in Table 1, the τ_j's of molecules having phenone and benzaldehyde groups are higher in comparison to other di- and tri-substituted para polar molecules. This is probably due to larger sizes of the rotating units. It is also interesting to note that variation of τ_j of such molecules as presented in Table 1 are irregular in disagreement with the Debye model of relaxation as observed elsewhere [4]. This may be explained by the fact that stretching of bond angles and bond moments of polar groups with temperature and the distribution of bond moments around the parent molecules leads to either symmetric or asymmetric shape of the molecules. The rest of the molecules show the lower values of τ decreasing with increase of temperature in agreement with the Debye relaxation in spite of the fact that they are nonspherical.

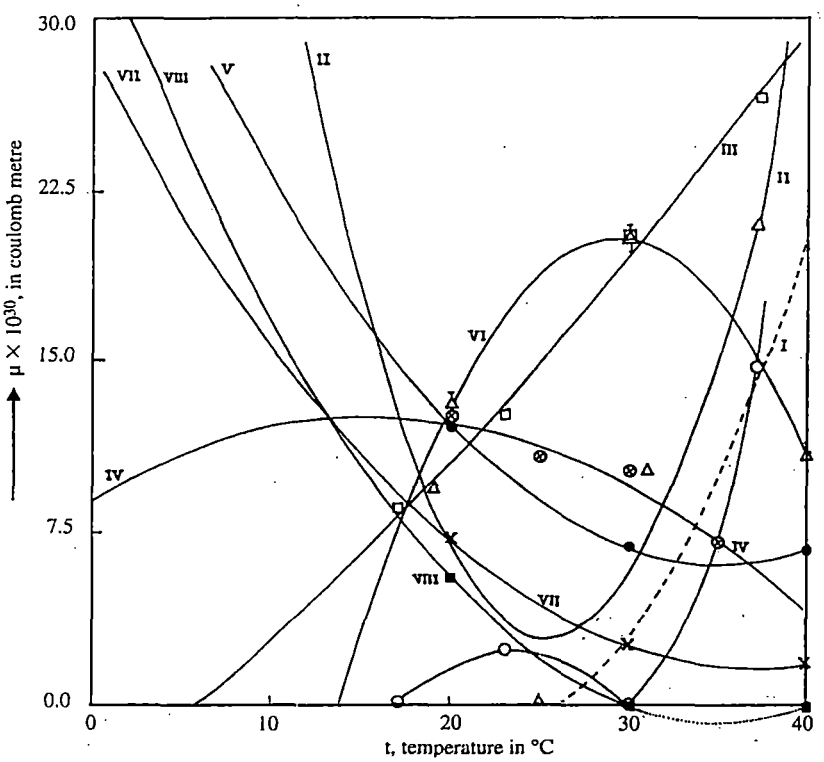

Figure 2. Variation of dipolemoments $\mu_i \times 10^{30}$ in Coulomb metre against t in °C, (I) parahydroxypropiophenone (—○—), (II) parachloropropiophenone (— △ —), (III) paraaceta-midobenzaldehyde (— □ —), (IV) parabenzyloxybenzaldehyde (— ⊗ —), (V) paraanisidine (—●), (VI) paraphenitidine (— ⊻ —), (VII) orthochloroparanitroaniline (—x—) and (VIII) parabromonitrobenzene (— ■ —).

The process of rotation of the rotating dipoles requires an activation energy sufficient to overcome the energy barrier, between two equilibrium positions, one can write according to Eyring et al [10] with the known τ_j by:

$$\tau_j = (A/T)e^{\Delta F_\tau / RT} \qquad (\Delta F_\tau = \Delta H_\tau - T\Delta S_\tau)$$

$$\text{or, } \ln(\tau_j T) = \ln(Ae^{-\Delta S_\tau / R}) + (\Delta H_\tau / RT)$$

$$= \ln A' + (\Delta H_\tau / R).(1/T) \qquad (12)$$

Equation (12) is a straight line of ln $(\tau_j T)$ against $1/T$ having intercept and slope to measure the thermodynamic energy parameters like enthalpy of activation (ΔH_τ), entropy of activation (ΔS_τ) and free energy of activation (ΔF_τ) of dielectric relaxation process of the molecules. The intercepts and slopes of the least squares fitted ln $(\tau_j T)$ against $1/T$ curves as illustrated graphically in Figure 1, were accurately obtained and placed in the 3rd and 4th column of Table 2. The variation of ln $\tau_j T$ against $1/T$ are linear for almost all the liquids with the available experimental data. The enthalpy of activation ΔH_η due to viscous flow of the solvent was, however, estimated from the slope of the linear equation of ln $(\tau_j T)$ against $\ln\eta$ at different experimental temperatures. As evident from Table 2, the values of γ $(= \Delta H_\tau / \Delta H_\eta) > 0.50$ for all the liquids except parabromonitrobenzene exhibit the solvent environment around the solute molecules which behave as solid phase rotators. The low value of γ, on the other hand, for p-bromonitrobenzene may indicate the weak molecular interaction of such dipole with benzene. The values of ΔS_τ's for the system like p-hydroxypropiophenone, p-phenitidine and p-bromonitrobenzene are negative. This is due to the fact that activated states are more ordered than the normal states unlike other molecules. The high values of ΔS_τ and ΔH_τ of p-chloropropiophenone and p-benzyloxybenzaldehyde indicate the activated states are not stable probably due to internal resistance suffered by larger dipole rotations. The rest of the molecules possess ΔH_τ of nearly the same magnitude. The ΔF_τ's between the activated and unactivated states of all the systems are, however, the same as the activation that is accomplished by the rupture of bonds of dipolar groups in the same degree of freedom [6,7]. Unlike the Kalman factor $\tau_j T/\eta^\gamma$ at different temperatures the Debye factor $\tau_j T/\eta$ is almost constant signifying the applicability of Debye model of relaxation behaviour for such para liquids [14]. The μ_j's from equation (10) of all the p-liquids were obtained from slopes β's of σ_{ij}–w_j curves and dimensionless parameters b's of equation (11) involved with measured τ_j's of equation (6). The slopes and intercepts of σ_{ij} against w_j as presented in Table 1 were obtained by careful regression technique and are found to be almost constant ($\sim 10^{-12}\ \Omega^{-1}\ m^{-1}$) at all the experimental temperatures under 3 cm. wavelength electric field perhaps for their same polarity. Thus σ'_{ij}, σ''_{ij} and σ_{ij} with w_j's could not be shown graphically. Parahydroxypropiophenone (curve I) and p-acetamidobenzaldehyde (curve III) showed the monotonic increase of μ_j with temperature (Figure 2) for their increasing molecular asymmetry at higher temperatures. The μ_j–t curves of p-benzyloxybenzaldehyde (curve IV) and p-phenitidine (curve VI) are convex in nature [15] showing zero values at lower and higher temperatures unlike the other four assuming minimum values at different temperatures as seen in Figure 2. The least squares fitted μ_j–t curve for p-bromonitrobenzene which showed 5.59×10^{-30} C.m at 20°C but zero values of μ_j at 30°C and 40°C for its strong symmetry attained at those temperatures was, however, obtained. Like curves II, V and VII of other p-compounds it (curve VIII) also showed minimum having-ve μ_j between 30°C to 40°C, shown by dotted line to satisfy the continuous curve. The usual variation of μ_j against t°C for p-hydroxypropiophenone (curve I) is shown by least squares fitted dotted line together with the solid line drawn through the estimated

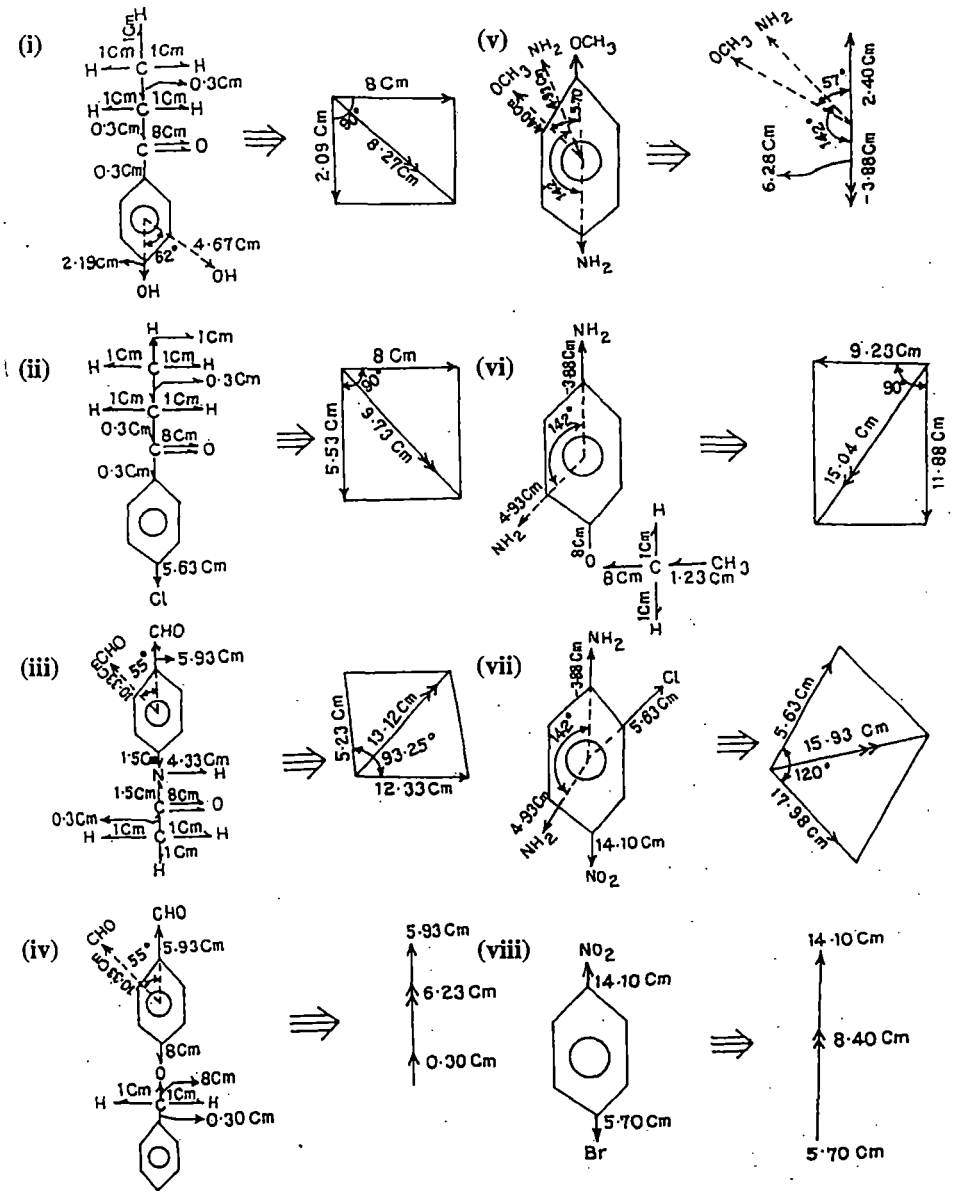

Figure 3. Conformational structures from availible bond moments and bond angles of para compounds : (i) para-hydroxypropiophenone (ii) para-chloropropiophenone (iii) para-acetamidobenzaldehyde (iv) para-benzyloxybenzaldehyde (v) para-anisidine (vi) para-phenitidine (vii) ortho-chloroparanitroaniline and (viii) para-bromonitrobenzene.

μ_j's. The above nature of μ_j–t curves are explained by the rupture of solute–solvent (monomer) and solute–solute (dimer) associations due to stretching of bond angles and bond moments of substituted polar groups at different temperatures.

The theoretical dipole moments μ_{theo}'s of all the p-liquids were also calculated from the vector addition of the available bond moments 4.67, 10.33, 4.40, 4.40, 1.00, 8.00, 5.63, 1.50, 14.10 and 5.70 multiples of 10^{-30} Coulomb metre (C.m) for C → OH, C → CHO, C → OCH_3 and C → NH_2 bonds making angles 62°, 55°, 57°, 142° and 0° for the rest C → H, C ⇉ O, C → Cl, C → N, C → NO_2 and C → Br bonds respectively with C atom of the parent molecules which are assumed to be planar structures, as shown in Figure 3. The μ_{theo}'s thus obtained are finally placed in the 12th column of Table 1. The slight disagreement between measured μ_j's and μ_{theo}'s reveals the presence of inductive and mesomeric moments of the substituent polar groups due to their aromaticity. In p-acetamidobenzaldehyde, p-phenetidine, orthochloroparanitroaniline and p-bromonitrobenzene, the μ_{theo}'s are larger while for others μ_{theo}'s are smaller than the measured values. This fact at once predicts that the substituent polar groups in former molecules push the electrons towards the electro-negative atoms and thereby inductive effect is less than in latter system where they pull the electrons. The electromeric effect is also prominent in the system containing C ⇉ O groups.

4. CONCLUSION

A very convenient method to evaluate τ_j's from the ratio of the individual slopes of σ''_{ij}–w_j and σ'_{ij}–w_j curves at $w_j \to 0$ and the corresponding μ_j's in SI units of several chain like para liquids at different experimental temperatures is suggested in order to avoid polar–polar interactions. The slopes of σ''_{ij}–σ'_{ij} curves are very often not linear in almost all liquids and hence could not be used to obtain τ_j's. Both τ_j's and hence μ_j's within the accuracy of 10% and 5% are now reliable. Para-hydroxypropiophenone, and p-chloropropiophenone show zero values of μ at certain temperatures owing to their symmetry gained at that temperatures. The variation of μ with temperature in °C is not a new concept, but for p-liquids the convex, concave or gradual increase occur probably due to association or dissociation of solute–solute and solute–solvent molecular associations and stretching, of bond moments of the substituent polar groups at different temperatures. Different thermodynamic energy parameters could, therefore, be estimated from the stand point of Eyring's rate theory [15,16] to infer the molecular dynamics of the nonspherical liquids. μ_{theo}'s of the molecules could, however, be found out from the available bond angles and bond moments of the substituent polar groups attached to the parent molecules. They are usually found to differ from the measured μ_j's indicating the existence of mesomeric and inductive effects in polar liquids due to their aromaticity.

References

[1] G S Kastha, J Dutta, J Bhattacharyya and S B Roy, Ind J Phys **43 B** (1965) 14.
[2] C R Acharyya, A K Chatterjee, P K. Sanyal and S Acharyya, Ind. J. Pure & Appl. Phys. **24** (1986) 234.
[3] U. Saha and S Acharyya Ind. J. Pure & Appl. Phys **31** (1993) 181.
[4] S Acharyya, A K Chatterjee, P Acharyya and I L Saha, Ind. J Phys. **56** (1982) 291.
[5] J P Shukla, S I Ahmed, D D Shukla and M C Saxena, J Phys. Chem **72** (1968) 1013.
[6] R L Dhar, A Mathur, J P Shukla and M C Saxena, Ind. J. Pure. & Appl Phys. **11** (1973) 568.

[7] S K S Somevanshi, S B I Misra and N K Mehrotra, Ind. J Pure and Appl Phys. **16** (1978) 57.
[8] M B R Murthy, R L Patil and D K Desh pande, Ind. J. Phys. **63 B** (1989) 491.
[9] R C Basak, A Karmakar, S K Sit and S Acharyya, Ind. J Pure & Appl. Phys. **37** (1999) 224.
[10] H Eyring, S Glasstone, and K J Laidler, The theory of rate process (Mc Graw Hill NY) 1941.
[11] F J Murphy and S O Morgan, Bell. Syst. Tech. J **18** (1939) 502.
[12] C P Smyth, Dielectric behaviour and structure (Mc Graw Hill New York) 1955.
[13] K V Gopala krishna, Trans. Faraday Soc. **53** (1957) 767.
[14] K Dutta, S K Sit and S Acharyya, Ind. J Pure & Appl Phys. Communicated 1999.
[15] H Eyring, J Chem Phys. **4** (1936) 283.
[16] W Kauzmann, Rev. mod. Phys. **14** (1942) 12.

INFORMATION FOR AUTHORS

Both review papers and original work will be published. Those intending to write a review are invited to get in touch with the Editor for a preliminary discussion of scope. There is no limitation on length, but it would be convenient if some idea could be given of the probable length of the contribution in pages of camera-ready copy.

Submission of papers
Authors are requested to submit three copies of their manuscript to:
Professor Josef Barthel, Institut für Physikalische und Theoretische Chemie, Universitat Regensburg, D-93040 Regensburg, Germany. Fax +49.941.943.4532.

Submission of an article is understood to imply that the article is original and unpublished and is not being considered for publication elsewhere. Upon acceptance of an article by the journal, author(s) will be asked to transfer the copyright of the article to the publisher. This transfer will ensure the widest dissemination of information.

Reprints
Fifty reprints will be supplied free of charge. Additional reprints can be ordered at prices shown on the reprint order form which will be sent after the Editor's acknowledgement of acceptance of the paper.

Instructions for the preparation of a camera-ready paper

The points mentioned below give a summary of the absolute minimum technical requirements to which your contribution should adhere. All text material and illustrations will be photographically reduced by 20–25%.

1. Format
21 cm x 16 cm (8.25" 8 x 6.25"): text dimensions (length and width) *for opening* page.
23 cm x 16 cm (9.00" 8 x 6.25"): text dimensions (length and width) for all subsequent pages.
Deviations from this text area are not acceptable.
Spacing: 1.0 (single line) spacing

2. Typefonts
Laser/jet printers:
Recommended fonts: 12 point 'Times Roman' (use this font wherever possible), 'Helvetica', 'Bookman Light', and 'New Century Schoolbook'.
Text length: equivalent to approximately 48 single-spaced lines.
Electric typewriter/daisywheel printer:
Recommended fonts: 10 pitch 'Courier', 12 pitch 'Letter Gothic'/'Prestige Elite'. Text width: can be translated into 63 or 76 characters per line using 10 and 12 pitch typing fonts, respectively.
Text length: equivalent to approximately 50 single-spaced lines.

Do not use small font sizes for footnotes. (Remember text reduction to 75–80%.)

3. Printout
Printout must be an original copy. Photocopies are not acceptable.
Paper: print onto either Elsevier camera-ready sheets, A4, or US Letter Paper format. If Elsevier's paper is not used, the paper must be plain white, high quality, and smooth. Print on only one side of the sheet.
Positioning of printout on paper: not critical provided approximately 3 cm (1") of space is left free above the first text line.
Quality of printout: must have uniform contrast over whole text page, be dark and sharp. Printout which is streaked, has lighting variations at the margins, is grey, fuzzy, broken or flecked is not acceptable.
Mathematical symbols and equations must be typed or drawn accurately; *handwritten characters are unacceptable.*

4. Illustrations
Illustrations must be original drawings or sharp black and white prints. Attach them on/near the page where they are first described with a few spots of suitable glue. Do not use transparent adhesive tape. All notations and details must be legible after reduction. Photocopies, colour plates, screened photographs, and slides are not generally acceptable.

5. Language
Use good, explicit English. Consult a native speaker and/or dictionary where necessary. Authors in Japan please note: Upon request, Elsevier Science Japan will provide authors with a list of people who can check and improve the English of their paper *(before submission).* Please contact our Tokyo office: Elsevier Science Japan, 1-9-15 Higashi-Azabu, Minato-ku, Tokyo 106-0044; Tel. (03)-5561-5033; Fax (03)-5561-5047.

6. Layout
The tables and illustrations must appear in the appropriate positions in the text with about 1 cm of space above and below. If illustrations need to be reduced they must fit in the available space left in the text. Tables and figures with legends must be incorporated in the text at the appropriate places; it is not acceptable to collect these on separate pages for later placement. The reference list should run on from the end of the text.

7. Miscellaneous
Text must be proof-read and checked for completeness. Label pages with your name and numerical order on their reverse side.

Indian Journal of Pure & Applied Physics
Vol. 38, August 2000, pp. 574-588

Structural and associational aspects of dielectropolar straight chain alcohols from relaxation phenomena

N Ghosh, A Karmakar, S K Sit & S Acharyya

Department of Physics, Raiganj College (University College), PO Raiganj, Dist Uttar Dinajpur, 733 134 (West Bengal)

Received 15 November 1999; revised 27 March 2000; accepted 6 June 2000

The structural and associational aspects of some straight chain aliphatic alcohols are inferred from their static dipole moments μ_s's and high frequency (hf) dipole moments μ_j's in terms of relaxation times τ_j's under effective dispersive region of nearly 24 GHz electric field. τ_j's are estimated from the slope of the linear variation of imaginary part σ''_{ij} with real part σ'_{ij} of hf complex conductivity σ^*_{ij} for different weight fractions w_j in order to compare with those obtained from the ratio of the individual slopes of σ''_{ij} and σ'_{ij} with w_j's of solutes. The linear coefficients of the static experimental parameter X_{ij} with w_j are used to obtain μ_s. The slopes β's of σ_{ij} with w_j's are employed to get hf μ_j in terms of τ_j's obtained by two methods only to see how far they agree with μ_1 and μ_2 from double relaxation method (Sit & Acharyya, 1996 and Sit *et al.*, 1997). It is observed that –OH bond of alcohols about ≡ C–O– bond rotates under GHz electric field. The slight disagreement of theoretical dipole moments μ_{theo}'s from available bond angles and bond moments with μ_j's and μ_s's suggest the strong hydrogen bonding in them, in addition to mesomeric and inductive moments of the substituent polar groups attached to the parent molecule.

1 Introduction

The relaxation phenomenon of a dielectropolar liquid in a solvent has attracted the attention of a large number of workers[1-3] as it is a very sensitive and useful tool to ascertain the shape, size and structure of a polar molecule. The technique provides one with much information about the stability[4] of the system undergoing relaxation phenomena. It also offers valuable insight into the solute-solute i.e. dimer and solute-solvent i.e.monomer formations[4]. Structural and associational aspects of a polar liquid in a nonpolar solvent can, however, be gained by measured static dipole moment μ_s and high frequency (hf) dipole moment μ_j in terms of relaxation time τ_j and slope β of hf conductivity σ_{ij} with weight fraction w_j.

Alcohols behaving like almost polymers have α, β and γ etc. dispersion regions. The strong dipole of –OH group rotates about ≡ C–O– bond without disturbing CH_3 or CH_2 groups and thus they have possibility to exhibit intramolecular as well as intermolecular rotations. Sit and Acharyya[5] and Sit *et al.*[6] studied the straight long chain alcohols like 1-butanol, 1-hexanol, 1-heptanol, 1-decanol in *n*-heptane[7], ethanol and methanol in benzene[8] (9.84GHz) and 2-methyl-3-heptanol, 3-methyl-3-heptanol, 4-methyl-3 heptanol, 5-methyl-3-heptanol, 4-octanol and 2-octanol, in *n*-heptane[9] at 25°C to observe that all the alcohols except methanol showed the double relaxation times τ_1 and τ_2 at all the frequencies in GHz range. The alcohols were again expected to exhibit the triple relaxation phenomena[7] for different frequencies of electric field in GHz range. Such long chain liquids under investigation have wide applications in the fields of biological research, medicine and industry. Moreover, the study of alcohols in terms of modern internationally accepted units and symbols appears to be superior for the unified, coherent and rationalized nature of the SI unit used.

The μ_s of all the associated dielectropolar molecules under static electric field was derived from static experimental parameter X_{ij}. X_{ij} is again involved with the dimensionless dielectric constants k_{0ij} and $k_{\infty ij}$ of Table 1, from the measured relaxation permittivities static ε_{0ij} and hf $\varepsilon_{\infty ij}$ of dimensions Farad metre^{-1} (F.m.$^{-1}$) based on Debye model[10]. The linear coefficients of the expected nonlinear experimental X_{ij} curves against w_j graphically shown in Fig. 1, of alcohols were conveniently used to estimate μ_s at a given temperature.

The τ_j of all the alcohols were, however, estimated from the slope of linear variation of imaginary σ''_{ij} against real σ'_{ij} parts[11] of hf complex conductivity σ^*_{ij} for different w_j's as seen in Fig. 2. The hf σ''_{ij} did not vary linearly with hf σ'_{ij} at higher or even lower concen-

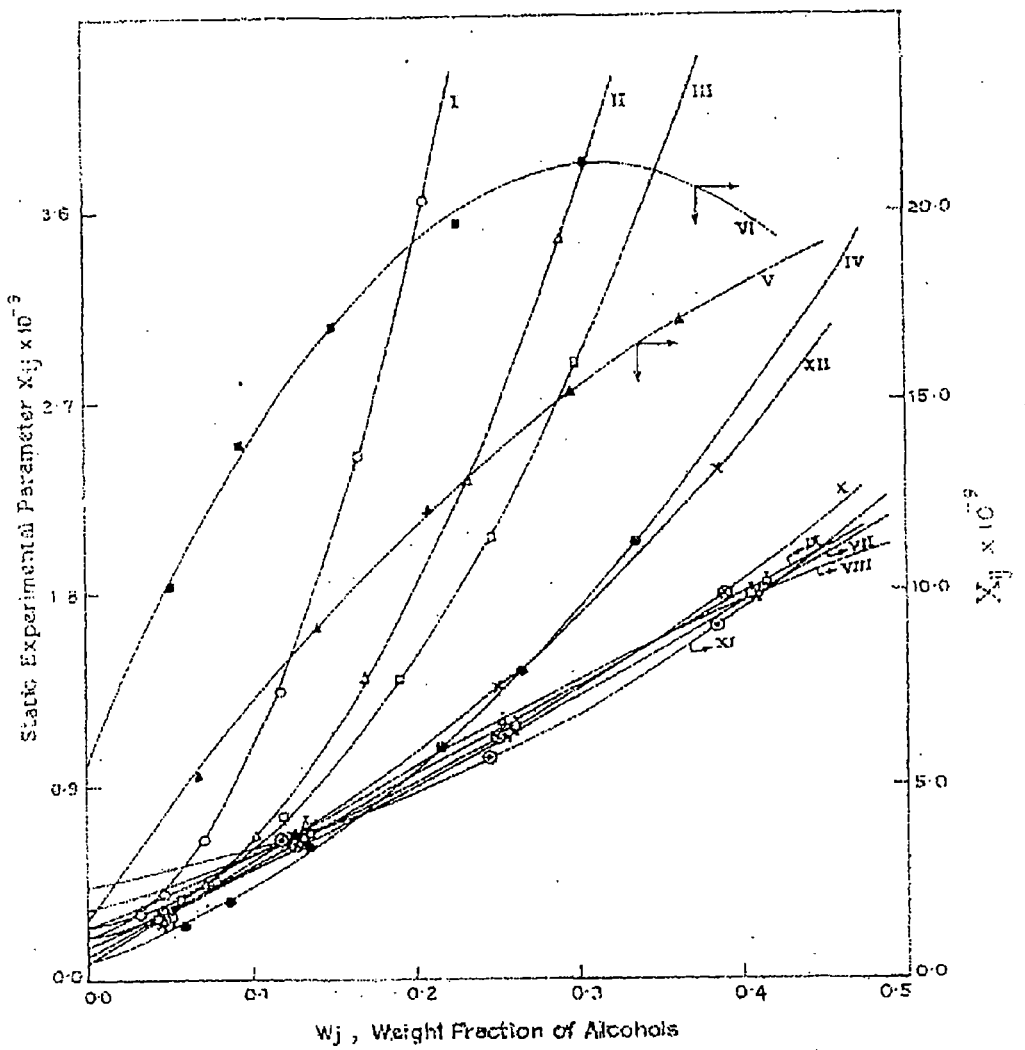

Fig. 1 — Variation of static experimental parameter ($X_{ij} \times 10^{-9}$) against weight fraction w_j of solute at 25°C under nearly 24 GHz electric field [ethanol and methanol at 9.84 GHz]

System – I 1-butanol (— O — O —);

System – II 1-hexanol (—Δ—Δ—);

System – III 1-heptanol (—□—□—);

System – IV 1-decanol (— ●—●—);

System – V ethanol (—▲—▲—);

System – VI methanol (—■—■—);

System – VII 2-methyl – 3 heptanol (—Φ—Φ—);

System – VIII 3-methyl –3 heptanol (—Ⱶ—Ⱶ—);

System – IX 4-methyl – 3 heptanol (—▯—▯—);

System – X 5-methyl – 3 heptanol (—⊗ — ⊗ —);

System – XI 4-Octanol (—Θ —Θ—);

System – XII 2-Octanol (— x — x —)

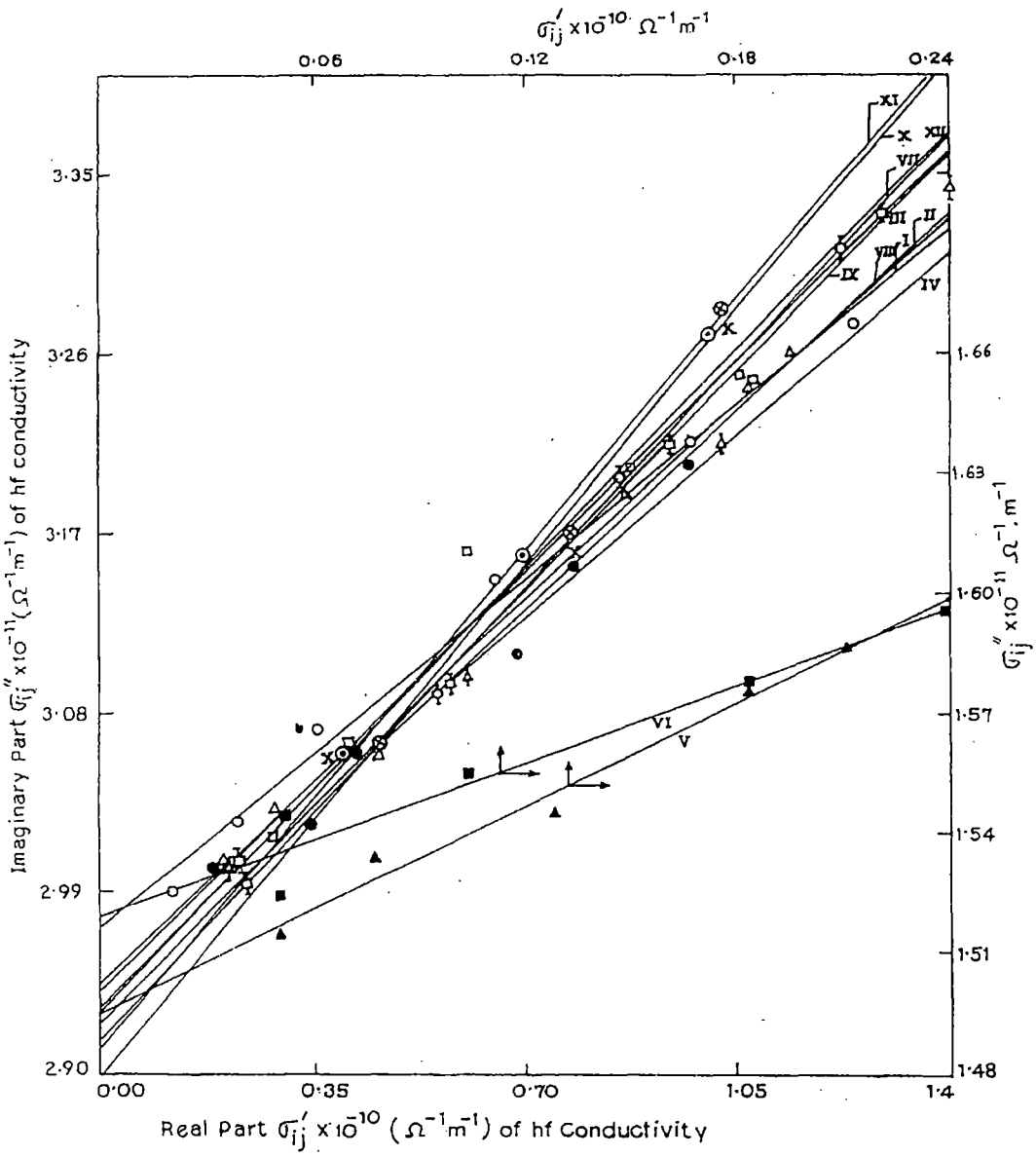

Fig. 2 — Variation of imaginary part of conductivity $\sigma''_{ij} \times 10^{-11}$ in $\Omega^{-1}\ m^{-1}$ against real part of conductivity $\sigma'_{ij} \times 10^{-10}$ in $\Omega^{-1}\ m^{-1}$

System – I 1-butanol (— O — O —);

System – II 1-hexanol (—Δ—Δ—);

System – III 1-heptanol (—□—□—);

System – IV 1-decanol (— ●—●—);

System – V ethanol (—▲—▲—);

System – VI methanol (—■—■—);

System – VII 2-methyl – 3 heptanol (—Φ—Φ—);

System – VIII 3-methyl –3 heptanol (—Ⱶ—Ⱶ—);

System – IX 4-methyl – 3 heptanol (—Ⱶ—Ⱶ—);

System – X 5-methyl – 3 heptanol (—⊗ — ⊗ —);

System – XI 4-Octanol (—Θ —Θ—);

System – XII 2-Octanol (— x — x —)

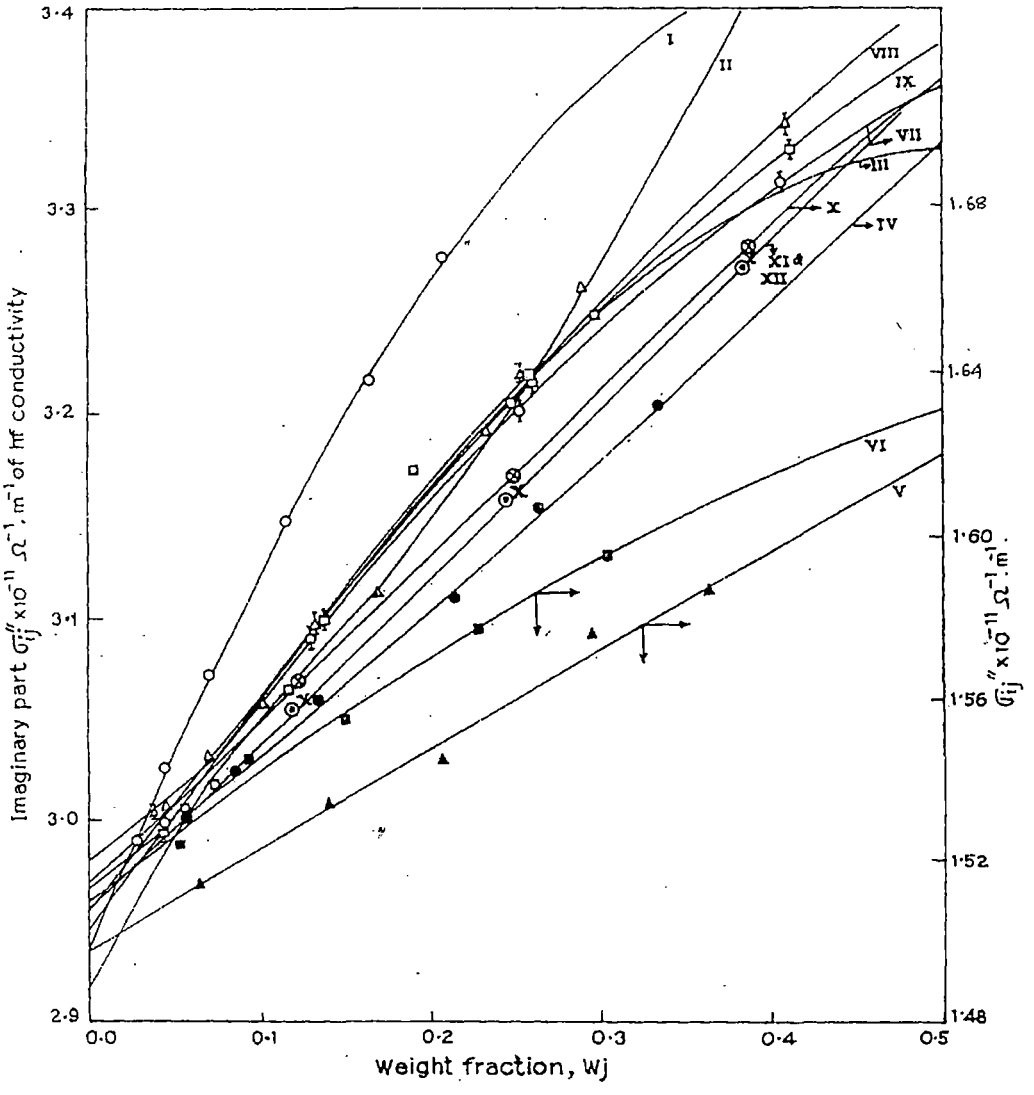

Fig. 3 — Plot of imaginary part of conductivity $\sigma''_{ij} \times 10^{-11}$ in Ω^{-1} m^{-1} against weight fraction w_j of solute at 25°C under nearly 24 GHz electric field. [ethanol and methanol at 9.84 GHz.]

System – I 1-butanol (— O — O —);

System – II 1-hexanol (—Δ—Δ—);

System – III 1-heptanol (—□—□—);

System – IV 1-decanol (— ● —● —);

System – V ethanol (—▲—▲—);

System – VI methanol (—■—■—);

System – VII 2-methyl – 3 heptanol (—Φ—Φ —);

System – VIII 3-methyl –3 heptanol (—Ⱥ —Ⱥ —);

System – IX 4-methyl – 3 heptanol (—I—I—);

System – X 5-methyl – 3 heptanol (—⊗ — ⊗ —);

System – XI 4-Octanol (—Θ —Θ—);

System – XII 2-Octanol (— x — x —)

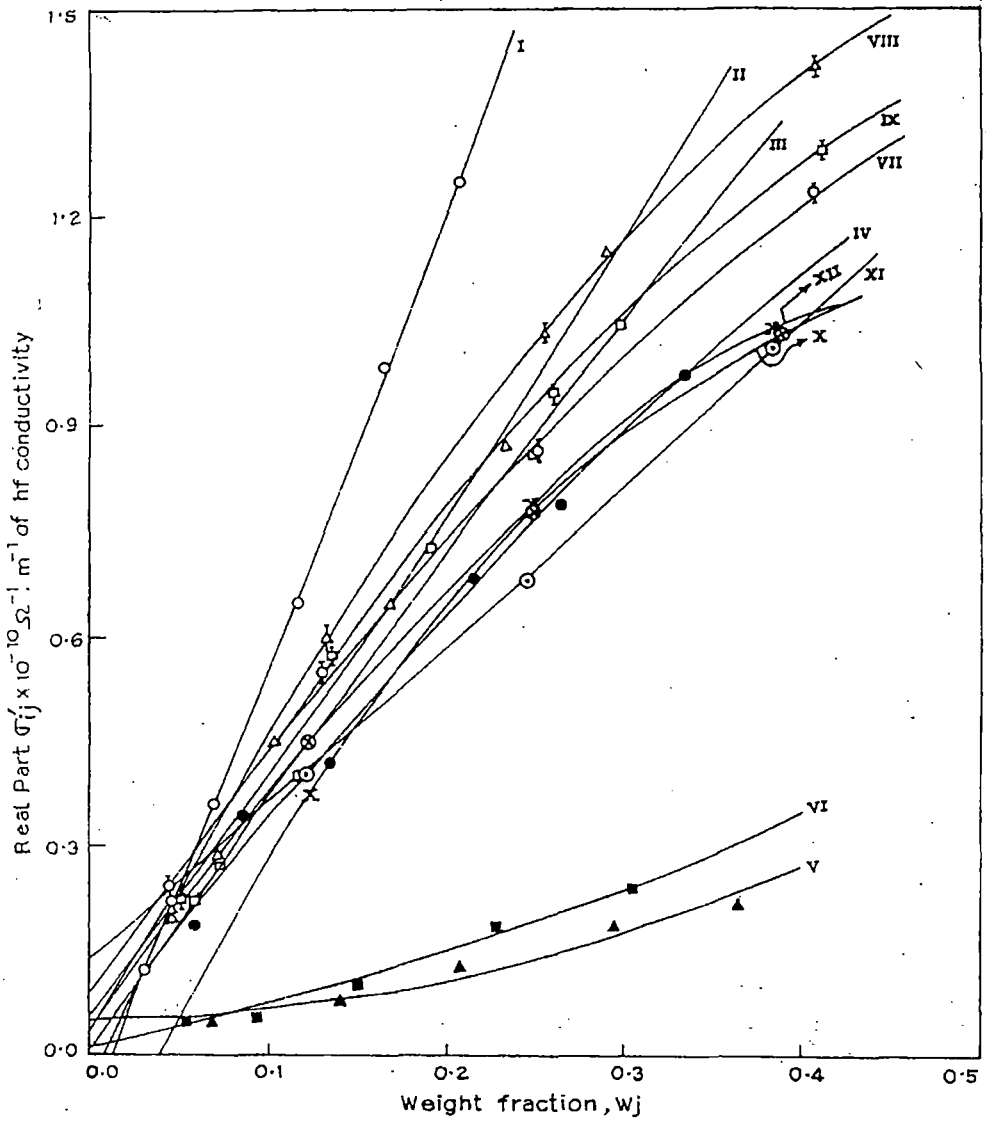

Fig. 4 — Plot of real part of conductivity $\sigma'_{ij} \times 10^{-10}$ in Ω^{-1} m^{-1} against weight fraction w_j of solute at 25°C under nearly 24 GHz electric field [ethanol and methanol at 9.84 GHz]

System – I 1-butanol (— O — O —);

System – II 1-hexanol (—Δ—Δ—);

System – III 1-heptanol (—□—□—);

System – IV 1-decanol (— ●—●—);

System – V ethanol (—▲—▲—);

System – VI methanol (—■—■—);

System – VII 2-methyl – 3 heptanol (—Φ—Φ—);

System – VIII 3-methyl –3 heptanol (—Ⱥ—Ⱥ—);

System – IX 4-methyl – 3 heptanol (—I—I—);

System – X 5-methyl – 3 heptanol (—⊗ — ⊗ —);

System – XI 4-Octanol (—Θ —Θ—);

System – XII 2-Octanol (— x — x —)

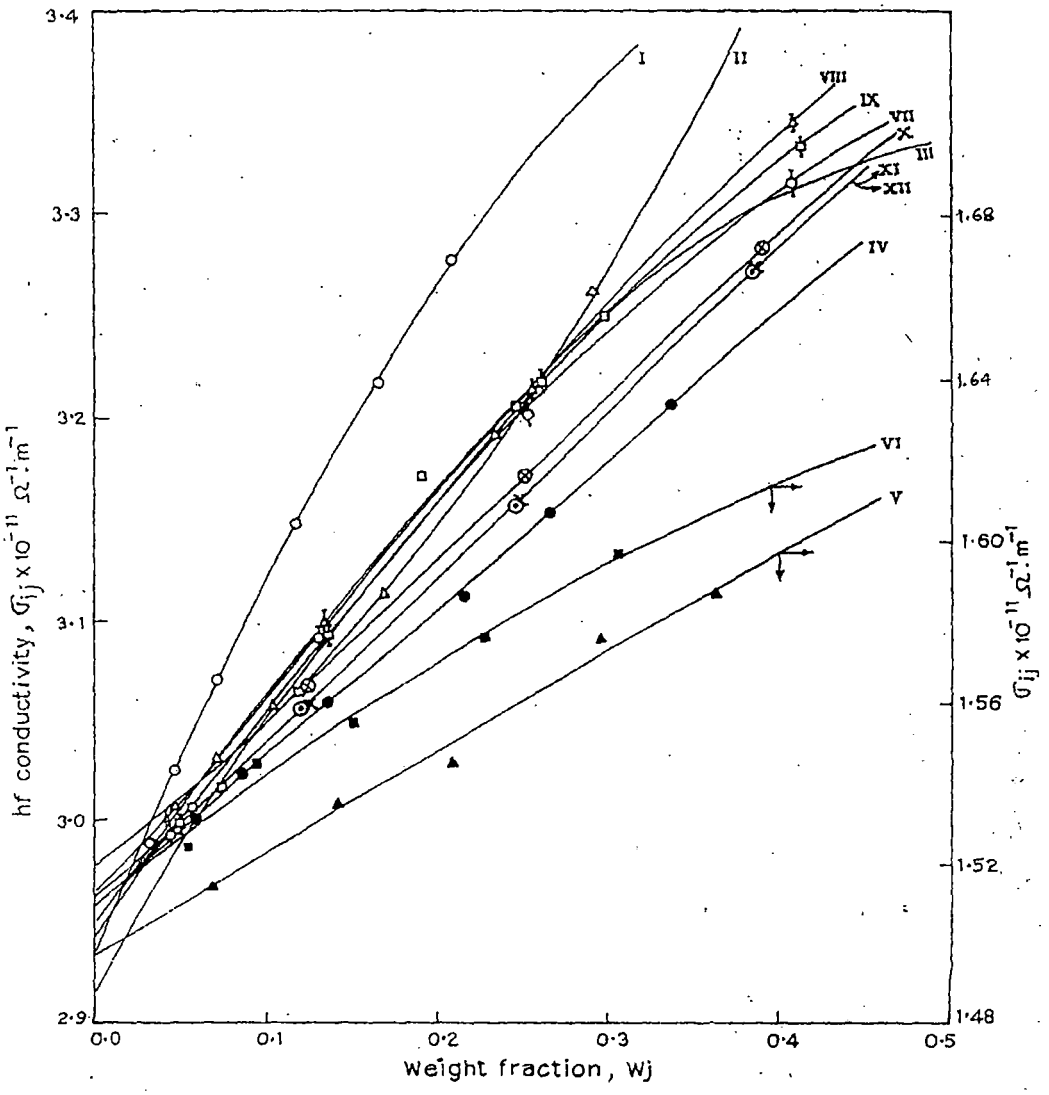

Fig. 5 — Variation of total hf conductivity $\sigma_{ij} \times 10^{-11}$ in Ω^{-1} m^{-1} against weight fraction w_j of solute at 25°C under nearly 24 GHz electric field [ethanol and methanol at 9.84 GHz]

System – I 1-butanol (— O — O —);

System – II 1-hexanol (—Δ—Δ—);

System – III 1-heptanol (—□—□—);

System – IV 1-decanol (— ●—●—);

System – V ethanol (—▲—▲—);

System – VI methanol (—■—■—);

System – VII 2-methyl – 3 heptanol (—Φ—Φ—);

System – VIII 3-methyl –3 heptanol (—Ⱥ—Ⱥ—);

System – IX 4-methyl – 3 heptanol (—Ⱡ—Ⱡ—);

System – X 5-methyl – 3 heptanol (—⊗ — ⊗ —);

System – XI 4-Octanol (—Θ —Θ—);

System – XII 2-Octanol (— x — x —)

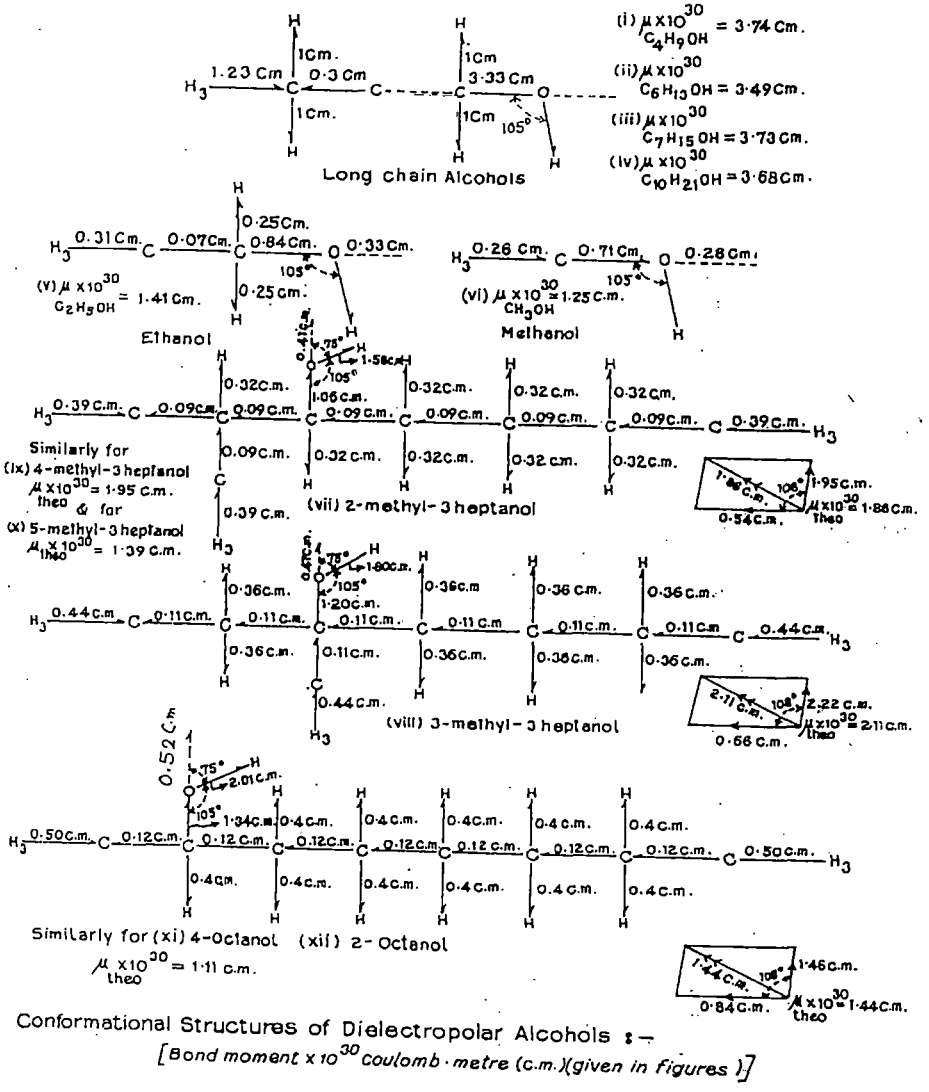

Fig. 6 — Conformational structures of dielectropolar alcohols (theoretical dipole moments μ_{theo} from bond angles and reduced bond moments)

trations[12]. It is therefore, better to use the ratio of slopes of individual variations of σ''_{ij} and σ'_{ij} both in Ω^{-1} m^{-1} with w_j's of Figs 3 and 4 to get the exact and accurate value of $d\sigma''_{ij}/d\sigma'_{ij}$ in the limit $w_j = 0$ to evaluate τ_j [13,14]. τ_j's thus obtained by both the methods are placed in Table 3 to see how far they are close in agreements. τ_j's of such dielectropolar molecules were, however, estimated at 1.233 cm for molecules like 1-butanol, 1-hexanol, 1-decanol, 2-methyl 3-heptanol, 3-methyl 3-heptanol, 4-methyl-3-heptanol, 5-methyl 3-heptanol, 4-octanol, 2-octanol and at 1.249 cm wavelength electric field for 1- heptanol at which measured ε''_{ij} of a given w_j of the solute when were graphically plotted against the electric field frequency "f" showed peak indicating the most effective dispersive region for such liquids.

The formulation to measure μ_j's of all the alcohols involves with the slopes β's of the expected σ_{ij}–w_j nonlinear curves of Fig. 5 and dimensionless parameter

Table 1 — Measured dielectric permittivities ε'_{ij}, ε''_{ij}, ε_{0ij}, $\varepsilon_{\infty ij}$ in farad metre^{-1} and dimensionless dielectric constants k'_{ij}, k''_{ij}, k_{0ij}, $k_{\infty ij}$ of some dielectropolar alcohols at 25°C of different weight fractions w_j

Systems with molecular weight M_j in kg	Weight Fraction w_j	ε'_{ij} in F.m^{-1}	ε''_{ij} in F.m^{-1}	ε_{0ij} in F.m^{-1}	$\varepsilon_{\infty ij}$ in F.m^{-1}	Dimensionless dielectric constants			
						$k'_{ij} \times 10^{-11}$	$k''_{ij} \times 10^{-9}$	$k_{0ij} \times 10^{-11}$	$k_{\infty ij} \times 10^{-11}$
(i)	0.0291	1.957	0.0079	1.971	1.928	2.2103	0.8922	2.2261	2.1775
1-butanol	0.0451	1.981	0.0147	2.000	1.945	2.2374	1.6603	2.2589	2.1967
$M_j = 0.074$	0.0697	2.011	0.0236	2.050	1.958	2.2713	2.6655	2.3153	2.2114
	0.1163	2.060	0.0425	2.175	1.978	2.3266	4.8001	2.4565	2.2340
	0.1652	2.105	0.0644	2.381	2.000	2.3774	7.2735	2.6892	2.2589
	0.2072	2.144	0.0818	2.621	2.020	2.4215	9.2388	2.9602	2.2814
(ii)	0.0458	1.968	0.0131	1.988	1.944	2.2227	1.4795	2.2453	2.1956
1-hexanol	0.0703	1.984	0.0190	2.015	1.952	2.2408	2.1459	2.2758	2.2046
$M_j = 0.102$	0.1028	2.001	0.0296	2.064	1.970	2.2600	3.3431	2.3311	2.2250
	0.1687	2.037	0.0425	2.196	1.989	2.3006	4.8001	2.4802	2.2464
	0.2335	2.088	0.0569	2.360	2.002	2.3582	6.4265	2.6655	2.2611
	0.2901	2.134	0.0748	2.580	2.018	2.4102	8.4481	2.9139	2.2792
(iii)	0.0564	1.968	0.0147	1.985	1.932	2.2227	1.6603	2.2419	2.1821
1-heptanol	0.0735	1.975	0.0182	2.008	1.945	2.2306	2.0556	2.2679	2.1967
$M_j = 0.116$	0.1175	2.007	0.0265	2.066	1.957	2.2668	2.9930	2.3334	2.2103
	0.1909	2.076	0.0482	2.195	1.989	2.3447	5.4439	2.4791	2.2464
	0.2465	2.097	0.0567	2.315	2.002	2.3684	6.4039	2.6146	2.2611
	0.2970	2.126	0.0693	2.464	2.008	2.4012	7.8270	2.7829	2.2679
(iv)	0.0572	1.965	0.0120	1.976	1.940	2.2193	1.3553	2.2317	2.1911
1-decanol	0.0857	1.979	0.0223	2.003	1.952	2.2351	2.5186	2.2622	2.2046
$M_j = 0.158$	0.1351	2.003	0.0273	2.050	1.964	2.2622	3.0833	2.3153	2.2182
	0.2140	2.036	0.0449	2.147	1.990	2.2995	5.0711	2.4249	2.2476
	0.2640	2.064	0.0513	2.220	2.008	2.3311	5.7940	2.5073	2.2679
	0.3353	2.097	0.0637	2.346	2.030	2.3684	7.1945	2.6496	2.2927
(v)	0.0664	2.450	0.0082	3.300	2.262	2.7671	0.9223	3.7271	2.5548
ethanol	0.1393	2.483	0.0124	4.300	2.190	2.8047	1.4023	4.8566	2.4734
$M_j = 0.046$	0.2077	2.500	0.0208	5.400	2.120	2.8236	2.3529	6.0989	2.3944
	0.2953	2.550	0.0297	7.000	2.062	2.8800	3.3600	7.9060	2.3289
	0.3638	2.567	0.0342	8.200	2.016	2.8988	3.8641	9.2613	2.2769
(vi)	0.0514	2.467	0.0082	4.800	2.214	2.7858	0.9284	5.4213	2.5006
methanol	0.0930	2.500	0.0083	6.500	2.155	2.8236	0.9408	7.3413	2.4339
$M_j = 0.032$	0.1495	2.517	0.0168	8.600	2.085	2.8423	1.8940	9.7131	2.3549
	0.2266	2.550	0.0298	11.400	2.016	2.8800	3.3601	12.8755	2.2769
	0.3049	2.583	0.0387	13.700	1.960	2.9177	4.3765	15.4732	2.2137
(vii)	0.0437	1.960	0.0156	1.971	1.930	2.2137	1.7619	2.2261	2.1798
2-methyl	0.1299	2.022	0.0361	2.059	1.966	2.2847	4.0772	2.3255	2.2205
3-heptanol	0.2522	2.095	0.0565	2.172	2.007	2.3661	6.3813	2.4531	2.2667
$M_j = 0.130$	0.4081	2.169	0.0809	2.330	2.054	2.4497	9.1371	2.6316	2.3198
(viii)	0.0450	1.965	0.0137	1.974	1.934	2.2193	1.5473	2.2295	2.1843
3-methyl	0.1334	2.028	0.0393	2.069	1.966	2.2905	4.4387	2.3368	2.2205
3-heptanol	0.2538	2.103	0.0674	2.180	2.004	2.3752	7.6124	2.4622	2.2634
$M_j = 0.130$	0.4085	2.188	0.0928	2.334	2.057	2.4712	10.4811	2.6361	2.3232
(ix)	0.0466	1.964	0.0146	1.976	1.936	2.2182	1.6490	2.2317	2.1866
4-methyl	0.1326	2.025	0.0375	2.065	1.969	2.2871	4.2354	2.3323	2.2238
3-heptanol	0.2590	2.104	0.0616	2.185	2.011	2.3763	6.9573	2.4678	2.2713
$M_j = 0.130$	0.4124	2.180	0.0849	2.352	2.065	2.4622	9.5889	2.6564	2.3323
(x)									
5-methyl	0.1228	2.008	0.0296	2.048	1.956	2.2679	3.3431	2.3131	2.2092
3-heptanol	0.2489	2.075	0.0511	2.168	2.004	2.3436	5.7714	2.4486	2.3634
$M_j = 0.130$	0.3898	2.148	0.0676	2.315	2.040	2.4260	7.6350	2.6146	2.3040
(xi)	0.1201	2.000	0.0265	2.040	1.948	2.2589	2.9930	2.3040	2.2001
4-octanol	0.2445	2.067	0.0449	2.148	1.997	2.3345	5.0711	2.4260	2.2555
$M_j = 0.130$	0.3838	2.140	0.0659	2.282	2.031	2.4170	7.4430	2.5764	2.2939
(xii)	0.1236	2.001	0.0245	2.049	1.954	2.2600	2.7671	2.3142	2.2069
2-octanol	0.2479	2.068	0.0513	2.195	1.996	2.3357	5.7940	2.4791	2.2543
$M_j = 0.130$	0.3844	2.141	0.0680	2.410	2.036	2.4181	7.6801	2.7219	2.2995

Table 2 — Coefficients a_0, a_1 and a_2 of static experimental parameter $X_{ij} = a_0 + a_1 w_j + a_2 w_j^2$ correlation coefficients (r), % of errors in getting X_{ij}, static or low frequency dipole-moments $\mu_s \times 10^{30}$ in Coulomb-metre, theoretical dipole-moments $\mu_{theo} \times 10^{30}$ in Coulomb-metre from reduced bond moments by μ_s/μ_{theo} and μ_1, μ_2 by double relaxation method

Systems with sl. no. & molecular weight M_j	Coefficients a_0, a_1 and a_2 in Eq. $X_{ij} \times 10^{-9} = a_0 + a_1 w_j + a_2 w_j^2$			Correlation coefficient (r)	% of error in fitting technique	$\mu_s \times 10^{30}$ in Coulomb-metre from Eq. (5)	Corrected $\mu_{theo} \times 10^{30}$ in Coulomb metre from bond angle & reduced bond moments	μ_1 and μ_2 in Coulomb metre from double relaxation method	
	a_0	a_1	a_2					$\mu_1 \times 10^{30}$ in Coulomb metre	$\mu_2 \times 10^{30}$ in Coulomb metre
(i) 1-butanol in *n*-heptane $M_j = 0.074$ kg	0.2047	1.0852	75.2840	0.9824	0.96	3.74	$4.97 \times 0.7525 = 3.74$	3.63	29.17
(ii) 1-hexanol in *n*-heptane $M_j = 0.102$ kg	0.1951	1.0710	34.8550	0.9896	0.57	3.49	$4.37 \times 0.7986 = 3.49$	3.43	21.20
(iii) 1-heptanol in *n*-heptane $M_j = 0.116$ kg	0.2553	0.8932	26.4890	0.9867	0.73	3.73	$4.07 \times 0.9165 = 3.73$	3.73	27.00
(iv) 1-decanol in *n*-heptane $M_j = 0.158$ kg.	0.0901	2.3826	10.1760	0.9924	0.42	3.68	$3.17 \times 1.1609 = 3.68$	3.83	17.24
(v) ethanol in benzene $M_j = 0.046$ kg	1.6141	59.1892	−44.9614	0.9919	0.49	1.41	$5.57 \times 0.2531 = 1.41$	1.70	490.73
(vi) methanol in benzene $M_j = 0.032$ kg.	5.6331	99.8090	−159.9120	0.9672	1.94	1.25	$5.87 \times 0.2129 = 1.25$	–	293.96
(vii) 2-methyl 3-heptanol in *n*-hepatane $M_j = 0.130$ kg.	0.1372	3.7778	0.5639	0.9997	0.02	1.86	$5.87 \times 0.3168 = 1.86$	3.83	16.00
(viii) 3-methyl 3-heptanol in *n*-heptane $M_j = 0.130$ kg.	0.0830	4.8577	−1.7495	0.9986	0.09	2.11	$5.87 \times 0.3594 = 2.11$	3.83	8.60
(ix) 4-methyl 3-heptanol in *n*-heptane $M_j = 0.130$ kg.	0.1032	4.1481	0.0885	0.9998	0.01	1.95	$5.87 \times 0.3322 = 1.95$	3.90	13.90
(x) 5-methyl 3-heptanol in *n*-heptane $M_j = 0.130$ kg.	0.3270	2.1113	4.1567	0.9972	0.22	1.39	$5.87 \times 0.2368 = 1.39$	3.37	9.50
(xi) 4-octanol in *n*-heptane $M_j = 0.130$ kg.	0.4402	1.1341	5.2073	0.9946	0.42	1.11	$3.60 \times 0.3083 = 1.11$	3.43	10.97
(xii) 2-octanol in *n*-heptane $M_j = 0.130$ kg.	0.2591	2.2977	8.3285	0.9955	0.35	1.45	$3.60 \times 0.4028 = 1.45$	3.43	16.00

Table 3 — Intercept (c) and slope (m) of $\sigma''_{ij} - \sigma'_{ij}$ equation (Fig. 2), correlation coefficient (r), percentage of error (%), relaxation time τ_j in psec Eq. (10), ratio of slopes of σ''_{ij} and σ'_{ij} with w_j (= x/y), relaxation time τ_j in psec from (Eq. 11), calculated relaxation time τ_j in psec from Gopalakrishana's method for some dielectropolar alcohols under nearly 24 GHz electric field (Q–Band Microwave) at 25 °C

System with sl. no. and molecular weight	Intercept & slope of σ''_{ij}–σ'_{ij} fitted Equation $c \times 10^{-11}$ m		Correlation coefficient (r)	% of error	Estimated relaxation time τ_j in psec from Eq. (10)	Ratio of the slopes of σ''_{ij} & σ'_{ij} with w_j $x/y = (d\,\sigma''_{ij}/dw_j)/(d\,\sigma'_{ij}/dw_j)$	Estimated relaxation time τ_j in psec from Eq (11)	Relaxation time τ_j in psec estimated from Gopalakrishna's method
(i) 1-butanol in *n*-heptane $M_j = 0.074$ kg.	2.9731	2.4816	0.9959	0.22	2.64	$\frac{2.0789 \times 10^{11}}{5.7404 \times 10^{10}} = 3.6215$	1.81	2.47
(ii) 1-hexanol in *n*-heptane $M_j = 0.102$ kg.	2.9457	2.7315	0.9959	0.22	2.40	$\frac{5.8541 \times 10^{10}}{3.2779 \times 10^{10}} = 1.7859$	3.66	2.25
(iii) 1-heptanol in *n*-heptane $M_j = 0.116$ kg.	2.9414	2.9898	0.9973	0.15	2.19	$\frac{1.5295 \times 10^{11}}{3.8161 \times 10^{10}} = 4.0080$	1.65	2.07
(iv) 1-decanol in *n*-heptane $M_j = 0.158$ kg.	2.9465	2.5881	0.9925	0.41	2.53	$\frac{6.8315 \times 10^{10}}{3.3881 \times 10^{10}} = 2.0163$	3.24	2.39
(v) ethanol in benzene $M_j = 0.046$ kg.	1.4952	4.2872	0.9880	0.72	3.77	$\frac{2.5827 \times 10^{10}}{5.6872 \times 10^{9}} = 4.5412$	3.56	3.62
(vi) methanol in benzene $M_j = 0.032$ kg.	1.5188	3.2088	0.9633	2.17	5.04	$\frac{3.4467 \times 10^{10}}{5.1439 \times 10^{9}} = 6.7005$	2.41	4.87
(vii) 2-methyl 3-heptanol in *n*-heptane $M_j = 0.130$ kg.	2.9162	3.2340	0.9994	0.04	2.02	$\frac{1.2112 \times 10^{11}}{3.6429 \times 10^{10}} = 3.3248$	1.97	1.86
(viii) 3-methyl 3-heptanol in *n*-heptane $M_j = 0.130$ kg.	2.9361	2.8021	0.9976	0.16	2.33	$\frac{1.1146 \times 10^{11}}{5.1067 \times 10^{10}} = 2.1826$	3.00	2.26
(ix) 4-methyl 3-heptanol in *n*-heptane $M_j = 0.130$ kg.	2.9254	3.0946	0.9988	0.08	2.11	$\frac{1.2125 \times 10^{11}}{4.3826 \times 10^{10}} = 2.7666$	2.36	1.95
(x) 5-methyl 3-heptanol in *n*-heptane $M_j = 0.130$ kg.	2.8973	3.6562	0.9949	0.40	1.79	$\frac{8.3993 \times 10^{10}}{3.7395 \times 10^{10}} = 2.2461$	2.91	1.63
(xi) 4-octanol in *n*-heptane $M_j = 0.130$ kg.	2.9129	3.5515	0.9999	0.01	1.84	$\frac{8.5252 \times 10^{10}}{2.1993 \times 10^{10}} = 3.8763$	1.69	1.68
(xii) 2-octanol in *n*-heptane $M_j = 0.130$ kg.	2.9320	3.1511	0.9875	0.97	2.08	$\frac{8.3278 \times 10^{10}}{5.3226 \times 10^{10}} = 1.5646$	4.18	1.93

Table 4 — Coefficients α, β, γ of hf σ_{ij} against w_j curves (Fig. 5) correlation coefficients (r) percentage of error, dimensionless parameter b using τ_j from Eq. (10) and (11), computed $\mu_j \times 10^{30}$ in Coulomb metre from Eqs (10) and (16) and Eqs (11) and (16) estimated $\mu_j \times 10^{30}$ in Coulomb metre from Gopalakrishna's method for some dielectropolar alcohols under nearly 24 GHz electric field (Q-Band micro wave) at 25 ° C

System with sl. no. & molecular weight	Coefficients of σ_{ij}-w_j fitted Equation			Correlation coefficient (r)	% of error	Dimensionless parameter using τ_j from Eq. (10) $b = 1/(1 + \omega^2\tau_j^2)$	Dimensionless parameter using τ_j from Eq. (11) $b = 1/(1 + \omega^2\tau_j^2)$	Computed $\mu_j \times 10^{30}$ in Coulomb metre		Estimated $\mu_j \times 10^{30}$ in Coulomb metre from Gopalakrishna's method
	$\alpha \times 10^{-11}$	$\beta \times 10^{-11}$	$\gamma \times 10^{-11}$					hf method of Eqs (10) &(16)	hf method of Eqs (11) &(16)	
(i) 1-butanol in *n*-heptane $M_j = 0.074$ kg.	2.9351	2.0769	–2.0776	0.9978	0.12	0.8601	0.9289	4.28	4.11	3.58
(ii) 1-hexanol in *n*-heptane $M_j = 0.102$ kg.	2.9807	0.5846	–1.3346	0.9961	0.21	0.8815	0.7618	2.63	2.83	3.35
(iii) 1-heptanol in *n*-heptane $M_j = 0.116$ kg.	2.9173	1.5312	–1.3817	0.9928	0.39	0.9016	0.9417	4.52	4.42	3.59
(iv) 1-decanol in *n*-heptane $M_j = 0.158$ kg.	2.9639	0.6848	0.1087	0.9995	0.03	0.8699	0.8032	3.57	3.71	3.55
(v) ethanol in benzene $M_j = 0.046$ kg.	1.4970	0.2584	–0.0233	0.9927	0.44	0.9485	0.9538	1.44	1.43	1.33
(vi) methanol in benzene $M_j = 0.032$ kg.	1.5098	0.3444	–0.2046	0.9928	0.43	0.9116	0.9783	1.41	1.36	1.18
(vii) 2-methyl 3-heptanol in *n*-heptane $M_j = 0.130$ kg.	2.9437	1.2203	–0.7548	0.9958	0.28	0.9130	0.9169	4.22	4.21	3.42
(vii) 3-methyl 3-heptanol in *n*-heptane $M_j = 0.130$ kg.	2.9515	1.1644	–0.4868	0.9985	0.10	0.8875	0.8264	4.18	4.33	3.54
(ix) 4-methyl 3-heptanol in *n*-heptane $M_j = 0.130$ kg.	2.9454	1.2172	–0.6697	0.9970	0.02	0.9058	0.8849	4.23	4.28	3.48
(x) 5-methyl 3-heptanol in *n*-heptane $M_j = 0.130$ kg.	2.9658	0.8446	–0.0754	0.9999	0.01	0.9304	0.8349	3.47	3.67	3.24
(xi) 4-octanol in *n*-heptane $M_j = 0.130$ kg.	2.9546	0.8544	–0.0762	0.9999	0.01	0.9267	0.9375	3.56	3.48	3.27
(xii) 2-octanol in *n*-heptane $M_j = 0.130$ kg.	2.9542	0.8399	–0.0280	0.9999	0.01	0.9083	0.7103	3.51	3.97	3.32

b in terms of τ_j's obtained by both the methods as τ_j's were not found to agree excellently in Table 3. The σ''_{ij} and σ'_{ij} in Ω^{-1} m^{-1} are not linear with w_j as evident from Figs 3 and 4. μ_j's thus obtained are finally compared with μ_{theo}'s from available bond angles and bond moments of the substituent polar groups attached to parent ones. The slight disagreement between the measured μ_j's and μ_s's from μ_{theo}'s indicates the existence of inductive and mesomeric moments of different substituent polar groups present in such dielectropolar molecules in addition to strong hydrogen bonding in them as displayed by the molecular conformations of Fig 6.

The solvent C_6H_6 unlike n-heptane is a cyclic compound with three double bonds and six p-electrons on six carbon atoms. Hence π-π interaction or resonance effect combined with inductive effect known as mesomeric effect is expected to play an important role in the measured μ_j's under hf electric field. A special attention is to be paid to have the conformational structures of the alcohols to evaluate μ_{theo}'s as seen in Fig 6 and Table 2 from the reduction of the available bond moments[5,6] of different substituent polar groups by the ratio of μ_s/μ_{theo}. This takes into account of H- bonding, in addition to inductive effect in them. Thus the conclusion regarding the molecular association of such long chain associated aliphatic alcohols may also be the reason to yield higher dipole moments.

2 Static Relaxation Parameter X_{ij} and Static Dipole Moment μ_s

Under static electric field μ_s of a dielectropolar molecule ($_j$) in a non polar solvent ($_i$) may be obtained from the following equation[10].

$$\frac{(\varepsilon_0 k_{0ij}-1)}{(\varepsilon_0 k_{0ij}+2)}-\frac{(\varepsilon_0 k_{\infty ij}-1)}{(\varepsilon_0 k_{\infty ij}+2)}=$$

$$\frac{(\varepsilon_0 k_{0i}-1)}{(\varepsilon_0 k_{0i}+2)}-\frac{(\varepsilon_0 k_{\infty i}-1)}{(\varepsilon_0 k_{\infty i}+2)}+\frac{N\mu_s^2}{3\varepsilon_0 k_B T}\,c_j \qquad ...(1)$$

where $k_{0ij}=\varepsilon_{0ij}/\varepsilon_0$ and $k_{\infty ij}=\varepsilon_{\infty ij}/\varepsilon_0$ are the dimensionless static and infinite frequency dielectric constants of solution (ij). ε_0 is the permittivity of free space $= 8.854 \times 10^{-12}$ F.m.$^{-1}$, c_j is the molar concentration of the solute where $c_j = \rho_{ij} w_j/M_j$ and the other symbols carry usual meanings.

A polar liquid of weight W_j and volume V_j is mixed with a nonpolar solvent of weight W_i and volume V_i to get the solution density ρ_{ij} where

$$\rho_{ij}=\frac{W_i+W_j}{V_i+V_j}=\frac{W_i+W_j}{W_i/\rho_i+W_j/\rho_j}=$$

$$\frac{\rho_i\,\rho_j}{\rho_j\,W_i/(W_i+W_j)+\rho_i\,W_j/(W_i+W_j)}=$$

$$\frac{\rho_i\,\rho_j}{\rho_j\,w_i+\rho_i\,w_j}=\rho_i(1-\gamma\,w_j)^{-1} \qquad ...(2)$$

The weight fractions w_j and w_i of solute and solvent are given by :

$$w_j=\frac{W_j}{W_i+W_j} \text{ and } w_i=\frac{W_i}{W_i+W_j} \text{ such that } w_i+w_j=1$$

and $\gamma = (1-\rho_i/\rho_j)$, ρ_i and ρ_j are densities of pure solvent and solute respectively.

Now, Eq. (1) may be written as:

$$\frac{k_{0ij}-k_{\infty ij}}{(\varepsilon_0 k_{0ij}+2)(\varepsilon_0 k_{\infty i}+2)}=\frac{k_{0i}-k_{\infty i}}{(\varepsilon_0 k_{0i}+2)(\varepsilon_0 k_{\infty ij}+2)}$$

$$+\frac{N\rho_i\mu_s^2}{9\varepsilon_0^2 M_j k_B T}w_j(1-\gamma\,w_j)^{-1}$$

$$X_{ij}=X_i+\frac{N\rho_i\mu_s^2}{9\varepsilon_0^2 M_j k_B T}w_j+\frac{N\rho_i\mu_s^2}{9\varepsilon_0^2 M_j k_B T}\gamma w_j^2+... \qquad ...(3)$$

The right hand side of Eq. (3) is obviously a polynomial equation of w_j like

$$X_{ij}=a_0+a_1 w_j+a_2 w_j^2+... \qquad ...(4)$$

Now, comparing the linear coefficients of Eqs (3) and (4) one gets μ_s from:

$$\mu_s=\left(\frac{9\varepsilon_0^2 M_j k_B T}{N\rho_i}a_1\right)^{1/2} \qquad ...(5)$$

where a_1 is the slope of X_{ij}-w_j curve of Fig. 1. But μ_s from higher coefficients of Eqs (3) or (4) are not reliable as they are involved with various effects of solvent, relative density, solute-solute association, internal field, macroscopic viscosity etc. μ_s's from Eq. (5) along with a_1 are placed in Table 2 to compare with hf μ_j's presented in Table 4.

3 High Frequency Dipole Moment μ_j and Relaxation Time τ_j

Under hf electric field of GHz range the dimensionless complex dielectric constant k^*_{ij} is:

$$k^*_{ij}=k'_{ij}-jk''_{ij} \qquad ...(6)$$

where $k'_{ij} = \varepsilon'_{ij}/\varepsilon_0$ and $k''_{ij} = \varepsilon''_{ij}/\varepsilon_0$ are the real and imaginary parts of complex dielectric constant. ε'_{ij} and ε''_{ij} are the real and imaginary parts of complex permittivity ε^*_{ij} in F.m.$^{-1}$ and ε_0 = permittivity of free space = 8.854×10^{-12} F.m.$^{-1}$. The hf complex conductivity σ^*_{ij} of a polar-nonpolar liquid mixture of[15] weight fraction w_j is:

$$\sigma^*_{ij} = \omega\varepsilon_0 k''_{ij} + j\omega_0\varepsilon_0 k'_{ij} \qquad ...(7)$$

where $\sigma'_{ij} = \omega\varepsilon_0 k''_{ij}$ and $\sigma''_{ij} = \omega\varepsilon_0 k'_{ij}$ are real and imaginary parts of complex conductivity and j is a complex number = $(-1)^{1/2}$

The hf conductivity σ_{ij} is, however, obtained from :

$$\sigma_{ij} = \omega\varepsilon_0 (k''^{\,2}_{ij} + k'^{\,2}_{ij})^{1/2} \qquad ...(8)$$

σ''_{ij} is related to σ'_{ij} by

$$\sigma''_{ij} = \sigma_{\infty ij} + (1/\omega\tau_j)\sigma'_{ij} \qquad ...(9)$$

where $\sigma_{\infty ij}$ is the constant conductivity at $w_j \to 0$ and τ_j is the relaxation time of a polar molecule.

Eq. (9) on differentiation with respect to σ'_{ij} becomes[11]

$$d\sigma''_{ij}/d\sigma'_{ij} = 1/\omega\tau_j \qquad ...(10)$$

to yield τ_j

It is often better to use the ratio of slopes of individual variation of σ''_{ij} and σ'_{ij} with w_j at $w_j \to 0$ to avoid polar-polar interaction in a given solvent to get τ_j from:

$$(d\sigma''_{ij}/dw_j)/(d\sigma'_{ij}/dw_j) = 1/\omega\tau_j$$

$$\text{or } x/y = 1/\omega\tau_j \qquad ...(11)$$

where $\omega = 2\pi f$, f being the frequency of alternating electric field.

In hf region of GHz range, it is often observed that $\sigma''_{ij} \equiv \sigma_{ij}$ and Eq. (9) becomes:

$$\sigma_{ij} = \sigma_{\infty ij} + (1/\omega\tau_j)\,\sigma'_{ij} \qquad ...(12)$$

$$\beta = 1/\omega\tau_j\,(d\sigma'_{ij}/dw_j) \qquad ...(13)$$

where β - $(d\sigma_{ij}/dw_j)$ is the slope of σ_{ij}-w_j curve at $w_j \to 0$

The σ'_{ij} of a solution of weight fraction w_j of a polar molecule at T K is given by Smyth[14,16] as:

$$\sigma'_{ij} = \frac{N\rho_{ij}\mu_j^2}{27\,\varepsilon_0 M_j k_B T}\left(\frac{\omega^2\tau}{1+\omega^2\tau^2}\right)(\varepsilon_0 k_{0ij}+2)(\varepsilon_0 k_{\infty ij}+2)\,w_j \qquad ...(14)$$

Eq. (14) on differentiation with respect to w_j and at $w_j \to 0$ yields:

$$(d\sigma'_{ij}/dw_j)_{w_j\to 0} = \frac{N\rho_i\mu_j^2}{3\,\varepsilon_0 M_j k_B T}\left(\frac{\varepsilon_i+2}{3}\right)^2\left(\frac{\omega^2\tau}{1+\omega^2\tau^2}\right) \qquad ...(15)$$

where N = Avogadro's number, ρ_i = density of solvent

ε_i = permittivity of solvent;

M_j = Molecular weight of solute and

k_B = Boltzmann constant.

From Eqs (13) and (15) one gets hf μ_j as:

$$\mu_j = \left[\frac{27\,\varepsilon_0 M_j k_B T}{N\rho_i(\varepsilon_i+2)^2}\,\frac{\beta}{\omega b}\right]^{1/2} \qquad ...(16)$$

where $b = 1/(1+\omega^2\tau_j^{\,2})$ ...(17)

is a dimensionless parameter involved with estimated τ_j from Eqs (10) and (11). All the computed hf μ_j's in terms of slopes β's and b's are placed in Table 4 in order to compare with μ_{theo}'s, μ_s and μ_1 , μ_2 of the flexible part and end-over-end rotation of the whole molecule[5,6] presented in Table 2.

4 Results and Discussions

The dimensionless real k'_{ij} and imaginary k''_{ij} of the complex dielectric constants k^*_{ij} as well as the static k_{0ij} and infinite frequency $k_{\infty ij}$ of dielectric constants were obtained from the measured relaxation permittivities $\varepsilon'_{ij}\varepsilon''_{ij}$, ε_{0ij} and $\varepsilon_{\infty ij}$ in F.m^{-1} for different w_j's of alcohols in different solvents at 25°C. The data thus obtained are placed in Table 1. The static experimental solution parameters X_{ij}'s involved with k_{0ij} and $k_{\infty ij}$ of Table 1 are shown in Fig. 1; for different w_j of alcohols. The nature of variation of X_{ij} with w_j's are parabolic in nature satisfying a polynomial equation : $X_{ij} = a_0 + a_1 w_j + a_2 w_j^{\,2}$. The coefficients of X_{ij}—w_j curves i.e. a_0, a_1 and a_2 are placed in the 2nd, 3rd and 4th columns of Table 2. As evident from Fig. 1, the X_{ij}—w_j curves for methanol, ethanol and 3-methyl-3-heptanol are convex in nature as their coefficients of quadratic terms in Table 2 are negative. The remaining X_{ij}'s on the other hand, showed a gradual increase with w_j's for all the coefficients of the curves are positive as seen in Table 2. The anomalous behaviour of X_{ij}—w_j curves from linearity for all the alcohols in different solvents at a given temperature in °C may rouse an interesting relaxation mechanism in such long chain associated liquids. In comparison to octyl alcohols, the curves of normal alcohols in higher concentrations are highly concave hav-

ing a tendency to meet at a common point on the X_{ij} axis at $w_j \to 0$. This sort of behaviour of X_{ij}—w_j curves of Fig. 1 arises either due to solute-solute i.e. dimer or solute-solvent i.e. monomer formations in comparatively high concentrations. The convex shape of ethanol and methanol occurs for the probable experimental uncertainty in their ε_{0ij} and $\varepsilon_{\infty ij}$ measurements. The identical nature of variations of all the octyl alcohols have almost the same slope, but of different intercepts as a result of solvation effect. Their X_{ij}'s have tendency to become closer within $0.1 \leq w_j \leq 0.2$ indicating various molecular association in them.

In case of non-associated liquids a_2's were found to be vanishingly small in comparison to a_0 and a_1 to yield almost linear variation of X_{ij} against w_j. The estimated correlation coefficient (r) and the percentage of error (%) entered in 5th and 6th columns of Table 2 for all the alcohols are such that one may rely on the linear term of X_{ij}—w_j curve to compute μ_s's from Eq. (5). μ_s's thus computed are placed in the 7th column of Table 2 to compare with μ_{theo}'s obtained from bond angles and bond moments of the substituent polar groups, as presented in Fig. 6 and μ_1 and μ_2 of the flexible part and the whole molecule by the double relaxation method[5,6] at nearly 24 GHz electric field. The smaller and larger deviations of X_{ij}'s from linearity with w_j's as seen in Fig. 1, confirm the molecular associations of such associated dielectropolar liquids in different solvents.

The relaxation times τ_j's are, however, derived from the slope of linear[11] variation of σ''_{ij} with σ'_{ij} of Fig. 2 for all the alcohols. Although, the experimental data, on the other hand, did not strictly fall on the fitted linear curves of σ''_{ij} and σ'_{ij} both in Ω^{-1} m^{-1} as drawn in Fig. 2, the slope of σ''_{ij} against σ'_{ij} of Fig. 2 was, however, used to obtain τ_j from Eq. (10). The 2nd, 3rd and 6th columns of Table 3 contain all the estimated intercepts and slopes together with the measured τ_j's. The linearity of σ''_{ij} curves against σ'_{ij} as shown graphically in Fig. 2 is again tested by correlation coefficients r's and % of errors. They are entered in the 4th and 5th columns of Table 3 only to see how far σ''_{ij} and σ'_{ij} are correlated to each other. But it is often better to use the ratio of the individual slopes of variation of σ''_{ij} and σ'_{ij} with w_j at $w_j \to 0$ to get τ_j. τ_j's by using Eq. (11) are not in close agreement with those obtained from Eq. (10) and by freshly calculated Gopalakrishna's method, as seen in Table 3. Figs (3) and (4) showed that both σ''_{ij} and σ'_{ij} vary nonlinearly with w_j. The nonlinear behaviour of σ''_{ij} and σ'_{ij} as seen in Figs 3 and 4 with w_j's invites the associational and structural aspects of such long chain dielectropolar associated molecules. The latter method to measure τ_j's thus appears to be a significant improvement[12,13] over the former one[11] as it eliminates the polar-polar interaction in a given solvent.

The hf μ_j from Eq. (16) was obtained from the slope β of the nonlinear variation of σ_{ij} in Ω^{-1} m^{-1} with w_j's of Fig. 5 and dimensionless parameter b of Eq. (17) in terms of τ_j obtained by both the methods. The intercept α and slope β of hf σ_{ij} with w_j curves of Fig. 5 are entered in the 2nd and 3rd columns of Table 3. It is interesting to note that the curves of σ_{ij}—w_j variation of Fig. 5 are almost identical with σ''_{ij}—w_j curves of Fig. 3. This fact at once confirms the applicability of the approximation that $\sigma''_{ij} \cong \sigma_{ij}$ as done in Eqs (9) and (12). The imaginary σ''_{ij} and total hf σ_{ij} in case of normal alcohols in Figs 3 and 5 decrease gradually with w_j's of 1-butanol to methanol except ethanol. This can be explained on the basis of the fact that the polarity of the molecules decreases from 1-butanol to methanol. Both σ''_{ij}'s and σ_{ij}'s in Figs 3 and 5 of all the octyl alcohols are found to be closer only to show their nearly same polarity. The almost coincident curves of 4-octanol (–Θ–) and 2-octanol(–X–) arise due to their identical polarity as estimated in Fig. 6.

The estimated μ_s's and μ_j's in Table 2 and 4 are then compared with the μ_1 and μ_2 in Table 2 by double relaxation method[5,6] and those by freshly calculated Gopalakrishna's method. For all the normal alcohols μ_j's and μ_s's are in excellent agreement with Gopalakrishna's μ_j's (reported data) and μ_1. The estimated μ_j's for octyl alcohols agree with reported μ_j's and μ_1. All these discussions made above establish the fact that a part of the molecule is rotating under GHz electric field. Slight disagreement in μ's and the reported ones arises due to steric hindrances of the substituent polar units of their structural configurations of Fig. 6 and the existence of associative nature for their hydrogen bonding. Unlike normal alcohols, μ_s's are always lower than μ_j's and μ_1's for octyl alcohols. This at once reveals under static electric field the possible formation of dimers which undergo to rupture into the solute solvent association i.e. monomer in the hf electric field to increase μ's. It is also evident that dimer formation is favourable in octyl alcohols than normal alcohols due to existence of strong

inductive effect for their –OH groups at the end of the molecular chains.

The theoretical dipole moments μ_{theo}'s of all the alcohols under study were calculated from the available bond angles and bond moments of the substituent polar groups like H_3 — C, C—H, C—O, O—H ($\angle 105°$) and C—C of 1.23×10^{-30}, 1.0×10^{-30}, 3.33×10^{-30}, 1.30×10^{-30} and 0.3×10^{-30} Coulomb-meter (C.m.) as presented elsewhere[5,6]. The values thus estimated are then made closer with the measured static μ_s's or even μ_j's by reducing the available bond moments by a factor μ_s/μ_{theo} which takes into account of the inductive and mesomeric effects of the substituent polar groups as shown in Fig. 6. An inductive effect of polar unit acts along the chain of the molecular axis of the normal alcohols to make them strongly polar due to presence of –OH group at their ends of the axis. The comparatively lower μ_{theo}'s in octyl alcohols is probably due to screening effect of their –OH groups by other polar groups like H_3—C, C—H which favour the dimer formation of these alcohols through H-bonding to make their μ_s's and μ_j's lower than the normal alcohol as seen in Fig. 6.

5 Conclusion

The modern internationally accepted symbols of dielectric terminologies and parameters in SI unit are conveniently used to obtain static and hf dipole moments μ_s and μ_j in terms of relaxation time τ_j of a polar molecule. τ_j's measured from the slope of imaginary σ''_{ij} against real σ'_{ij} of complex hf conductivity σ^*_{ij} for different w_j are not in agreement with those measured from the ratio of the individual slopes of $\sigma''_{ij} - w_j$ and $\sigma'_{ij} - w_j$ curves at $w_j \rightarrow 0$ indicating the applicability of the latter method in long chain dielectropolar alcohols. This method of determination of τ_j is a significant improvement over the previous one as it eliminates polar-polar interactions in a given solvent. The comparison of μ_j's and μ_s's with μ_1 and μ_2 of the flexible part and the whole molecule by double relaxation method and μ_{theo}'s from bond angles and bond moments seems to be an interesting phenomenon to have deep insight into relaxation mechanism of dielectropolar alcohols.

The results indicate that a part of the molecule is rotating under GHz electric field. The slight departure among the measured μ_s, μ_j and μ_{theo} reveals different associational aspects of dielectropolar alcohols in different solvents through the frequency dependence of relaxation parameters. It also shows the strong polar nature of normal alcohols which favour solute-solvent association due to the presence of —OH group at the end of their bond axis. But the comparatively lower values of μ_j's in octyl alcohols indicates the solute-solute association due to –H bonding supported by the fact that –OH being screened by $-CH_3$ and a large number of $> CH_2$ polar groups. The μ_s/μ_{theo}'s are almost constant for all the alcohols to take into account of all these facts in addition to their material property of the system. This study further supports the rotation of –OH group along the ≡C–O– bond of all the alcohols under static and hf electric fields. Moreover, the methodology so far developed within the frame work of Debye and Smyth model appears to be sound, simple, straightforward and useful to arrive at associational and structural aspects of alcohols which are thought to be non-Debye in relaxation behaviour.

References

1 Gopalakrishna K V, *Trans Farad Soc*, 33 (1957) 767.

2 Kastha G S, Dutta J, Bhattacharyya J & Roy S B, *Indian J Phys*, 43 (1969) 14.

3 Dutta S K, Acharyya C R & Acharyya S, *Indian J Phys*, 55B (1981) 140.

4 Sit S K, Ghosh N, Saha U & Acharyya S, *Indian J Phys*, 71B (1997) 533.

5 Sit S K & Acharyya S, *Indian J Phys*, 70B (1996) 19.

6 Sit S K, Ghosh N & Acharyya S, *Indian J Pure & Appl Phys*, 35 (1997) 329.

7 Glasser L, Crossley J & Smyth C P, *J Chem Phys*, 57 (1972) 3977.

8 Ghosh A K, PhD Dissertation, N B U, (1981).

9 Crossley J, Glasser L & Smyth C P, *J Chem Phys*, 55 (1971) 2197.

10 Debye P, *Polar Molecules* (Chemical Catalogue), 1929.

11 Murthy M B R, Patil R L & Deshpande D K, *Indian J Phys*, B63 (1989) 491.

12 Ghosh N, Basak R C, Sit S K & Acharyya S, *J Mol Liq*, Germany, (Accepted for publication), 2000.

13 Basak R C, Sit S K, Nandi N & Acharyya S, *Indian J Phys*, B70 (1996) 37.

14 Basak R C, Karmakar A, Sit S K & Acharyya S, *Indian J Pure & Appl Phys*, 37 (1999) 224.

15 Murphy F J & Morgan S O, *Bell Syst Tech J*, 18 (1939) 502.

16 Smyth C P, *Dielectric behaviour and structure*, (McGraw-Hill, New York), 1955.

INSTITUTE OF PHYSICS PUBLISHING JOURNAL OF PHYSICS D: APPLIED PHYSICS
J. Phys. D: Appl. Phys. 34 (2001) 379–388 www.iop.org/Journals/jd PII: S0022-3727(01)18296-3

Structural and associational aspects of isomers of anisidine and toluidine under a gigahertz electric field

N Ghosh, S K Sit, A K Bothra and S Acharyya

Department of Physics, Raiganj College (University College), P.O. Raiganj, District Uttar Dinajpur, PIN - 733134, (WB), India

Received 25 October 2000

Abstract

The relaxation times τ_1 and τ_2 for rotations of the flexible parts and the whole molecules of the isomers of anisidine and toluidine (j) in benzene (i) under a 9.945 GHz electric field are predicted from the slope and intercept of a linear equation of $(\chi_{0ij} - \chi'_{ij})/\chi'_{ij}$ against χ''_{ij}/χ'_{ij} for different weight fractions w_j's of solute at 35 °C. χ'_{ij} and χ''_{ij} are the real and imaginary parts of the high-frequency complex orientational susceptibility χ^*_{ij} and χ_{0ij} is the low-frequency susceptibility which is real. The τ's; dimensionless parameters b's involved with τ's and linear coefficients β's of χ'_{ij}–w_j curves are used to obtain dipole moments μ_1 and μ_2 of the flexible parts and the whole molecules. The theoretical weighted contributions c_1 and c_2 due to τ_1 and τ_2 towards dielectric dispersions from Fröhlich's equations are worked out to compare with experimental ones by graphical variations of χ'_{ij}/χ_{0ij} and χ''_{ij}/χ_{0ij} at $w_j \to 0$. The estimated τ's from the ratio of the individual slopes of χ''_{ij} and χ'_{ij} with w_j's at $w_j \to 0$ are compared with those of Murthy *et al* (1989 *Indian J. Phys.* B **63** 491) and reported τ's.
The symmetric and characteristic relaxation times τ_s and τ_{cs} by symmetric and asymmetric distribution parameters γ and δ are computed to suggest the symmetric relaxation behaviour of the molecules. The measured μ_1 and μ_2 from double relaxation phenomena and the reported μ's signify the fact that a part of the molecule is rotating under a gigahertz electric field. The slight disagreement between the theoretical dipole moment μ_{theo} from available bond angles and bond moments of substituent polar groups attached to the parent molecules and measured μ_1 demands the inductive and mesomeric effects suffered by the substituent polar groups, in addition to structural and associational aspects of such molecules.

1. Introduction

The dielectric relaxation of a polar liquid molecule in a non-polar solvent under static and high-frequency (hf) electric fields provides one with valuable information on various types of molecular associations [1, 2] and the structural configuration of the polar molecule from relaxation parameters such as the relaxation time τ and dipole moment μ, measured by any standard method [3, 4]. μ_j's determined by concentration variation of the real part of the hf dielectric susceptibility are concerned with the orientational polarization and are further used to shed more light on the structural and associational aspects of a polar molecule [5].

Srivastava and Chandra [6] measured the real ϵ'_{ij} and imaginary ϵ''_{ij} parts of the relative complex permittivity, ϵ^*_{ij} and the static and infinitely hf relative permittivities, ϵ_{0ij} and $\epsilon_{\infty ij}$, of isomers of anisidines and toluidines in C_6H_6 under 2.02, 3.86 and 22.06 GHz electric fields at 35 °C. The purpose of such a study was to observe the solute–solvent and solute–solute molecular associations, besides the possible existence of either double or single relaxation behaviour of anisidines and toluidines.

Nowadays, the usual practice is to study dielectric relaxation phenomena by dimensionless complex hf dielectric orientational susceptibility χ^*_{ij} [5] rather than the relative hf permittivity ϵ^*_{ij} or hf conductivity σ^*_{ij}. The ϵ^*_{ij} includes within

0022-3727/01/030379+10$30.00

it all types of polarizations while σ_{ij}^* is concerned with the transport of bound charges. Hence it is better to work with χ_{ij} for its more direct link with orientational polarization. Moreover, the present system of study in the modern concept of internationally accepted symbols of dielectric terminology and parameters in SI units is interesting because of its rationalized, coherent and unified nature.

Under such a context we derived a linear equation (5) (see below) in terms of the real $\chi'_{ij} = (\epsilon'_{ij} - \epsilon_{\infty ij})$ and imaginary $\chi''_{ij} = \epsilon''_{ij}$ parts of the complex hf χ^*_{ij} and low-frequency dielectric susceptibility $\chi_{0ij} = (\epsilon_{0ij} - \epsilon_{\infty ij})$, which is real as presented in table 1 under a 9.945 GHz electric field, to obtain τ_1 and τ_2 of the flexible parts and the whole molecules in C_6H_6 at 35 °C.

The electric field frequency of $f = 9.945$ GHz was claimed to be the most effective dispersive region for such molecules [7]. When χ''_{ij}s were plotted against frequency (f) they showed a peak in the neighbourhood of 9.945 GHz, at which point the dielectric orientation processes of polar molecules [8, 9] are invariably maximum. At this frequency χ'_{ij}, χ''_{ij} and χ_{0ij} were again adjusted by a careful graphical interpolation technique [7]. One could make a strong conclusion of double relaxation phenomena of a polar molecule in a non-polar solvent based on single-frequency measurement of the relaxation parameters, provided the accurate value of χ_{0ij} involved with ϵ_{0ij} and $\epsilon_{\infty ij}$ is available. The use of n^2_{Dij} for $\epsilon_{\infty ij}$ [6] may often introduce additional error into the calculation. Nevertheless, the data are accurate up to 5% for χ''_{ij} and 2% for χ'_{ij} and χ_{0ij}. The liquid molecules at this f absorb electric energy much more strongly to exhibit reasonable τ_1 and τ_2 for all the chemical systems under identical environments. τ_1 and τ_2 are, however, measured from the intercept and slope of the derived straight-line equation (see equation (5) below) of $(\chi_{0ij} - \chi'_{ij})/\chi'_{ij}$ against χ''_{ij}/χ'_{ij} of figure 1 for different weight fractions w_j's of polar solute at the single frequency ω ($=2\pi f$), signifying the material property of the systems. The correlation coefficients τ's and minimum chisquare values to test the linearity of the curves of figure 1, along with the estimated τ_1 and τ_2, are given in table 2. In absence of reliable τ, the ratio of the individual slopes of variation of χ''_{ij} and χ'_{ij} with w_j's at $w_j \to 0$, as seen in figures 2 and 3, were conveniently used to evaluate τ_j to compare with those of Murthy *et al* [10] of figure 4 and Gopalakrishna's method [11].

The theoretical weighted contributions c_1 and c_2 due to the estimated τ_1 and τ_2 presented in table 3, towards dielectric dispersions, were calculated from Fröhlich's equations [12] in order to compare with the experimental contributions by the graphical extrapolation technique of figures 5 and 6 at $w_j \to 0$. The symmetric and asymmetric distribution parameters γ and δ were, however, worked out from the variation of χ'_{ij}/χ_{0ij} and χ''_{ij}/χ_{0ij} with w_j in the limit $w_j = 0$ to conclude the symmetric distribution behaviour obeyed by such molecules. The characteristic relaxation time τ_{cs} from δ and ϕ of figure 7 along with the symmetric relaxation time τ_s in terms of γ are found out to compare with τ_1, τ_2 and τ_j in table 2.

The dipole moments μ_1, μ_2 and μ_0, in Coulomb metres (C m), in terms of b_1, b_2 and b_0 involved with τ_1, τ_2 and τ_0, where τ_0 is the most probable relaxation time ($= \sqrt{\tau_1\tau_2}$) and linear coefficient β's of χ'_{ij} against w_j curves of figure 3

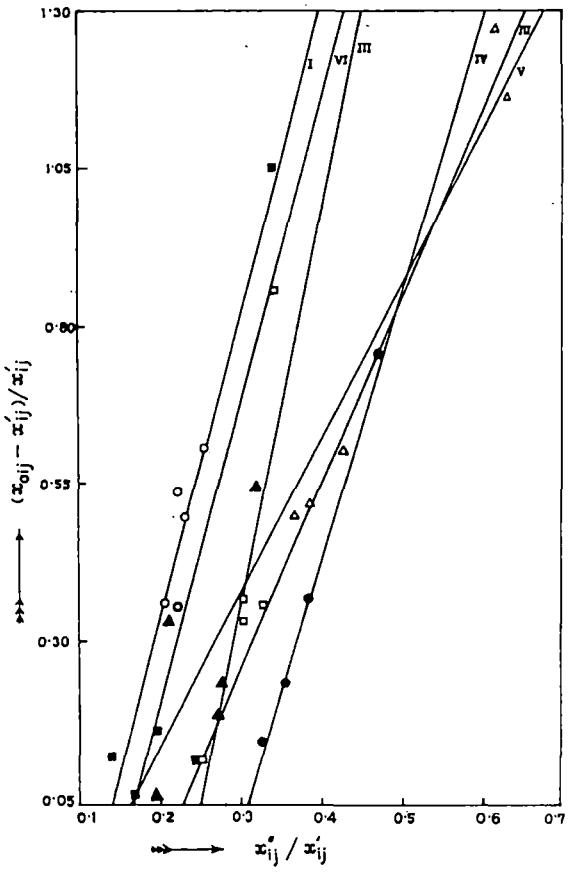

Figure 1. Linear variation of $(\chi_{0ij} - \chi'_{ij})/\chi'_{ij}$ against χ''_{ij}/χ'_{ij} of isomers of anisidines and toluidines in benzene at 35 °C under a 9.945 GHz electric field: (I) *o*-anisidine (——○——), (II) *m*-anisidine (——△——), (III) *p*-anisidine (——□——), (IV) *o*-toluidine (——●——), (V) *m*-toluidine (——▲——) and (VI) *p*-toluidine (——■——).

were determined in order to place them in table 4. The comparison, however, indicates that the flexible parts of the molecules rotate under X-band gigahertz electric fields. They are compared with μ_{theo}'s obtained from available bond angles and bond moments of the substituent polar groups attached to the parent molecules, as displayed in figure 8, and μ_j by freshly calculated Gopalakrishna's method of table 4. The slight disagreement between the measured μ's and μ_{theo}'s invites the existence of inductive and mesomeric effects of substituent polar groups.

2. Theoretical formulations for τ_1, τ_2 and τ_0

Bergmann *et al*'s equations [13] are concerned with molecular orientational polarization processes. We therefore introduce χ_{ij}'s to avoid clumsiness of algebra as $\epsilon_{\infty ij}$ includes a fast polarization process and frequently appears as a subtracted term in the equations. Thus, with the established symbols of parameters of dielectric terminology like $\chi'_{ij} = (\epsilon'_{ij} - \epsilon_{\infty ij})$, $\chi''_{ij} = \epsilon''_{ij}$ and $\chi_{0ij} = (\epsilon_{0ij} - \epsilon_{\infty ij})$ of table 1, Bergmann *et al*'s

Table 1. Concentration variations of the measured real ϵ'_{ij} and imaginary ϵ''_{ij} parts of the hf complex relative permittivity under a 9.945 GHz electric field, the static and hf relative permittivities ϵ_{0ij} and $\epsilon_{\infty ij}$ along with the real χ'_{ij} and imaginary χ''_{ij} parts of the complex dimensionless dielectric orientational susceptibility χ^*_{ij} and the low-frequency susceptibility χ_{0ij} which is real for isomers of anisidine and toluidine in benzene at 35 °C.

System with serial number and molecular weight (M_j)	Weight fraction, w_j, of solute	Measured dielectric relative permittivities				Dimensionless dielectric orientational susceptibilities		
		ϵ'_{ij}	ϵ''_{ij}	ϵ_{0ij}	$\epsilon_{\infty ij}$	χ'_{ij}	χ''_{ij}	χ_{0ij}
(i) *o*-anisidine	0.0326	2.3104	0.0148	2.336	2.239	0.0714	0.0148	0.097
$M_j = 0.123$ kg	0.0604	2.3520	0.0244	2.404	2.247	0.1050	0.0244	0.157
	0.0884	2.4064	0.0340	2.459	2.255	0.1514	0.0340	0.204
	0.1135	2.4416	0.0400	2.538	2.262	0.1796	0.0400	0.276
	0.1361	2.4672	0.0512	2.588	2.267	0.2002	0.0512	0.321
(ii) *m*-anisidine	0.0160	2.2720	0.0234	2.315	2.235	0.0370	0.0234	0.080
$M_j = 0.123$ kg	0.0336	2.3040	0.0390	2.384	2.241	0.0630	0.0390	0.143
	0.0579	2.3904	0.0618	2.477	2.246	0.1444	0.0618	0.231
	0.0823	2.4544	0.0744	2.553	2.253	0.2014	0.0744	0.300
	0.1109	2.5344	0.1056	2.675	2.261	0.2734	0.1056	0.414
(iii) *p*-anisidine	0.0319	2.3104	0.0252	2.373	2.237	0.0734	0.0252	0.136
$M_j = 0.123$ kg	0.0597	2.3904	0.0474	2.442	2.246	0.1444	0.0474	0.196
	0.0848	2.5088	0.0642	2.539	2.250	0.2588	0.0642	0.289
	0.1106	2.5376	0.0840	2.638	2.262	0.2756	0.0840	0.376
	0.1396	2.6272	0.1086	2.745	2.269	0.3582	0.1086	0.476
(iv) *o*-toluidine	0.0137	2.2752	0.0162	2.301	2.241	0.0342	0.0162	0.060
$M_j = 0.107$ kg	0.0459	2.3648	0.0408	2.392	2.250	0.1148	0.0408	0.142
	0.0622	2.4032	0.0570	2.457	2.255	0.1482	0.0570	0.202
	0.1048	2.5376	0.0900	2.577	2.264	0.2736	0.0900	0.313
(v) *m*-toluidine	0.0264	2.3136	0.0150	2.337	2.243	0.0706	0.0150	0.094
$M_j = 0.107$ kg	0.0538	2.3552	0.0342	2.413	2.248	0.1072	0.0342	0.165
	0.0781	2.4576	0.0402	2.470	2.252	0.2056	0.0402	0.218
	0.1015	2.4840	0.0618	2.526	2.258	0.2260	0.0618	0.268
	0.1225	2.5280	0.0732	2.591	2.262	0.2660	0.0732	0.329
(vi) *p*-toluidine	0.0213	2.3100	0.0102	2.319	2.237	0.0730	0.0102	0.082
$M_j = 0.107$ kg	0.0428	2.3040	0.0204	2.367	2.244	0.0600	0.0204	0.123
	0.0616	2.3904	0.0276	2.413	2.249	0.1414	0.0276	0.164
	0.0916	2.4704	0.0384	2.483	2.254	0.2164	0.0384	0.229
	0.1048	2.4960	0.0582	2.523	2.260	0.2360	0.0582	0.263

equations become

$$\frac{\chi'_{ij}}{\chi_{0ij}} = c_1 \frac{1}{1+\omega^2\tau_1^2} + c_2 \frac{1}{1+\omega^2\tau_2^2} \tag{1}$$

and

$$\frac{\chi''_{ij}}{\chi_{0ij}} = c_1 \frac{\omega\tau_1}{1+\omega^2\tau_1^2} + c_2 \frac{\omega\tau_2}{1+\omega^2\tau_2^2} \tag{2}$$

assuming the molecules possess two separate broad dispersions for which the relative weight factors c_1 and c_2 are such that $c_1 + c_2 = 1$. χ'_{ij} and χ''_{ij} are the real and imaginary parts of the hf complex susceptibility χ^*_{ij} and χ_{0ij} is the static or low-frequency susceptibility which is real.

Let $\alpha_1 = \omega\tau_1$ and $\alpha_2 = \omega\tau_2$, equations (1) and (2) are solved to obtain

$$c_1 = \frac{(\chi'_{ij}\alpha_2 - \chi''_{ij})(1+\alpha_1^2)}{\chi_{0ij}(\alpha_2 - \alpha_1)} \tag{3}$$

and

$$c_2 = \frac{(\chi''_{ij} - \chi'_{ij}\alpha_1)(1+\alpha_2^2)}{\chi_{0ij}(\alpha_2 - \alpha_1)} \tag{4}$$

provided $\alpha_2 > \alpha_1$. Now adding equations (3) and (4), since $c_1 + c_2 = 1$, one obtains

$$\frac{\chi_{0ij} - \chi'_{ij}}{\chi'_{ij}} = \omega(\tau_1 + \tau_2)\frac{\chi''_{ij}}{\chi'_{ij}} - \omega^2\tau_1\tau_2. \tag{5}$$

Equation (5) gives a straight line between the variables $(\chi_{0ij} - \chi'_{ij})/\chi'_{ij}$ and χ''_{ij}/χ'_{ij} having intercept $-\omega^2\tau_1\tau_2$ and slope $\omega(\tau_1 + \tau_2)$. It was solved for different concentrations w_j's of each of the polar molecules of table 1 for a given fixed value of the angular frequency ω $(=2\pi f)$ of the applied electric field at 35 °C, where $f = 9.945$ GHz. The values of τ_1 and τ_2 from the intercept and slope of equation (5) are found as shown in table 2.

The theoretical values of c_1 and c_2 towards dielectric relaxations were obtained from equations (3) and (4) using values of χ'_{ij}/χ_{0ij} and χ''_{ij}/χ_{0ij} of Fröhlich's [12] following equations, (6) and (7), in terms of the estimated τ_1 and τ_2 of table 2 from the intercepts and slopes of equation (5):

$$\chi'_{ij}/\chi_{0ij} = 1 - \frac{1}{2A}\ln\left(\frac{1+\omega^2\tau_2^2}{1+\omega^2\tau_1^2}\right) \tag{6}$$

$$\chi''_{ij}/\chi_{0ij} = \frac{1}{A}[\tan^{-1}(\omega\tau_2) - \tan^{-1}(\omega\tau_1)]. \tag{7}$$

The theoretical c_1 and c_2 are given in table 3 in order to compare them with the experimental values obtained by graphically extrapolated values of χ'_{ij}/χ_{0ij} and χ''_{ij}/χ_{0ij} in the limit $w_j = 0$ in figures 5 and 6 and equations (3) and (4). The Fröhlich's parameter A, where $A = \ln(\tau_2/\tau_1)$ is given in table 3 for each compound.

Table 2. Slope and intercept of the linear equations of $(\chi_{0ij} - \chi'_{ij})/\chi'_{ij}$ against χ''_{ij}/χ'_{ij}, correlation coefficient (r), minimum chisquare values, relaxation times τ_1 and τ_2 of the flexible part as well as the whole molecules, measured τ from equations (9) and (10), reported τ (Gopalakrishna) and most probable relaxation time τ_0, together with symmetric τ_s and characteristic τ_{cs} from symmetric and asymmetric distribution parameters γ and δ of some monosubstituted anilines at 35 °C under a 9.945 GHz (X-band microwave) electric field.

System with serial number and molecular weight (M_j)	Intercept and slope from (5) for $((\chi_{0ij} - \chi'_{ij})/\chi'_{ij})$ against χ''_{ij}/χ'_{ij}		Correlation coefficient	Chisquare value	Estimated relaxation times τ_1 and τ_2		Most probable relaxation time	Measured τ	Ratio of slopes of χ''_{ij} and χ'_{ij} with w_j of (10)
	Intercept (c)	Slope (m)	(r)	($\times 10^2$)	(ps)		$\tau_0 = \sqrt{\tau_1 \tau_2}$	(ps)[a]	$\frac{(d\chi''_{ij}/dw_j)_{w_j \to 0}}{(d\chi'_{ij}/dw_j)_{w_j \to 0}}$
(i) *o*-anisidine $M_j = 0.123$ kg	0.6373	4.8390	0.7743	4.36	2.17	75.31	12.78	4.18	0.1560
(ii) *m*-anisidine $M_j = 0.123$ kg	0.6075	2.9047	0.9888	1.22	3.63	42.88	12.48	5.20	0.3033
(iii) *p*-anisidine $M_j = 0.123$ kg	1.4948	6.2149	0.8310	24.77	4.01	95.50	19.57	4.47	0.1824
(iv) *o*-toluidine $M_j = 0.107$ kg	1.2684	4.2603	0.9986	0.13	5.15	63.06	18.02	4.95	0.4025
(v) *m*-toluidine $M_j = 0.107$ kg	0.3501	2.4337	0.6864	30.10	2.46	36.51	9.48	4.18	0.1605
(vi) *p*-toluidine $M_j = 0.107$ kg	0.7348	4.7136	0.8687	−23.25	2.58	72.89	13.71	3.36	0.1755

System with serial number and molecular weight (M_j)	Relaxation times			
	τ (ps)[b]	τ (ps)[c]	τ (ps)[d]	τ (ps)[e]
(i) *o*-anisidine $M_j = 0.123$ kg	2.50	3.29	2.46	130.40
(ii) *m*-anisidine $M_j = 0.123$ kg	4.86	4.28	3.02	64.22
(iii) *p*-anisidine $M_j = 0.123$ kg	2.92	3.70	140.19	305.52
(iv) *o*-toluidine $M_j = 0.107$ kg	6.44	4.15	16.05	82.37
(v) *m*-toluidine $M_j = 0.107$ kg	2.57	4.01	5.85	458.51
(vi) *p*-toluidine $M_j = 0.107$ kg	2.81	3.34	1.38	12.07

[a] Measured by the slope of χ''_{ij} against χ'_{ij} using the straight-line equation (9).
[b] From the ratio of individual slopes.
[c] By Gopalakrishna's method [11].
[d] From the symmetric distribution parameter γ of (17).
[e] From the asymmetric distribution parameter δ of (19).

3. Theoretical formulation for the dipole moment

The real ϵ'_{ij} and imaginary ϵ''_{ij} parts of the hf complex relative permittivity are written as

$$\epsilon'_{ij} = \epsilon_{\infty ij} + (1/\omega\tau)\epsilon''_{ij}$$

or

$$\epsilon'_{ij} - \epsilon_{\infty ij} = (1/\omega\tau)\epsilon''_{ij}$$

or

$$\chi'_{ij} = (1/\omega\tau)\chi''_{ij} \tag{8}$$

and

$$(d\chi''_{ij}/d\chi'_{ij}) = \omega\tau_j. \tag{9}$$

The variation of susceptibility χ''_{ij} with χ'_{ij} of equation (9) is caused by variation in concentrations, w_j's, of the polar liquids under the fixed frequency of the electric field. As χ''_{ij} is, however, claimed to vary linearly with χ'_{ij} [10] of different concentrations and the frequency is fixed, the slope of χ''_{ij} with χ'_{ij} can conveniently be used to obtain τ_j from equation (9).

However, in case of monosubstituted anilines the variations of χ''_{ij} with χ'_{ij}, as seen in figure 4, are not strictly linear. The ratio of individual slopes from the variations of χ''_{ij} and χ'_{ij} with w_j's in figures 2 and 3 is, however, thought to be a better representation of equation (9) to obtain τ_j where polar–polar interactions are supposed to be fully avoided.

Table 3. Fröhlich's parameter A, relative contributions c_1 and c_2 due to τ_1 and τ_2 theoretical values of χ'_{ij}/χ_{0ij} and χ''_{ij}/χ_{0ij} of Fröhlich's equations, (6) and (7), and those by the graphical method at $w_j \to 0$, symmetric γ and asymmetric δ distribution parameters of some monosubstituted anilines at 35 °C under a 9.945 GHz (X-band microwave) electric field.

System with serial number	Fröhlich's Parameter $A = \ln(\tau_2/\tau_1)$	Estimated values of χ'_{ij}/χ_{0ij} and χ''_{ij}/χ_{0ij} of Frohlich's equations (6) and (7)		Weighted contributions c_1 and c_2 from (3) and (4)		Estimated values of χ'_{ij}/χ_{0ij} and χ''_{ij}/χ_{0ij} from figures 5 and 6 at $w_j \to 0$		Weighted contributions c_1 and c_2 from the graphical technique		Symmetric distribution parameter γ	Asymmetric distribution parameter δ
				c_1	c_2			c_1	c_2		
(i) *o*-anisidine	3.5469	0.5598	0.3458	0.5099	1.3664	0.7100	.0.1470	0.7117	0.2570	0.5716	0.1360
(ii) *m*-anisidine	2.4692	0.5848	0.4011	0.4997	0.8952	0.3339	0.3094	0.2508	0.7791	0.2475	0.5671
(iii) *p*-anisidine	3.1703	0.4419	0.3656	0.4222	1.6317	0.2114	0.1523	0.2062	0.6360	0.4813	0.4111
(iv) *o*-toluidine	2.5051	0.4600	0.4035	0.4296	1.1665	0.4995	0.2638	0.5197	0.4708	0.3821	0.3524
(v) *m*-toluidine	2.6974	0.6661	0.3726	0.5517	0.7879	0.5894	0.1308	0.5839	0.1173	0.6650	0.1422
(vi) *p*-toluidine	3.3412	0.5432	0.3576	0.4818	1.3361	0.9550	0.1148	0.9889	−0.1933	0.1617	0.1853

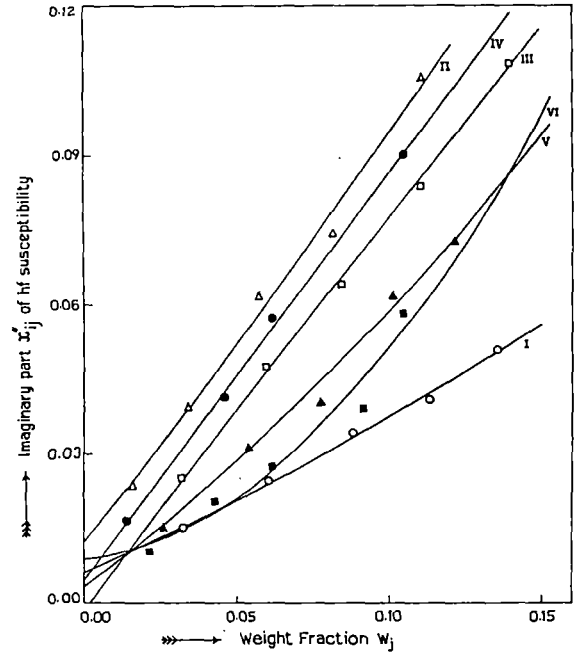

Figure 2. Variation of the imaginary part χ''_{ij} of the hf susceptibility against the weight fraction w_j of solute in benzene at 35 °C under a 9.945 GHz electric field: (I) *o*-anisidine (——○——), (II) *m*-anisidine (——△——), (III) *p*-anisidine (——□——), (IV) *o*-toluidine (——●——), (V) *m*-toluidine (——▲——) and (VI) *p*-toluidine (——■——).

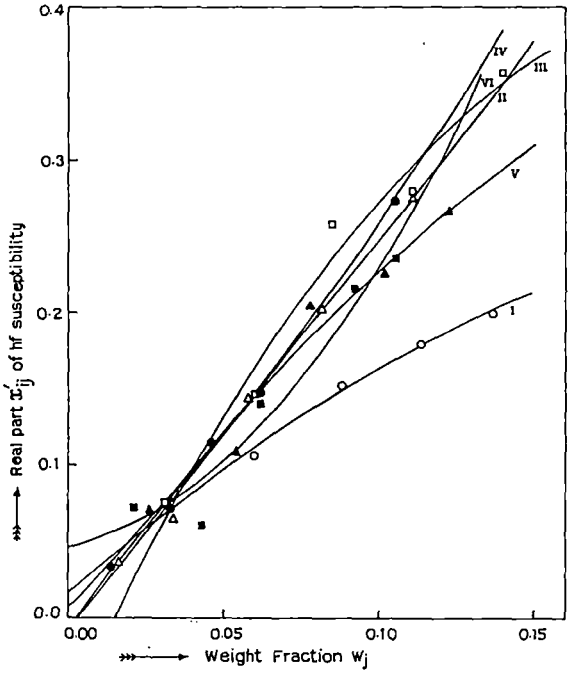

Figure 3. Variation of the real part χ'_{ij} of the hf susceptibility against the weight fraction w_j of solute in benzene at 35 °C under a 9.945 GHz electric field: (I) *o*-anisidine (——○——), (II) *m*-anisidine (——△——), (III) *p*-anisidine (——□——), (IV) *o*-toluidine (——●——), (V) *m*-toluidine (——▲——) and (VI) *p*-toluidine (——■——).

Thus

$$\left(\frac{d\chi''_{ij}}{dw_j}\right)_{w_j\to 0}\left[\left(\frac{d\chi'_{ij}}{dw_j}\right)_{w_j\to 0}\right]^{-1} = \omega\tau_j. \qquad (10)$$

The imaginary part χ''_{ij} of χ^*_{ij} is [14, 15]

$$\chi''_{ij} = \frac{N\rho_{ij}\mu_j^2}{27\epsilon_0 M_j k_B T}\left(\frac{\omega\tau}{1+\omega^2\tau^2}\right)(\epsilon_{ij}+2)^2 w_j. \qquad (11)$$

Equation (11), when differentiated with respect to w_j and at $w_j \to 0$ yields

$$\left(\frac{d\chi''_{ij}}{dw_j}\right)_{w_j\to 0} = \frac{N\rho_i\mu_j^2}{27\epsilon_0 M_j k_B T}\left(\frac{\omega\tau}{1+\omega^2\tau^2}\right)(\epsilon_i+2)^2. \qquad (12)$$

At $w_j \to 0$, the density of solution ρ_{ij} and $(\epsilon_{ij}+2)^2$ tends to ρ_i and $(\epsilon_i+2)^2$ where ρ_i and ϵ_i are the density and relative permittivity of solvent i, respectively.

In comparison to earlier works presented elsewhere [15, 16] the approximation that $\chi_{ij} \simeq \chi''_{ij}$, as $\sigma_{ij} \simeq \sigma''_{ij}$, is not necessary to obtain the μ_j's from the τ_j's where σ''_{ij} is the

Table 4. Coefficients α, β and γ of the χ'_{ij}–w_j curve (figure 3) with correlation coefficients and percentage of errors, dimensionless parameter b, estimated μ_j's where μ is from $\mu_1 = \mu_2(c_1/c_2)^{1/2}$ and theoretical μ from bond angles and bond moments together with reported μ (Gopalakrishna [11]) of some monosubstituted anilines in benzene at 35 °C under a 9.945 GHz (X-band microwave) electric field.

Systems with serial number and molecular weight (M_j)	Coefficients of the equation $\chi'_{ij} = \alpha + \beta w_j + \gamma w_j^2$			Correlation coefficient of the χ'_{ij}–w_j equation	Percentage error involved in the χ'_{ij}–w_j equations	Dimensionless parameters			Estimated dipole moments μ ($\times 10^{30}$ C m)		
	α	β	γ			b_0^a	b_1^b	b_2^c	μ_0	μ_1	μ_2
(i) *o*-anisidine $M_j = 0.123$ kg	0.0149	1.7546	−2.8056	0.9960	0.24	0.6108	0.9820	0.0432	6.17	4.87	23.21
(ii) *m*-anisidine $M_j = 0.123$ kg	−0.0094	2.5108	0.4641	0.9968	0.19	0.6221	0.9511	0.1224	7.31	5.91	16.49
(iii) *p*-anisidine $M_j = 0.123$ kg	−0.0634	4.4003	−10.2107	0.9962	0.23	0.4010	0.9410	0.0273	12.06	7.87	46.23
(iv) *o*-toluidine $M_j = 0.107$ kg	0.0063	2.0495	4.7368	0.9979	0.14	0.4412	0.9062	0.0606	7.32	5.11	19.75
(v) *m*-toluidine $M_j = 0.107$ kg	−0.0078	2.8140	−4.6071	0.9782	1.30	0.7404	0.9769	0.1613	6.62	5.76	14.19
(vi) *p*-toluidine $M_j = 0.107$ kg	0.0464	0.3863	14.5432	0.9593	2.41	0.5770	0.9747	0.0460	2.78	2.14	9.84

Systems with serial number and molecular weight (M_j)	Dipole moments		
	Estimated μ ($\times 10^{30}$ Cm)[d]	Theoretical μ ($\times 10^{30}$ Cm)[e]	μ ($\times 10^{30}$ Cm)[f]
(i) *o*-anisidine $M_j = 0.123$ kg	14.18	3.40	4.50
(ii) *m*-anisidine $M_j = 0.123$ kg	12.32	5.50	6.17
(iii) *p*-anisidine $M_j = 0.123$ kg	23.51	6.30	6.53
(iv) *o*-toluidine $M_j = 0.107$ kg	11.98	4.63	5.77
(v) *m*-toluidine $M_j = 0.107$ kg	11.87	3.43	5.17
(vi) *p*-toluidine $M_j = 0.107$ kg	5.91	5.13	5.30

[a] $b_0 = \dfrac{1}{1+\omega^2\tau_0^2}$.

[b] $b_1 = \dfrac{1}{1+\omega^2\tau_1^2}$.

[c] $b_2 = \dfrac{1}{1+\omega^2\tau_2^2}$.

[d] From $\mu_1 = \mu_2\left(\dfrac{c_1}{c_2}\right)^{1/2}$.

[e] From bond angles and bond moments.

[f] From Gopalakrishna's method [11].

imaginary part of the complex hf conductivity and σ_{ij} is the total hf conductivity of the polar–non-polar liquid mixture.

From equations (8) and (12) one obtains

$$\omega\tau_j\left(\frac{d\chi'_{ij}}{dw_j}\right)_{w_j\to 0} = \frac{N\rho_i\mu_j^2}{27\epsilon_0 M_j k_B T}\left(\frac{\omega\tau_j}{1+\omega^2\tau_j^2}\right)(\epsilon_i+2)^2$$

or

$$\mu_j = \left[\frac{27\epsilon_0 M_j k_B T\beta}{N\rho_i(\epsilon_i+2)^2 b}\right]^{1/2} \qquad (13)$$

where τ_j and μ_j are the relaxation time and the dipole moment of the jth solute and ϵ_0 is the permittivity of free space, 8.854×10^{-12} F m^{-1}. Here N is the Avogadro number, 6.023×10^{23}; ρ_i is the density of the solvent, 865 kg m^{-3}; k_B is the Boltzmann constant, 1.38×10^{-23} J mol^{-1} k^{-1}; ϵ_i is the dielectric relative permittivity of the solvent, benzene, 2.253; M_j is the molecular weight of the solute in kilogrammes; β is the linear coefficient of the $\chi'_{ij} - w_j$ curve at $w_j \to 0$; and $b = 1/(1+\omega^2\tau_j^2)$ is a dimensionless parameter involved with the measured τ_j.

The μ_1, μ_2 and μ_0 in terms of b_1, b_2 and b_0 involved with τ_1, τ_2 and τ_0, respectively, were then computed with the knowledge of β of χ'_{ij}–w_j curves of figure 3. The μ's thus obtained from equation (13) are given in table 4 in order to compare with those of Gopalakrishna [11] and μ_{theo}'s obtained

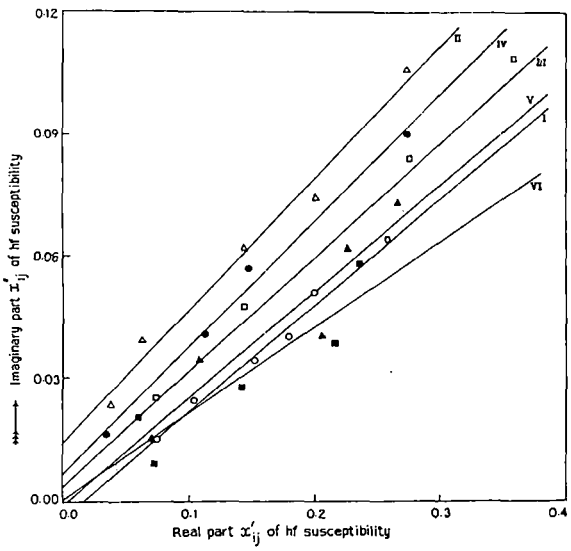

Figure 4. Linear plot of the imaginary part χ''_{ij} of the hf susceptibility against the real part χ'_{ij} of the isomers of the anisidine and toluidine in benzene at 35 °C under a 9.945 GHz electric field: (I) *o*-anisidine (——○——), (II) *m*-anisidine (——△——), (III) *p*-anisidine (——□——), (IV) *o*-toluidine (——●——), (V) *m*-toluidine (——▲——) and (VI) *p*-toluidine (——■——).

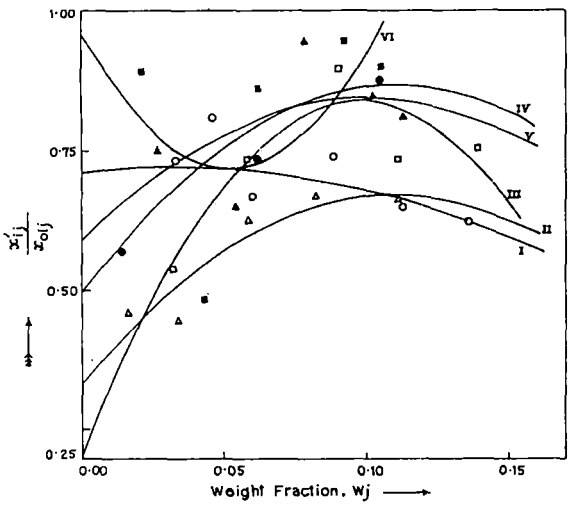

Figure 5. Plot of χ'_{ij}/χ_{0ij} against the weight fraction w_j of the solute of the isomers of the anisidine and toluidine in benzene at 35 °C under a 9.945 GHz electric field: (I) *o*-anisidine (——○——), (II) *m*-anisidine (——△——), (III) *p*-anisidine (——□——), (IV) *o*-toluidine (——●——), (V) *m*-toluidine (——▲——) and (VI) *p*-toluidine (——■——).

from bond angles and bond moments of the substituent polar groups of the molecules of figure 8.

4. Symmetric and characteristic relaxation times τ_s and τ_{cs}

The symmetric and asymmetric distribution parameters γ and δ appear in the following equations:

$$\chi^*_{ij}/\chi_{0ij} = \frac{1}{1 + (j\omega\tau_s)^{1-\gamma}} \tag{14}$$

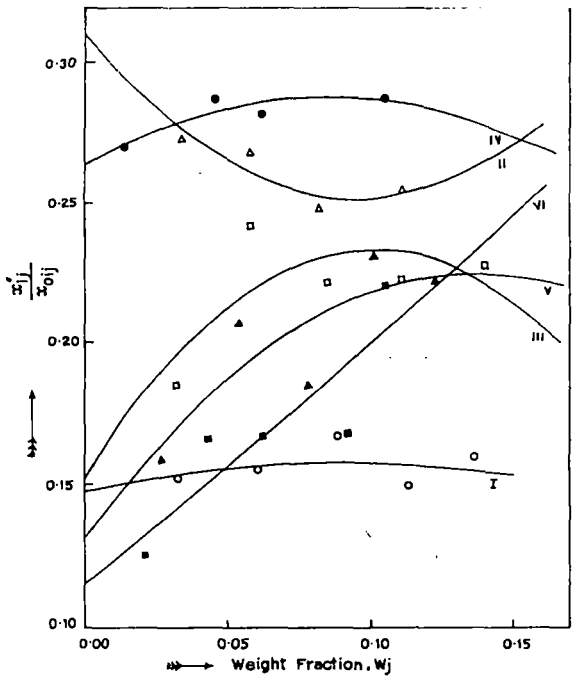

Figure 6. Plot of χ''_{ij}/χ_{0ij} against the weight fraction w_j of the solute of the isomers of the anisidine and toluidine in benzene at 35 °C under a 9.945 GHz electric field: (I) *o*-anisidine (——○——), (II) *m*-anisidine (——△——), (III) *p*-anisidine (——□——), (IV) *o*-toluidine (——●——), (V) *m*-toluidine (——▲——) and (VI) *p*-toluidine (——■——).

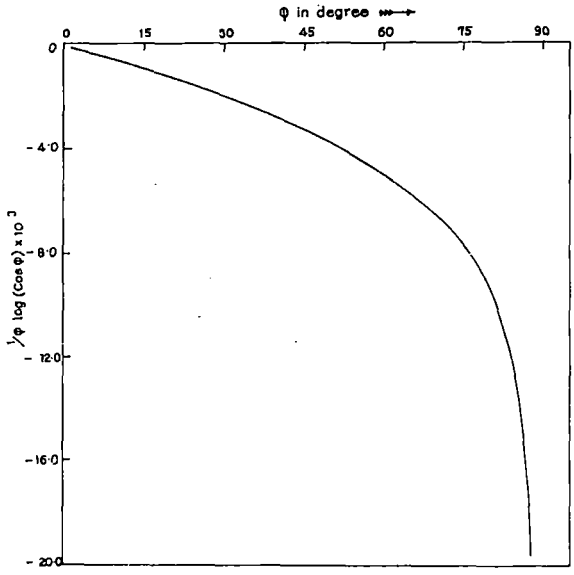

Figure 7. Variation of $(1/\phi)\log(\cos\phi) \times 10^3$ against ϕ in degrees.

$$\chi^*_{ij}/\chi_{0ij} = \frac{1}{(1 + j\omega\tau_{cs})^{\delta}}. \tag{15}$$

Although the left-hand side of equations (14) and (15) are identical, the former is associated with the symmetric relaxation time τ_s and latter with the characteristic relaxation

time τ_{cs}. Separating the real and imaginary parts of equations (14) and (15) and rearranging them in terms of $(\chi'_{ij}/\chi_{0ij})_{w_j\to 0}$ and $(\chi''_{ij}/\chi_{0ij})_{w_j\to 0}$ obtained from figures 5 and 6 the γ and τ_s were found using

$$\gamma = \frac{2}{\pi}\tan^{-1}\left[\left(1-\frac{\chi'_{ij}}{\chi_{0ij}}\right)\frac{\chi'_{ij}}{\chi''_{ij}}-\frac{\chi''_{ij}}{\chi_{0ij}}\right] \tag{16}$$

and

$$\tau_s = \frac{1}{\omega}\left[\frac{1}{(\chi'_{ij}/\chi''_{ij})\cos(\gamma\pi/2)-\sin(\gamma\pi/2)}\right]^{1/(1-\gamma)}. \tag{17}$$

Again δ and τ_{cs} can be obtained from equation (15)

$$\tan(\phi\delta) = \frac{\chi''_{ij}}{\chi'_{ij}} \tag{18}$$

and

$$\tan\phi = \omega\tau_{cs}. \tag{19}$$

As ϕ cannot be evaluated directly, an arbitrary theoretical curve between $(1/\phi)\log(\cos\phi)$ against ϕ in degrees was drawn in figure 7, from which

$$\frac{1}{\phi}\log(\cos\phi) = \frac{\log[(\chi'_{ij}/\chi_{0ij})/\cos(\phi\delta)]}{\phi\delta} \tag{20}$$

can be found. The known value of $(1/\phi)\log(\cos\phi)$ is used to obtain ϕ. With known ϕ and δ, τ_{cs} were found out from equations (18) and (19). τ_s and τ_{cs} so evaluated are given in table 2 in order to compare with values of τ by Murthy *et al* [10], Gopalakrishna [11] and τ_1 and τ_2 determined by double relaxation methods. The estimated values of γ and δ are however, given in table 3.

5. Results and discussion

The least-squares fitted linear equations of $(\chi_{0ij}-\chi'_{ij})/\chi'_{ij}$ against χ''_{ij}/χ'_{ij} for different weight fractions w_j's of the monosubstituted anilines in benzene at 35 °C under a 9.945 GHz electric field are shown graphically in figure 1, with the symbols denoting the experimental points. The experimental points are found to satisfy equation (5). χ'_{ij} and χ''_{ij} are the real and imaginary parts of the complex dielectric orientational susceptibility χ^*_{ij} and χ_{0ij} is the low-frequency dielectric susceptibility which is real. They are, however, derived from the measured relative permittivities [7] ϵ'_{ij}, ϵ''_{ij}, ϵ_{0ij} and $\epsilon_{\infty ij}$ of table 1. The linearity of all the curves of figure 1 are confirmed by correlation coefficients, τ's, lying in the range 0.6894–0.9986. The chisquare test of all the curves were again made to support their linearity. The slopes and intercepts of all the linear curves of figure 1 are placed in the second and third columns of table 2. The chisquare -values are, however, large for *o*-anisidine, *p*-anisidine and *m*-toluidine probably because of the large errors introduced in the ϵ'_{ij}, ϵ''_{ij}, ϵ_{0ij} and $\epsilon_{\infty ij}$ measurements for the molecules. In order to find the existence of double relaxation phenomena, accurate measurements of ϵ_{0ij} and $\epsilon_{\infty ij}$ are necessary. The refractive index n_{Dij} measured by Abbe's refractometer yields $\epsilon_{\infty ij} = n^2_{Dij}$ [6], although a Cole–Cole [3, 4] plot often gives $\epsilon_{\infty ij}$ as 1–1.15 times n^2_{Dij}.

The slope and intercept of each straight-line equation, (5), obtained from χ'_{ij}, χ''_{ij} and χ_{0ij} of different w_j's of table 1 by least-squares fitting are used to determine τ_1 and τ_2 for each compound, as seen in the sixth and seventh columns of table 2. τ_2's are found to increase gradually from the *meta* to the *ortho* and to the *para* forms for all the anisidines and toluidines, probably due to the presence of the C → NH_2 group in them. The electric field of nearly 3 cm wavelength greatly influences the C → NH_2 group. On the other hand, τ_1 increases from *ortho* to *para* for the anisidines, while the reverse is true for the toluidines. The increase in the τ_1 values indicates that the flexible parts of the molecules are more loosely bound to the parent molecules [17, 18], which signifies that the material property of the system is undergoing relaxation.

In the absence of a reliable τ_j under a hf electric field we tried to calculate τ_j's from the slopes of the least-squares fitted straight-line equations of χ''_{ij} against χ'_{ij} as claimed by Murthy *et al* [10], and give them in the ninth column of table 2. The available experimental points were found to deviate from linearity as illustrated in figure 4. The individual plots of χ'_{ij} and χ''_{ij} against the w_j's of the isomers of the anisidines and toluidines are not strictly linear as observed in figures 2 and 3. This at once prompted us to use the ratio of the individual slopes of variations of χ''_{ij} and χ'_{ij} with the w_j's at $w_j \to 0$ of figures 2 and 3 to obtain τ_j's. The τ_j's thus obtained agree well with τ_1 from double relaxation and Gopalakrishna's [11] methods. This confirms the basic soundness of the latter method to determine τ_j where polar–polar interactions are fully avoided. Moreover, it shows that the hf dielectric susceptibility measurement yields a microscopic relaxation time whereas the double relaxation method gives both microscopic and macroscopic τ_1 and τ_2, as observed elsewhere [19].

Larger τ_2's signify the larger sizes of the rotating units of solute–solvent, i.e. monomer formation under a hf electric field. The existence of a distribution of τ's between τ_2 and τ_1 helps us to test the symmetric and asymmetric distribution parameters γ and δ of such compounds. These are calculated from equations (16) and (18) with the values of χ'_{ij}/χ_{0ij} and χ''_{ij}/χ_{0ij} at $w_j \to 0$ of figures 5 and 6. The values of $(1/\phi)\log(\cos\phi)$ against ϕ in degrees as shown in figure 7 is essential to obtain δ. Knowing ϕ from the curve of figure 7, δ's were obtained. γ and δ so obtained are seen in the 11th and 12th columns of table 3. The values of γ establishes the non-rigid behaviour of the molecules in benzene in a 9.945 GHz electric field. They obey symmetric relaxation phenomena as δ's are found to be low.

The symmetric relaxation time τ_s from equation (17) agrees with the τ_1's and τ's due to Gopalakrishna's method [11] indicating symmetric relaxation behaviour for such molecules; but in case of *p*-anisidine the agreement is poor. It may probably be due to the experimental uncertainty or the presence of two flexible polar units in a line. The characteristic relaxation time τ_{cs} obtained from δ gives high values. They thus rule out the applicability of asymmetric relaxation behaviour for such polar molecules in benzene.

We find the relative contributions c_1 and c_2 towards dielectric dispersions for each polar compound, reported in tables and figures from equations (3) and (4) for fixed τ_1 and τ_2 of equation (5) and χ'_{ij}/χ_{0ij} and χ''_{ij}/χ_{0ij} of Fröhlich's equations, (6) and (7). The same could, however, be obtained

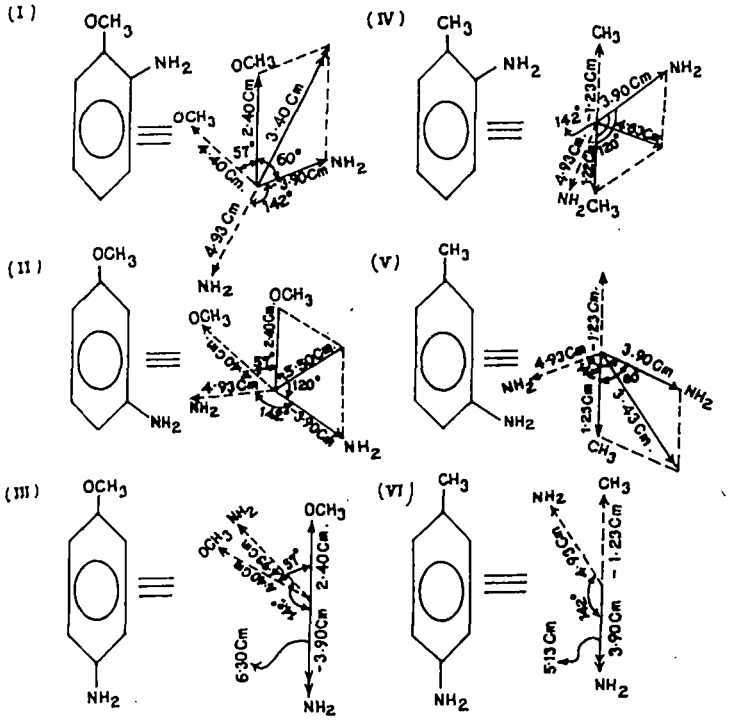

Figure 8. *Conformational structures of the isomers of the anisidine and toluidine. (The bond moments ($\times 10^{30}$ C m) are given in the figures).*

by a graphical technique. The c_1 and c_2 by both the methods are given in table 3. The Fröhlich's equations, (6) and (7), are related to Fröhlich's parameter, A, which predicts the temperature variation of the width of the distribution of τ. A is equal to $\ln(\tau_2/\tau_1)$. c_1 and c_2 obtained with χ'_{ij}/χ_{0ij} and χ''_{ij}/χ_{0ij} of Fröhlich's equations and the least-squares fitted graphically estimated values from figures 5 and 6 satisfy $c_1 + c_2 \simeq 1$. The variation of χ'_{ij}/χ_{0ij} and χ''_{ij}/χ_{0ij} with w_j usually do not obey Bergmann *et al*'s [13] equations, (1) and (2), as observed elsewhere [17, 18]. For *p*-toluidine c_2 becomes negative as seen in the tenth column of table 3. This arises due to the inertia of the whole molecule with respect to its flexible part under a nearly 10 GHz electric field [7, 19].

The dipole moments μ_1 and μ_2 of the flexible parts and whole molecules of all the compounds under investigation were obtained in terms of the dimensionless parameters b_1 and b_2 related to τ_1 and τ_2 and the linear coefficient β of the χ'_{ij}–w_j curve of figure 3. They are placed in the 11th and 12th columns of table 4 together with μ_0 in terms of b_0 related to τ_0, where τ_0 is the most probable relaxation time ($= \sqrt{\tau_1\tau_2}$) for the distribution of τ's between two fixed values. The correlation coefficients, τ's, of the χ'_{ij}–w_j curves were also estimated and are entered in the fifth column of table 4, but only to show how far the χ'_{ij}'s are correlated with the w_j's. The corresponding percentage of error in terms of τ are entered in the sixth column of table 4. The variation of the χ'_{ij}'s with the w_j's gives a reliable slope of β to yield reliable μ_1, μ_2 and μ_0 values. Almost all χ'_{ij}–w_j curves in figure 3 show a tendency to be closer in the region $0.00 \leqslant w_j \leqslant 0.03$, indicating an almost identical polarity of the solute molecules in addition to solute–solvent (monomer) and solute–solute (dimer) formations [9].

The solvent, benzene, is a cyclic compound with three double bonds and six p-electrons on six carbon atoms. Hence the π–π interaction or resonance effect combined with an inductive effect, known as the mesomeric effect, is expected to play an important role in the measured hf μ_j. Special attention is therefore paid to obtain the conformational structures of the isomers of anisidine and toluidine from the available bond angles and bond moments of the substituent polar groups. The polar groups C $\rightharpoonup$ NH_2 ($\angle 142°$), C $\rightharpoonup$ OCH_3 ($\angle 57°$) and C $\rightharpoonup$ CH_3 ($\angle 180°$) having bond moments of 3.90×10^{-30}, 2.40×10^{-30} and 1.23×10^{-30} C m, respectively, are used to obtain the theoretical μ_{theo} of figure 8. In the case of the anisidines, the amino group, $-NH_2$, exhibits a mesomeric effect by pushing the electrons towards the C atom of the benzene ring, but the inductive effect is more prominent in the $-OCH_3$ group rather than mesomeric effect; so the latter pulls the electrons from the C atom of the ring. Hence the resultant μ_{theo} increases from the *para* to the *ortho* and to the *meta* forms, as seen in table 4. In the case of the methyl group, $-CH_3$, in toluidines the inductive effect is important as the sp^2 hybridized C atom of benzene is more electronegative than the C atom of the $-CH_3$ group, which is sp^3 hybridized. Thus the direction of the bond moment is towards the benzene ring. For the $-NH_2$ group the mesomeric and inductive effects act oppositely, but as the mesomeric effect is more pronounced so resultant bond moment is towards the C_6H_6 ring. In the *ortho*, *meta* and *para* toluidines, the angle between the $-CH_3$ and $-NH_2$ groups are 60°, 120° and 180°, respectively. Hence there is an increment in μ_{theo} from the *ortho* to the *meta* and to the *para* forms (table 4).

In the absence of reliable μ_j values of these compounds Gopalakrishna's method [11] was employed to obtain hf μ_j's

(reported data). The close agreement between the reported μ_j (Gopalakrishna), μ_1 and μ_{theo} as seen in table 4 establishes the basic soundness of the method prescribed for obtaining hf μ_j. It also confirms the fact that a part of the molecule is rotating under a nearly 3 cm wavelength electric field.

6. Conclusions

The theoretical considerations for the effective utilization of the established symbols of the dielectric susceptibilities, χ_{ij}'s, from the dielectric relative permittivities ϵ_{ij}'s appear to be sound to study the dielectric relaxation mechanism as χ_{ij}'s are directly concerned with orientational polarization. The significant equations in terms of the χ_{ij}'s help one to grasp new physical insight into polar–polar and polar–non-polar molecular interactions in solution. The single-frequency measurement of the relaxation parameters thus provides a unique method to obtain macroscopic and microscopic relaxation times and hence dipole moments of the whole and the flexible parts of the molecules. The estimation of τ from the linear equation (5) is a very simple, straightforward and significant one to obtain μ from equation (13) in terms of linear coefficient β of the familiar χ'_{ij}–w_j curve. The correlation coefficient τ and the chisquare values signify the minimum error introduced into the desired parameters. The molecules under identical states show interesting phenomena of a double or, often, a single relaxation mechanism depending upon the solvent used. The probability of showing the double relaxation phenomena of monosubstituted anilines in benzene depends upon the electric field frequency of nearly 10 GHz. Various types of molecular associations, such as solute–solute and solute–solvent interactions, are thus inferred from the usual departure of graphically fitted plots of χ'_{ij}/χ_{0ij} and χ''_{ij}/χ_{0ij} with w_j following Bergmann's equations [13]. Non-rigid characteristics of the molecules are ascertained by estimation of symmetric and asymmetric distribution parameters in benzene. The molecular associations are also supported by the conformational structures of the molecules in which the mesomeric, inductive and electromeric effects play prominent roles.

References

[1] Sharma A and Sharma D R 1992 *J. Phys. Soc. Japan* **61** 1049
[2] Sit S K, Ghosh N, Saha U and Acharyya S 1997 *Indian J. Phys.* B **71** 533
[3] Cole K S and Cole R H 1941 *J. Chem. Phys.* **9** 341
[4] Davidson D W and Cole R H 1951 *J. Chem. Phys.* **19** 1484
[5] Jonscher A K 1980 *Physics of Dielectric Solids, Invited Papers* CHL Goodman
[6] Srivasta S C and Chandra S 1975 *Indian J. Pure Appl. Phys.* **13** 101
[7] Sit S K and Acharyya S 1996 *Indian J. Pure Appl. Phys.* **34** 255
[8] Jonscher A K 1980 *Inst. Phys. Conf. (Canterbury)* ed C H L Goodman
[9] Ghosh N, Karmakar A, Sit S K and Acharyya S 2000 *Indian J. Pure Appl. Phys.* **38** 574
[10] Murthy M B R, Patil R L and Deshpande D K 1989 *Indian J. Phys.* B **63** 491
[11] Gopalakrishna K V 1957 *Trans. Faraday Soc.* **53** 767
[12] Fröhlich H 1949 *Theory of Dielectrics* (Oxford: Oxford University Press)
[13] Bergmann K, Roberti D M and Smyth C P 1960 *J. Chem. Phys.* **64** 665
[14] Smyth C P 1955 *Dielectric Behaviour and Structure* (New York: McGraw-Hill)
[15] Dutta K, Sit S K and Acharyya S 2000 *Pramana: J. Phys.* at press
[16] Ghosh N, Basak R C, Sit S K and Acharyya S 2000 *J. Mol Liquids* **85** 375
[17] Saha U, Sit S K, Basak R C and Acharyya S 1994 *J. Phys. D: Appl. Phys.* **27** 596
[18] Sit S K, Basak R C, Saha U and Acharyya S 1994 *J. Phys. D: Appl. Phys.* **27** 2194
[19] Sit S K, Ghosh N and Acharyya S 1997 *Indian J. Pure Appl. Phys.* **35** 329

journal of
MOLECULAR
LIQUIDS

Editor-in-Chief:
Professor Josef Barthel

Institute of Physical and
Theoretical Chemistry
University of Regensburg
93040 Regensburg
Germany
Tel. No.: +49-941-943-4042
Fax No.: +49-941-943-4532
e-mail: Josef.Barthel@chemie.uni-regensburg.de

Associate Edito
Professor Werner Kur

Institute of Physical ar
Theoretical Chemistr
University of Regensbur
93040 Regensbur
German
Tel. No.: +49-941-943-404
Fax No.: +49-941-943-453
e-mail: Werner.Kunz@chemie.uni-regensburg.d

Dr. S. Acharyya
Dept. of hysics
Raiganj College
Raiganj – 733134
Uttar Dinajpur, India
e-mail: gkdutta@rediffmail.com

27.11.01

Our Ref.: MS 01045

Dear Dr. Acharrya

Thank you for the revised version of your paper MS 01026:

Double Relaxation Phenomena of Monosubstituted Anilinles in Benzene under High Frequency Electric Field.
N. Gosh, S.K.Sit and S. Acharyya

I will continue the publishing procedure. If there is no serious argument by the referees, you will not receive further mail. Minor errors of spelling etc. will be corrected here. You will be contacted by the publishing company for the copy-right and the reprints.

Please, do not hesitate to contact me when you think that I could be of any help to you.

We highly appreciated receiving a manuscript from you and hope that you will submit more manuscripts to us in the future.

With kind regards.

J. Barthel

Yours sincerely

Received on 7. 12. 01

Josef Barthel
Editor-in-Chief

Double relaxation phenomena of monosubstituted anilines in benzene under high frequency electric field.

N. Ghosh, S. K. Sit and S. Acharyya

Department of Physics, Raiganj College (University College) P.O. Raiganj, Dist. Uttar Dinajpur, Pin- 733134 (W.B.), India.

ABSTRACT

The intercept and slope of a derived linear equation : $(\chi_{oij} - \chi'_{ij}) / \chi'_{ij} = \omega (\tau_1+\tau_2) \chi''_{ij}/\chi''_{ij} - \omega^2\tau_1\tau_2$ for different weight fractions w_j's of monosubstituted anilines (j) in benzene(i) at 35°C under different electric field frequencies are used to yield the double relaxation times τ_1 and τ_2 of the flexible parts and the whole molecules. χ'_{ij} and χ''_{ij} are the real and imaginary parts of hf complex dielectric orientational susceptibility χ^*_{ij} and χ_{oij} is the low frequency dielectric susceptibility which is real. τ_j's obtained from the ratio of the individual slopes of variations of χ''_{ij} and χ'_{ij} with w_j's at $w_j \rightarrow 0$ are compared with Murthy et al (Indian J Phys **63 B** 1989 491) and Gopalakrishna (Trans Faradey. Soc. **53** 1957 767).The theoretical weighted contributions c_1 and c_2 for τ_1 and τ_2 from Fröhlichs' equations are compared with the experimental ones from the graphically fitted curves of χ'_{ij}/χ_{oij} and χ''_{ij}/χ_{oij} with w_j's in the limit $w_j = 0$. The values of $(\chi'_{ij}/\chi_{oij})w_j \rightarrow 0$ and $(\chi''_{ij}/\chi_{oij})w_j \rightarrow 0$ are again employed to get symmetric and asymmetric distribution parameters γ and δ, the latter one is from the curve of $1/\varphi \log \cos\varphi$ against φ^0 to yield the symmetric and characteristic relaxation times τ_s and τ_{cs} respectively only to show that symmetric relaxation behaviour obeyed by the molecules. The dipole moments μ_1 and μ_2 for the rotation of flexible parts and the whole molecules are measured from τ_1 and τ_2 and linear coefficient β's of the variations of χ_{ij}' and hf conductivity σ_{ij} with w_j's. The measured μ_1 and μ_2 are compared with the reported μ's and μ_{theo}'s of available bond angles and bond moments of the substituent polar groups of the parent molecules. The slight disagreement of measured μ's from μ_{theo}'s indicates the existence of inductive,mesomeric and electromeric effects suffered by the polar groups under hf electric field.

1. INTRODUCTION

In recent years, single or double relaxation phenomenon of polar liquid molecules in nonpolar solvents under high frequency (hf) electric field attracted the attention of a large number of workers [1, 2]. The study often provides the valuable information on the shape, size and structure, in addition to solute-solvent or solute-solute molecular associations in terms of the measured relaxation time τ and dipole moment μ by any conventional method [3, 4]. The stability and unstability [5] of the molecules towards dielectric relaxations, is, however, inferred from such study. τ_1 and τ_2 of the double relaxation method, τ_j from the ratio of slopes of the individual variations of χ''_{ij} and χ'_{ij} with weight fractions w_j's in the limit $w_j=0$ and μ_j's from the linear coefficient β's of either χ'_{ij}- w_j or hf conductivity σ_{ij}- w_j curves shed more light on the structural aspects of such dielectropolar liquid molecules [6] .

The real ε'_{ij} and imaginary ε''_{ij} parts of hf complex relative permittivity ε^*_{ij} together with the low frequency or static and optical relative permittivities ε_{oij} and $\varepsilon_{\infty ij}$ of isomers of methoxy substituted anilines (anisidines) and methyl substituted anilines (toluidines) in benzene under 2.02, 3.86 and 22.06 GHz electric field for different weight fractions w_j's were measured by Srivastava and Chandra [7] at 35°C. The analytical grade ortho, para toluidines and para-anisidines were supplied by M/S Riedel (Germany) and the others were of M/S BDH (London). The liquids were further purified by repeated fractional distillations and their physical constants like density ρ, viscosity η and refractive indices n_{Dij} were carefully checked in agreement with the literature values before use . The purpose of the study [7] was to detect the possible existence of solute-solvent (monomer) and solute-solute (dimer) molecular associations in the mixtures of various concentrations.

Nowadays, the usual trend is to study the dielectric relaxation processes in terms of hf complex dielectric orientational susceptibility χ^*_{ij} rather than hf complex conductivity σ^*_{ij} or hf relative permittivity ε^*_{ij}. ε^*_{ij} includes within it all types of polarisations while σ^*_{ij} is associated with transport of bound molecular charges. Hence it is more reasonable to work with χ_{ij}'s as they have direct link with the orientational polarisations [8]. Moreover, the present method of study in S.I unit is superior because of its unified, coherent and rationalised nature.

The dielectric susceptibilities like real $\chi'_{ij}=(\varepsilon'_{ij} - \varepsilon_{\infty ij})$ imaginary $\chi''_{ij} = \varepsilon''_{ij}$ parts of complex susceptibility $\chi^*_{ij} = (\varepsilon^*_{ij} - \varepsilon_{\infty ij})$ and the low frequency susceptibility $\chi_{oij} = (\varepsilon_{oij} - \varepsilon_{\infty ij})$ which is real, were derived from the measured relative permittivities ε'_{ij}, ε''_{ij}, ε_{oij} and $\varepsilon_{\infty ij}$ in each system for different w_js of the respective solute [7]. The experimental results of χ_{ij}'s for different w_j's are thus collected together in Table 1 for use. One could make a strong conclusion of double relaxation phenomena of a polar molecule in a nonpolar solvent based on single frequency measurement of the relaxation parameters provided the accurate value of χ_{oij} involved with ε_{oij} and $\varepsilon_{\infty ij}$ is available. The use of n^2_{Dij} for $\varepsilon_{\infty ij}$ [7] may often introduce additional error in the calculation. Nevertheless, the data presented in Table 1 are accurate up to 5% for χ''_{ij} and 2% for χ'_{ij} and χ_{oij} respectively.

The polar liquids like monosubstituted anilines often posses two or more τ's in GHz electric field for the rotation of their flexible polar groups to the parent molecules and the whole molecule itself [9]. Bergmann et al [10] devised a graphical method to obtain double relaxation times τ_1 and τ_2 and hence weighted contributions c_1 and c_2 towards dielectric dispersions for some complex polar liquid molecules. The mothod is based on plotting the measured values of ε', ε'', ε_0, ε_∞ at various frequencies ω on a semicircle in a complex plane. A point was then selected on the chord through two fixed points on the semicircle drawn in consistency with the experimental data. Bhattacharyya et al [11] subsequently modified the above procedure to get the same with experimental values measured at two different frequencies of GHz range.

Thus the object of the present paper is to detect the double relaxation times τ_1 and τ_2 due to rotations of the flexible parts and the whole molecules using χ_{ij}'s based on a single frequency measurement technique [7,12-13]. The aniline derivatives are thought to absorb electric energy much more strongly at nearly 10 GHz electric field. The parameters measured at 2.02, 3.86 and

Table-1 : Real ε'_{ij} and imaginary ε''_{ij} parts of hf complex relative permittivity ε_{ij}^* static and optical frequency hf relative permittivities ε_{oij} and $\varepsilon_{\infty ij}$ together with real χ'_{ij} and imaginary χ''_{ij} parts of hf complex dielectric orientational susceptibility χ^*_{ij} along with low frequency susceptibility χ_{oij} which is real for some monosubstituted anilines in benzene under different electric field frequencies at 35°C for various concentrations.

Systems with serial number & molecular weight M_j	Frequency (f) in GHz	Weight fraction w_j of solute	Measured dielectric relative permittivities				Dimensionless dielectric orientational susceptibilities		
			ε'_{ij}	ε''_{ij}	ε_{oij}	$\varepsilon_{\infty ij}$	χ'_{ij}	χ''_{ij}	χ_{oij}
(I)	(a)	0.0326	2.32	0.011	2.336	2.239	0.081	0.011	0.097
o-anisi-	3.86	0.0604	2.37	0.021	2.404	2.247	0.123	0.021	0.157
dine in		0.0884	2.44	0.029	2.459	2.255	0.185	0.029	0.204
benzene		0.1135	2.49	0.033	2.538	2.262	0.228	0.033	0.276
		0.1361	2.53	0.041	2.588	2.267	0.263	0.041	0.321
M_j=	(b)								
		0.0326	2.31	0.015	2.336	2.239	0.071	0.015	0.097
0.123kg	22.06	0.0604	2.36	0.026	2.404	2.247	0.113	0.026	0.157
		0.0884	2.40	0.041	2.459	2.255	0.145	0.041	0.204
		0.1135	2.42	0.053	2.538	2.262	0.158	0.053	0.276
		0.1361	2.56	0.065	2.588	2.267	0.293	0.065	0.321
		0.0160	2.31	0.018	2.315	2.235	0.075	0.018	0.080
		0.0336	2.25	0.026	2.384	2.241	0.009	0.026	0.143
(II)		0.0579	2.43	0.043	2.477	2.246	0.184	0.043	0.231
m-anisi	(a)	0.0823	2.51	0.059	2.553	2.253	0.257	0.059	0.300
dine in	3.86	0.1109	2.61	0.084	2.675	2.261	0.349	0.084	0.414
benzene									
M_j=		0.0160	2.29	0.021	2.315	2.235	0.055	0.021	0.080
0.123kg.	(b)	0.0336	2.32	0.038	2.384	2.241	0.079	0.038	0.143
	22.06	0.0579	2.36	0.068	2.477	2.246	0.114	0.068	0.231
		0.0823	2.40	0.080	2.553	2.253	0.147	0.080	0.300
		0.1109	2.43	0.115	2.675	2.261	0.169	0.115	0.414
(III)o-tolui-	2.02	0.0137	2.30	0.005	2.301	2.241	0.059	0.005	0.060
dine in		0.0459	2.38	0.013	2.392	2.250	0.130	0.013	0.142
benzene		0.0622	2.42	0.015	2.457	2.255	0.165	0.015	0.202
M_j=0.107kg.		0.1048	2.55	0.022	2.577	2.264	0.286	0.022	0.313
(IV) m-tolui-		0.0264	2.31	0.007	2.337	2.243	0.067	0.007	0.094
dine in	3.86	0.0538	2.37	0.016	2.413	2.248	0.122	0.016	0.165
benzene		0.0781	2.44	0.024	2.470	2.252	0.188	0.024	0.218
M_j =0.107kg.		0.1015	2.39	0.036	2.526	2.258	0.132	0.036	0.268
		0.1225	2.54	0.045	2.591	2.262	0.278	0.045	0.329
		0.0213	2.31	0.010	2.319	2.237	0.073	0.010	0.082
(V)	(a)	0.0428	2.32	0.016	2.367	2.244	0.076	0.016	0.123
p-tolui	3.86	0.0616	2.38	0.018	2.413	2.249	0.131	0.018	0.164
dine in		0.0916	2.46	0.029	2.483	2.254	0.206	0.029	0.229
benzene		0.1048	2.48	0.046	2.523	2.260	0.220	0.046	0.263
M_j = 0.107		0.0213	2.31	0.009	2.319	2.237	0.073	0.009	0.082
kg	(b)	0.0428	2.33	0.020	2.367	2.244	0.086	0.020	0.123
	22.06	0.0616	2.36	0.033	2.413	2.249	0.111	0.033	0.164
		0.0916	2.40	0.046	2.483	2.254	0.146	0.046	0.229
		0.1048	2.44	0.058	2.523	2.260	0.180	0.058	0.263

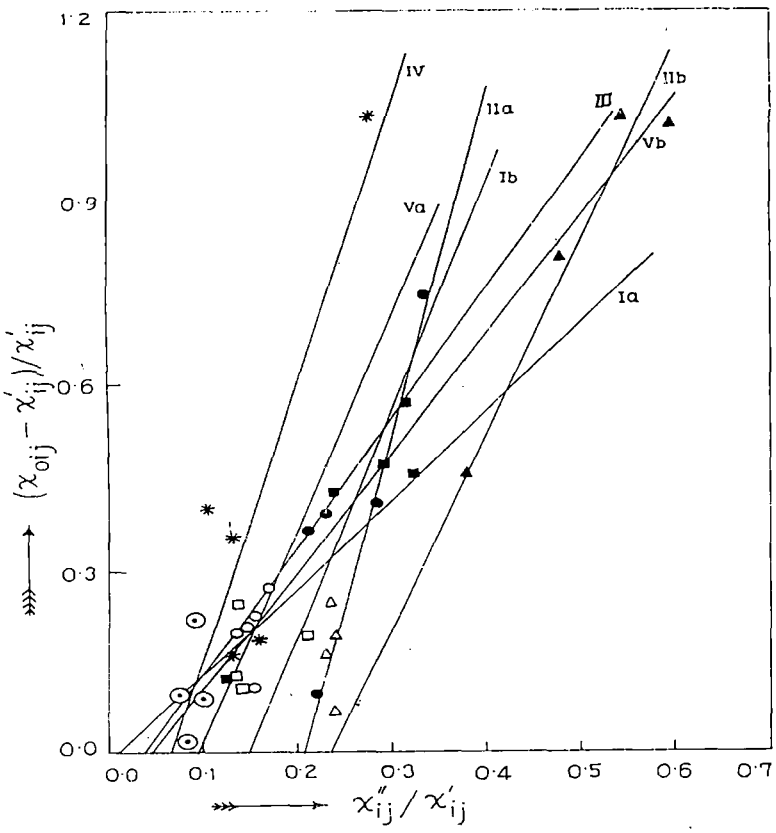

Figure 1 : Linear variation of $(\chi_{oij}-\chi'_{ij})/\chi'_{ij}$ against χ''_{ij}/χ'_{ij} of monosubstituted anilines in benzene at 35°C under GHz electric field.

(Ia) o-anisidine at 3.86 GHz (–O–), (Ib) o-anisidine at 22.06 GHz (–●–), (IIa) m-anisidine at 3.86 GHz (–Δ–), (IIb) m-anisidine at 22.06 GHz (–▲–), (III) o-toluidine at 2.02 GHz (–Θ–), (IV) m-toluidine at 3.86 GHz (–*–), (Va) p-toluidine at 3.86 GHz (–□–) and (Vb) p-toluidine at 22.06 (GHz (–■–) respectively.

22.06 GHz electric fields may yield considerable τ_1 and τ_2. Moreover, the present systems in terms of new physical parameters like χ_{ij}'s seem to yield a better insight into the relaxation phenomena. One is further tempted to see how far the linear coefficients β's of the variations of χ'_{ij}'s and σ_{ij} with w_j affect μ's. The aspect of molecular orientational polarisation, is, however, achieved by introducing χ_{ij}'s because $\varepsilon_{\infty ij}$ which includes the fast polarisation, always appears as a subtracted term in Bergmann et al's equations [10]. Thus in order to exclude the fast polarisation process and to avoid the clumsiness of algebra the established symbols of dielectric terminologies and parameters like $\chi'_{ij} = (\varepsilon'_{ij} - \varepsilon_{\infty ij})$, $\chi''_{ij} = \varepsilon''_{ij}$ and $\chi_{oij} = (\varepsilon_{oij} - \varepsilon_{\infty ij})$ of Table 1 are used in the Bergmann et. al's equations [10]:

$$\chi'_{ij}/\chi_{oij} = c_1/(1+\omega^2\tau_1^2) + c_2/(1+\omega^2\tau_2^2) \quad (1)$$

$$\chi''_{ij}/\chi_{oij} = c_1\omega\tau_1/(1+\omega^2\tau_1^2) + c_2\omega\tau_2/(1+\omega^2\tau_2^2) \quad (2)$$

assuming two separate broad dispersions for which the sum of c_1 and c_2 is unity. Equations (1) and (2) are now solved to get

$$(\chi_{oij} - \chi'_{ij})/\chi'_{ij} = \omega(\tau_1+\tau_2)\,\chi''_{ij}/\chi'_{ij} - \omega^2\tau_1\tau_2 \quad (3)$$

When the variables $(\chi_{oij} - \chi'_{ij})/\chi'_{ij}$ and χ''_{ij}/χ'_{ij} of equation (3) are plotted for different w_j's of a polar liquid at any given frequency ω of the applied electric field, a straight line results with intercept $-\omega^2\tau_1\tau_2$ and slope $\omega(\tau_1+\tau_2)$, as shown in Figure1. The intercept and slope of equation (3) are, however, obtained by linear regression analysis on the measured χ_{ij}'s of different w_j's of the monosubstituted anilines in C_6H_6 of Table 1 to get τ_1 and τ_2 as entered in the 7th and 8th columns of Table 2 extracted from the data of Table 1. The reliability of the data are checked through chisquares values. In absence of reliable τ_j, the ratio of individual slopes of variations of χ''_{ij} and χ'_{ij} with w_j's at $w_j \to 0$, as seen in Figures 2 and 3; were conveniently used to evaluate τ_j to compare with those of Murthy et al [14] of Figure 4 and Gopalakrishna [15].

Table 2: Intercept and slope of linear equation of $(\chi_{oij} - \chi'_{ij}) / \chi'_{ij}$ against χ''_{ij} / χ'_{ij}, correlation coefficient (r) and chisquare values, estimated relaxation times τ_1 and τ_2 due to rotation of flexible polar group and whole molecule, measured τ_j from Eq (16) and (17), reported τ (Gopalakrishna) symmetric and characteristic relaxation times τ_s and τ_{cs} of Eq. (11) and (13) of some monosubstituted anilines in benzene at 35°C under different GHz electric field frequencies.

Systems with serial number	Frequency (f) in GHz	Intercept and slope of Eq (3)		Correlation coefficient(r) and chisquares values of Eq(3)		Estimated relaxation times τ_1 & τ_2 in p.sec		Measured τ (ps)[a]	Ratio of slopes of χ''_{ij}-w_j & χ'_{ij}-w_j curves at $w_j \rightarrow 0$
(I) o-anisidine in benzene	(a) 3.86	0.0179	1.4360	0.3032	0.07	0.52	58.73	6.29	0.1891
	(b) 22.06	0.5406	3.6741	0.8277	0.23	1.11	25.41	1.59	0.1601
(II) m-anisidine in benzene	(a) 3.86	1.1404	5.5485	0.9999	0.15	8.82	220.07	7.61	0.2188
	(b) 22.06	0.7318	3.1447	0.9803	0.02	1.83	20.87	5.55	0.5413
(III) o-toluidine in benzene	2.02	0.0773	2.0910	0.2402	0.02	2.97	161.86	5.70	0.1536
(IV) m-toluidine in benzene	3.86	0.2938	4.5092	0.8469	0.51	2.73	183.29	6.53	0.3792
(V) p-toluidine in benzene	(a) 3.86	0.3149	3.4446	0.6480	0.30	3.88	183.22	7.64	0.2116
	(b) 22.06	0.0821	1.9151	0.9408	0.03	0.32	13.51	3.19	46.1743

Systems with serial number	Frequency (f) in GHz	Relaxation times			
		τ (ps)[b]	τ (ps)[c]	τ_s (ps)	τ_{cs} (ps)
(I) o-anisidine in benzene	(a) 3.86	7.80	5.25	0.92	471.52
	(b) 22.06	1.15	1.56	0.90	—
(II) m-anisidine in benzene	(a) 3.86	9.02	8.05	12.30	90.52
	(b) 22.06	3.91	4.41	2.33	14.80
(III) o-toluidine in benzene	2.02	12.11	4.97	17.06	—
(IV) m-toluidine in benzene	3.86	15.64	7.05	2.23	1181.32
(V) p-toluidine in benzene	(a) 3.86	8.73	7.65	8.15	—
	(b) 22.06	333.30	5.53	2.11	—

a. Measured by slope of χ''_{ij} against χ'_{ij} using Eq. (16)

b. From the ratio of individual slopes

c. By Gopalakrishna's method [15]

The theoretical weighted contributions c_1 and c_2 due to measured τ_1 and τ_2 from equation (3) were worked out from Fröhlichs' equations [16] and are placed in Table 3 inorder to compare them with the experimental ones from the intercepts of the least squares fitted curves of χ'_{ij} / χ_{oij} and χ''_{ij} / χ_{oij} against w_j's from Figures 5 and 6 in the limit $w_j = 0$. The values of χ'_{ij} / χ_{oij} and χ''_{ij} / χ_{oij} at $w_j = 0$ together with arbitrary curve of $1/\varphi$ log (Cos φ) against φ in degrees shown elsewhere [17] are further used to obtain symmetric and asymmetric distribution parameters γ and δ as seen in Table 3 to conclude the symmetric relaxation behaviour of such molecules. Symmetric relaxation time τ_s from γ and characteristic relaxation time τ_{cs} from δ and φ are further estimated in order to compare with τ_1, τ_2 and τ_j of Table 2.

The dipole moments μ_1 and μ_2 by both hf susceptibility and conductivity measurement techniques are, however, worked out from linear coefficient β's of χ'_{ij}-w_j and σ_{ij}-w_j curves of Figures 3 and 7 interms of b_1, b_2 involved with the estimated τ_1, τ_2 by double relaxation method. The μ_1 and μ_2 thus obtained are placed in Table 4 to see how far they are affected by the orientational polarisation and bound molecular charge in connection with χ_{ij}'s and σ_{ij}'s respectively. The estimated μ_1 and μ_2 by both the methods are finally compared with reported μ's (Gopalakrishna) and μ_{theo}'s from bond angles and bond moments of polar groups of the molecules to support their conformations. The slight disagreement between measured μ_j's and μ_{theo}'s invites the existence of inductive, mesomeric and electromeric effects suffered by polar groups, in addition to weak molecular associations between the polar molecules.

2. WEIGHTED CONTRIBUTIONS C_1 AND C_2 FOR τ_1 AND τ_2

By putting $\alpha_1 = \omega\tau_1$ and $\alpha_2 = \omega\tau_2$ the equations (1) and (2) are solved to get

$$c_1 = \frac{(\chi'_{ij}\,\alpha_2 - \chi''_{ij})\,(1+\alpha_1^2)}{\chi_{oij}\,(\alpha_2 - \alpha_1)} \tag{4}$$

and

$$c_2 = \frac{(\chi''_{ij} - \chi'_{ij}\,\alpha_1)\,(1+\alpha_2^2)}{\chi_{oij}\,(\alpha_2 - \alpha_1)} \tag{5}$$

provided $\alpha_2 > \alpha_1$. The theoretical values of c_1 and c_2 towards dielectric relaxations were, however, obtained from equations (4) and (5) with the help of Fröhlich's following theoretical equations [16]:

$$\chi'_{ij}/\chi_{oij} = 1 - \frac{1}{2A} \ln\left[\frac{1+\omega^2\tau_2^2}{1+\omega^2\tau_1^2}\right] \tag{6}$$

$$\chi''_{ij} / \chi_{oij} = 1/A\,[\tan^{-1}(\omega\tau_2) - \tan^{-1}(\omega\tau_1)] \tag{7}$$

in terms of the measured τ_1 and τ_2 as presented in Table 2 from equation (3) of double relaxation method.

The theoretical c_1 and c_2 as entered in Table 3 are compared with the experimental ones obtained from the intercepts of fitted parabolic curves of χ'_{ij} / χ_{oij} and χ''_{ij} / χ_{oij} against w_j of Figures 5 and 6 in the limit $w_j = 0$ and equations (3) and (4). The curves in Figure 5 and 6 drawn

by the regression analysis of polynomial fitting, are thought to yield the accurate values of χ'_{ij}/χ_{oij} and χ''_{ij}/χ_{oij} in the limit $w_j = 0$ in comparison to earlier graphical extrapolation technique based on personal judgement. The Fröhlich's parameter $A = \ln(\tau_2/\tau_1)$ are placed in Table 3 for each compound at different frequencies.

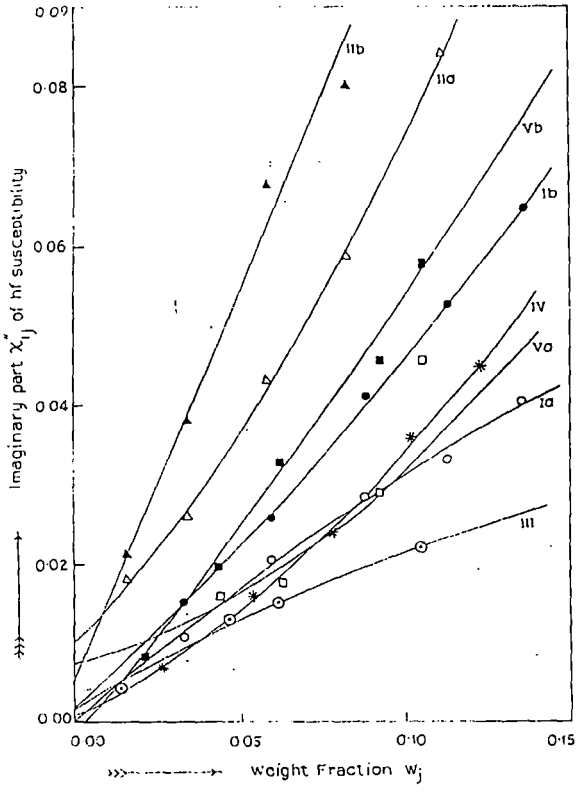

Figure 2 : Variation of imaginary part of hf susceptibility χ''_{ij} against weight fraction w_j of monosubstituted anilines in benzene at 35°C uner GHz electric field.

(Ia) o-anisidine at 3.86 GHz (–O–), (Ib) o-anisidine at 22.06 GHz (–●–), (IIa) m-anisidine at 3.86 GHz (–Δ–), (IIb) m-anisidine at 22.06 GHz (–▲–), (III) o-toluidine at 2.02 GHz (–O–), (IV) m-toluidine at 3.86 GHz (–*–), (Va) p-toluidine at 3.86 GHz (–□–) and (Vb) p-toluidine at 22.06 (GHz (–■–) respectively.

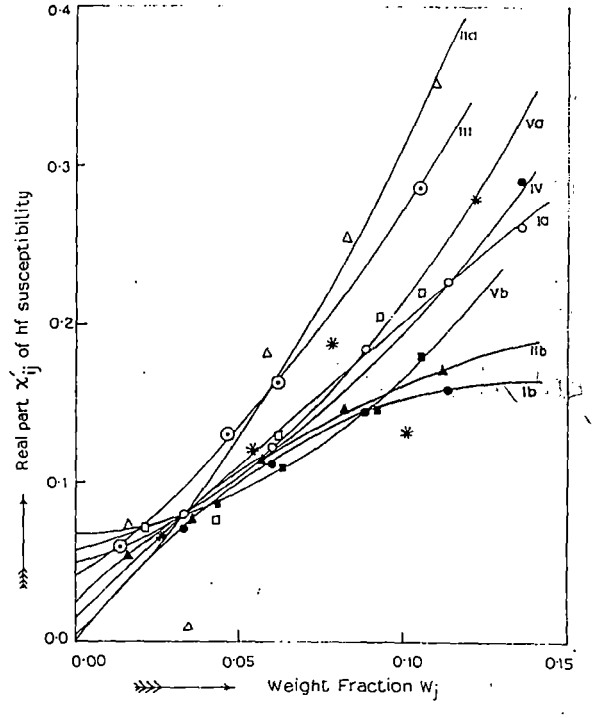

Figure 3 : Variation of real part of hf susceptibility χ'_{ij} against weight fraction w_j of monosub-stituted anilines in benzene at 35°C under GHz electric field.

(Ia) o-anisidine at 3.86 GHz (–O–), (Ib) o-anisidine at 22.06 GHz (–●–), (IIa) m-anisidine at 3.86 GHz (–Δ–), (IIb) m-anisidine at 22.06 GHz (–▲–), (III) o-toluidine at 2.02 GHz (–O–), (IV) m-toluidine at 3.86 GHz (–*–), (Va) p-toluidine at 3.86 GHz (–□–) and (Vb) p-toluidine at 22.06 (GHz (–■–) respectively.

3. SYMMETRIC AND CHARACTERISTIC RELAXATION TIMES τ_s AND τ_{cs}

The molecules under the present investigation appear to behave like non-rigid ones at 2.02, 3.86 and 22.06 GHz electric field having either symmetric or asymmetric distribution parameters γ and δ involved in the equations (8) and (9):

$$\frac{\chi_{ij}^*}{\chi_{oij}} = \frac{1}{1 + (j\omega\tau_s)^{1-\gamma}} \qquad (8)$$

$$\frac{\chi_{ij}^*}{\chi_{oij}} = \frac{1}{(1 + j\omega\tau_{cs})^{\delta}} \qquad (9)$$

Table 3 : Fröhlich's parameter A, χ'_{ij}/χ_{oij} and χ''_{ij}/χ_{oij} values estimated from Fröhlichs equations (6) and (7) with estimated τ_1 and τ_2 and those obtained from figures (5) and (6) at $w_j \rightarrow 0$, weighted contributions c_1 and c_2 from Fröhlichs method and those by graphical technique together with symmetric and asymmetric distribution parameters γ and δ of some monosubstituted anilines in benzene at 35°C under different electric field frequencies in GHz range.

Systems with serial number	Frequ.-ency (f) in GHz	Fröhlich para-meter (A)	Estimated values of χ'_{ij}/χ_{oij} & χ''_{ij}/χ_{oij} of Fröhlich's equations (6) &(7)		Weighted cont-ributions c_1 & c_2 from Eqs(4) &(5)		Estimated values of χ'_{ij}/χ_{oij} & χ''_{ij}/χ_{oij} from Figs.(5) & (6) at $w_j \rightarrow 0$	
(I) o-anisi-dine	(a) 3.86	4.7269	0.8829	0.2001	0.7491	0.4053	0.7613	0.0859
	(b) 22.06	3.1308	0.5893	0.3646	0.5200	1.0893	1.0006	0.1086
(II) m-anisi dine	(a) 3.86	3.2169	0.4811	0.3650	0.4496	1.5081	0.7527	0.2389
	(b) 22.06	2.4340	0.5534	0.4063	0.4816	0.9439	0.7468	0.2508
(III) o-tolui-dine	2.02	3.9982	0.7936	0.2699	0.6755	0.6212	1.0700	0.0841
(IV) m-tolui-dine	3.86	4.2068	0.6401	0.3049	0.5826	1.2450	0.7858	0.0475
(V) p-tolui-dine	(a) 3.86	3.5730	0.6509	0.3320	0.5727	1.0167	0.9901	0.1639
	(b) 22.06	3.7429	0.7992	0.2766	0.6685	0.5943	1.1134	0.0399

Systems with serial number	Frequ-ency (f) in GHz	Weighted contribu-tions c_1 & c_2 from graphical tech-nique		symme-tric distribu-tion para-meter γ	Asymmetric distribution parameter δ
(I) o-anisi-dine	(a) 3.86	0.7073	0.1637	0.7089	0.0757
	(b) 22.06	1.0380	–0.1801	–0.0724	—
(II) m-anisi dine	(a) 3.86	0.7712	0.4485	0.3155	0.2688
	(b) 22.06	0.7699	0.2181	0.2969	0.2901
(III) o-tolui-dine	2.02	1.0498	0.1133	–0.4921	—
(IV) m-tolui-dine	3.86	0.7903	–0.0213	0.8230	0.0393
(V) p-tolui-dine	(a) 3.86	0.9769	0.2657	–0.0661	—
	(b) 22.06	1.1208	–0.0233	–0.8078	—

The former one (eq. 8) is associated with symmetric relaxation time τ_s and the latter one (eq. 9) with characteristic relaxation time τ_{cs}. Separating the real and imaginary parts of equations (8)

and (9) and rearranging them in terms of χ'_{ij} / χ_{oij} and χ''_{ij} / χ_{oij} at $w_j \rightarrow 0$ of Figures 5 and 6, γ and τ_s were obtained from :

$$\gamma = \frac{2}{\pi} \tan^{-1} \left[(1 - \chi'_{ij} / \chi_{oij}) \frac{\chi'_{ij}}{\chi''_{ij}} - \frac{\chi''_{ij}}{\chi_{oij}} \right] \tag{10}$$

and

$$\tau_s = \frac{1}{\omega} \left[\frac{1}{(\chi'_{ij} / \chi''_{ij}) \text{ Cos } (\gamma\pi / 2) - \text{Sin } (\gamma\pi / 2)} \right]^{1/(1-\gamma)} \tag{11}$$

Similarly, δ and τ_{cs} can be had from equation (9) :

$$\tan (\varphi\delta) = \frac{(\chi''_{ij} / \chi_{oij})\ w_j \rightarrow 0}{(\chi'_{ij} / \chi_{oij})\ w_j \rightarrow 0} \tag{12}$$

and, $\tan \varphi = \omega\tau_{cs}$ (13)

As φ can not be evaluated directly; an arbitrary theoretical curve between $1/\varphi \log \text{Cos } \varphi$ against φ in degrees was drawn elsewhere [17] from which

$$\frac{1}{\varphi} \log \text{Cos } \varphi = \log \left[\frac{\chi'_{ij} / \chi_{oij}}{\text{Cos } \varphi\delta} \right] / \varphi\delta \tag{14}$$

can be known. The known values of $1/\varphi \log \text{Cos } \varphi$, is used to know φ from $1/\varphi \log \text{Cos } \varphi$ against φ curve. With known φ equations (12) and (13) were used to obtain δ and τ_{cs} respectively. τ_s and τ_{cs} so evaluated are entered in Table 2 to compare with τ_j's by Murthy et al [14], freshly calculated Gopalakrishna [15] and τ_1 & τ_2 by double relaxation methods. Estimated γ and δ are shown in Table 3.

4. THEORETICAL FORMULATIONS TO OBTAIN HF DIPOLE MOMENT μ_j

(A) hf susceptibility method

The real ε'_{ij} and imaginary ε''_{ij} parts of hf complex relative permittivity ε^*_{ij} are related by:

$$\varepsilon'_{ij} = \varepsilon_{\infty ij} + (1/\omega\tau)\ \varepsilon''_{ij}$$

$$\varepsilon'_{ij} - \varepsilon_{\infty ij} = (1/\omega\tau)\ \varepsilon''_{ij}$$

$$\chi'_{ij} = (1/\omega\tau)\ \varepsilon''_{ij} \tag{15}$$

and, $$(d\chi''_{ij} / d\chi'_{ij}) = \omega\tau \tag{16}$$

χ''_{ij}'s are expected to vary linearly with χ'_{ij} [14] as seen in Figure 4. The slope of linear equation of χ''_{ij} and χ'_{ij} was used to get τ_j from equation (16).

But the variations of χ''_{ij} with χ'_{ij} in Figure 4 are not strictly linear, the ratio of individual slopes of variations of χ''_{ij} and χ'_{ij} with w_j's in Figures 2 and 3 is a better representation of

equation (16) to get τ_j where the polar - polar interactions are supposed to be almost eliminated. Thus

$$(d\chi''_{ij}/dw_j)\, w_j \to 0 \,/\, (d\chi'_{ij}/dw_j)\, w_j \to 0 = \omega\tau_j \qquad (17)$$

The imaginary part χ''_{ij} of χ^*_{ij} is [18,19]

$$\chi''_{ij} = (N\rho_{ij}\mu^2_j / 27\varepsilon_0 M_j K_B T).\omega\tau / (1+\omega^2\tau^2)(\varepsilon_{ij}+2)^2 w_j \qquad (18)$$

which on differentiation with respect to w_j and at $w_j \to 0$ yields that

$$(d\chi''_{ij}/dw_j) w_j \to 0 = (N\rho_i\mu^2_j / 27\varepsilon_0 M_j K_B T).\omega\tau/(1+\omega^2\tau^2)(\varepsilon_i+2)^2 \qquad (19)$$

From equations (17) and (19) one obtains

$$\omega\tau\,(d\chi'_{ij}/dw_j)\, w_j \to 0 = (N\rho_i\mu^2_j/27\varepsilon_0 M_j K_B T).\omega\tau/(1+\omega^2\tau^2)(\varepsilon_i+2)^2$$

or,
$$\mu_j = \left[\frac{27\varepsilon_0 M_j K_B T\beta}{N\rho_i(\varepsilon_i+2)^2 b}\right]^{1/2} \qquad (20)$$

Where ε_0 = the permittivity of free space = 8.854×10^{-12} F.m.$^{-1}$ and

β = linear coefficient of χ'_{ij}-w_j curves of Figure 3 at $w_j \to 0$.

(B) hf conductivity method

According to Murphy and Morgan [20] the real and imaginary parts of hf conductivity are related by :

$$\sigma''_{ij} = \sigma_{\infty ij} + (1/\omega\tau)\,\sigma'_{ij} \qquad (21)$$

$\sigma'_{ij} = \omega\varepsilon_0\varepsilon''_{ij}$ and $\sigma''_{ij} = \omega\varepsilon_0\varepsilon'_{ij}$ are the real and imaginary parts of hf complex conductivity σ^*_{ij}. $\omega = 2\pi f$ and f is the frequency of applied electric field in GHz.

$$(d\sigma''_{ij}/dw_j)\, w_j \to 0 = (1/\omega\tau)(d\sigma'_{ij}/dw_j)\, w_j \to 0$$

Since in hf region $\sigma''_{ij} \cong \sigma_{ij}$ and σ_{ij} = the total hf conductivity = $\omega\varepsilon_0(\varepsilon'^2_{ij} + \varepsilon''^2_{ij})^{1/2}$

one has $(d\sigma'_{ij}/dw_j) w_j \to 0 = \omega\tau\beta$ (22)

where β is the linear coefficient of σ_{ij} - w_j curve of Figure 7 in the limit $w_j = 0$.

Again, the real part σ'_{ij} of hf complex conductivity σ^*_{ij} is [18,22].

$$\sigma'_{ij} = \frac{N\mu^2_j\rho_{ij}}{27M_jK_BT}\left[\frac{\omega^2\tau}{1+\omega^2\tau^2}\right](\varepsilon_{ij}+2)^2 w_j \qquad (23)$$

which on differentiation with respect to w_j and at $w_j \to 0$ yields

$$(d\sigma'_{ij}/dw_j) w_j \to 0 = \frac{N\mu^2_j\rho_i}{27M_jK_BT}\left[\frac{\omega^2\tau}{1+\omega^2\tau^2}\right](\varepsilon_i+2)^2 \qquad (24)$$

From equations (22) and (24) one gets

$$\mu_j = \left[\frac{27M_jK_BT\beta}{N\rho_i(\varepsilon_i+2)^2\omega b}\right]^{1/2} \quad (25)$$

Where β = linear coefficient of σ_{ij} - w_j curve of Figure 7 at $w_j \rightarrow 0$. In both the equations (20) and (25) N= Avogadros number = 6.023 X 10^{23}, ρ_i = density of solvent (C_6H_6) = 865kg.m^{-3}, ε_i= relative permittivity of solvent (C_6H_6) = 2.253, M_j = molecular weight of solute in kg., K_B= Boltzmann constant = 1.38 X 10^{-23} J. $mole^{-1}$. K^{-1} and $b = 1/(1+\omega^2\tau^2)$ = dimensionless parameter involved with measured τ.

Dipole moments μ_1 & μ_2 in terms of b_1, b_2 involved with τ_1 & τ_2 were computed from both the equations (20) and (25) as well with the linear coefficients β's of both, χ'_{ij} - w_j and σ_{ij} - w_j curves of Figures 3 and 7 respectively. All μ_j's are placed in Table 4 together with μ_{theo}'s and reported μ_j's (Gopalakrishna) for comparison.

Table 4 : Linear coefficient β's, correlation coefficient (r) and % of error of χ'_{ij}-w_j and σ_{ij}-w_j curves of figures 3 and 7, estimated dipole moments μ_1 & μ_2 for rotations of flexible polar groups and whole molecule by susceptibility and conductivity measurement techniques, dimensionless parameters b_1 and b_2 together with theoretical dipole moment μ_{theo} obtained from bond angles and bond moments, reported μ (Gopalakrishna) of some monosubstituted anilines in benzene at 35°C under different electric field frequencies.

Systems with serial number & molecular weight M_j	Frequency (f) in GHz	Liner coefficient of curves of figs 3 & 7	Correlation coefficient and % of error involved in curves of figs 3 & 7		Dimensionless parameters $b_1 = 1/(1+\omega^2\tau_1^2)$	$b_2 = 1/(1+\omega^2\tau_2^2)$	Estimated $\mu \times 10^{30}$ in C.m from Eqs. (20) & (25) μ_1	μ_2	$\mu_{theo} \times 10^{30}$ in C.m	$\mu \times 10^{30}$ in C.m from Gopalakrishnas method
(I) o-anisidine in C_6H_6	(a) 3.86	1.9358 0.4890	0.9980 0.9984	0.12 0.10	0.9998	0.3304	5.07 5.50	8.81 9.56	3.40	5.03
M_j = 0.123kg	(b) 22.06	2.4031 17.3978	0.9102 0.9316	5.18 3.98	0.9769	0.0747	5.71 13.88	20.66 50.19		5.23
(II) m-anisidine in C_6H_6	(a) 3.86	1.8788 0.4623	0.9417 0.9508	3.41 2.89	0.9563	0.0339	5.10 5.46	27.10 29.01	5.50	6.33
M_j = 0.123kg.	(b) 22.06	1.8214 2.5571	0.9934 0.9963	0.40 0.22	0.9396	0.1068	5.07 5.42	15.03 16.08		5.13
(III) o-toluidine in C_6H_6	2.02	1.4846	0.9966	0.23	0.9986	0.1917	4.14	9.45	4.63	5.37
M_j=0.107kg.		0.1981	0.9981	0.13			4.51	10.30		
(IV) m-toluidine in C_6H_6	3.86	0.5720	0.8479	8.48	0.9956	0.0482	2.57	11.69	3.43	4.90
M_j=0.107kg.		0.1265	0.8732	7.16			2.61	11.87		
(V) p-toluidine in C_6H_6	(a) 3.86	0.4791 0.1638	0.9755 0.9825	1.46 1.04	0.9912	0.0818	2.36 2.98	8.22 10.38	5.13	5.00
M_j=0.107kg.	(b) 22.06	0.0109 0.3762	0.9819 0.9864	1.08 0.81	0.9980	0.2221	0.35 1.88	0.75 3.99		3.37

5. RESULTS AND DISCUSSION

The least squares fitted straight line equations in terms of χ'_{ij}, χ''_{ij} and χ_{oij} of Table 1 were worked out for each system as shown graphically in Figure 1 at different w_j of solute in benzene at 35°C under GHz electric field with the experimental points placed upon them. χ'_{ij} and χ''_{ij} are real and imaginary parts of hf complex dimensionless dielectric orientational susceptibility χ^*_{ij} and χ_{oij} is the static or low frequency real dielectric susceptibility. They are, however, derived from measured [7] relative permittivities ε'_{ij}, ε''_{ij}, ε_{oij} and $\varepsilon_{\infty ij}$ of Table 1. The correlation coefficients (r) and chisquare values placed in the 5th and 6th columns of Table 2 are estimated to show how far the variables $(\chi_{oij}-\chi'_{ij}) / \chi'_{ij}$ and χ''_{ij} / χ'_{ij} of equation (3) are correlated. It is seen that r is low for o-anisidine at 3.86 GHz and o-toluidine at 2.02 GHz possibly for errors introduced in the measurement of ε'_{ij}, ε''_{ij}, ε_{oij} and $\varepsilon_{\infty ij}$. This fact is also confirmed by remarkable deviations of experimental data from linear curves of Figure 1. In order to locate the double relaxation phenomena accurate measurements of ε_{oij} and $\varepsilon_{\infty ij}$ are essential. The refractive index n_{Dij} measured by Abbes refractometer often yields $\varepsilon_{\infty ij} = n^2_{Dij}$ [7] although Cole - Cole [3] and Cole - Davidson [21] plots give $\varepsilon_{\infty ij}$ as (1.0 - 1.15) times of n^2_{Dij}. The intercepts and slopes of linear curves of Figure 1 are seen in the 3rd and 4th columns of Table 2, to get τ_1 and τ_2 due to rotation of flexible polar groups and end over end rotations of the whole molecules. τ_1 and τ_2 thus measured are presented in the 7th and 8th columns of Table 2. τ_2's in Table 2 increases gradually from meta to ortho for anisidines at 22.06 GHz while the reverse is true at 3.86 GHz. But incase of toluidines τ_2 increases from para to ortho and to meta forms. This behaviour is, however, explained by the fact that C → NH_2 group is significantly influenced by GHz electric field. On the other hand τ_1 increases from ortho to meta forms for anisidines while it increases from meta to ortho and to para forms for toluidines. This behaviour, however, indicates that flexible parts of the molecules are loosely bound to the parent molecules [12, 13].

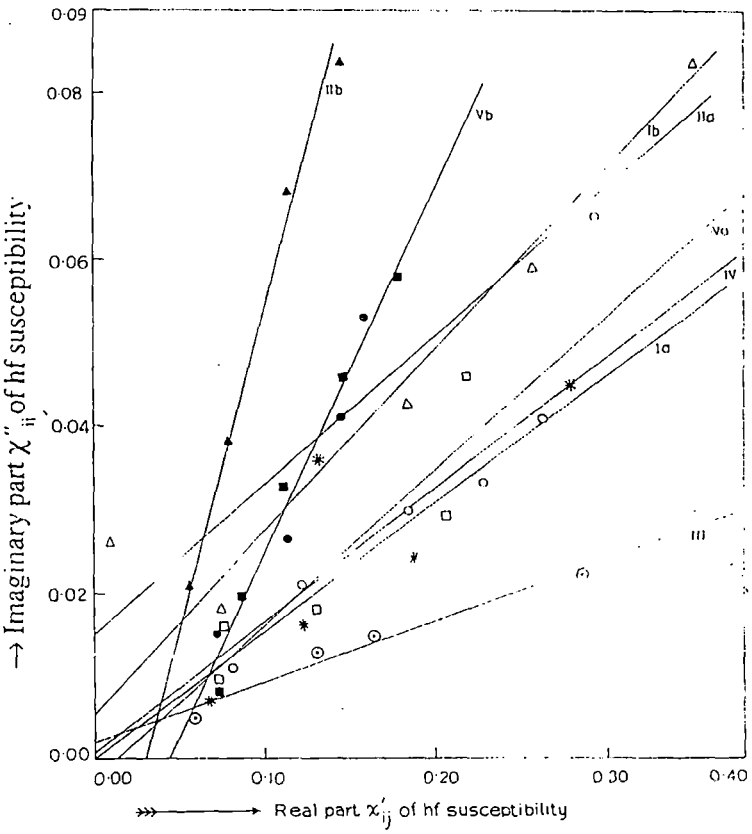

Figure 4 : Linear plot of imaginary part of hf susceptibility χ''_{ij} against real part χ'_{ij} of monosubstituted anilines in benzene at 35°C under GHz electric field.

(Ia) o-anisidine at 3.86 GHz (–○–), (Ib) o-anisidine at 22.06 GHz (–●–), (IIa) m-anisidine at 3.86 GHz (–Δ–), (IIb) m-anisidine at 22.06 GHz (–▲–), (III) o-toluidine at 2.02 GHz (–⊙–), (IV) m-toluidine at 3.86 GHz (–*–), (Va) p-toluidine at 3.86 GHz (–□–) and (Vb) p-toluidine at 22.06 (GHz (–■–) respectively.

In absence of reliable τ_j's of monosubstituted anilines the slopes of the least squares fitted straight line curves of χ''_{ij} against χ'_{ij} of Figure 4 as claimed by Murthy et al [14] were used to

get τ_j from equation (16). They are placed in the 9th column of Table 2. The experimental points of Table 1 are found to deviate from linearity of Figure 4 due to solute - solute molecular interactions. The individual variations of χ''_{ij} and χ'_{ij} with w_j are not strictly linear as seen in Figures 2 and 3 . This fact at once prompted one to use the ratio of slopes of the individual variations of χ''_{ij} and χ'_{ij} with w_j's entered in 10th column of Table 2 to evaluate τ_j from equation (17) at $w_j \rightarrow 0$. τ_j's thus obtained are in close agreement with τ_1 from double relaxation and Gopalakrishna's [15] method and are placed in the Table 2. τ_j for p-toluidine at 22.06 GHz shows large value probably for error introduced in ε'_{ij}, ε''_{ij}, ε_{oij} and $\varepsilon_{\infty ij}$ measurements. The basic soundness of the latter method in getting τ_j is thus confirmed because polar-polar interactions are fully avoided [22]. Moreover, it shows that hf susceptibility measurement yields microscopic τ where as double relaxation method gives both microscopic and macroscopic τ_1 and τ_2 as observed else where [23].

Larger τ_2 arises for the bigger size of rotating unit ($\tau_j T/\eta^{\gamma}$) due to solvent environment around solute molecules. The distribution of τ between two extreme τ_1 and τ_2 values yields the symmetric and asymmetric distribution parameters γ and δ. They are however, obtained from equations (10) and (12) with $(\chi'_{ij} / \chi_{oij})$ $w_j \rightarrow 0$ and $(\chi''_{ij} / \chi_{oij})$ $w_j \rightarrow 0$ of Figures 5 and 6. The value of $1/\varphi$ log Cos φ against φ in degree as shown elsewhere [17] is essential to know δ. Knowing φ, δ's were obtained. γ and δ are entered in Table 3.

The symmetric relaxation times τ_s from equation (11) in terms of γ of equation (10) are presented in Table 2. The close agreement of τ_s's with τ_1's and reported τ's by freshly calculated from Gopalakrishna's method, indicates symmetric relaxation behaviour of such molecules in C_6H_6. The agreement is however, poor incase of o-toluidine. The characteristic relaxation times τ_{cs} obtained from equation (13) for o-anisidine at 3.86 GHz, m-anisidine at 3.86 & 22.06 GHz and m-toluidine at 3.86 GHz as in Table 2 are found to be low due to high values of δ. For other systems τ_{cs} and δ could not be found out as $1/\varphi$ log Cos φ for them are positive. This fact rules out the applicability of asymmetric relaxation behaviour for such compounds.

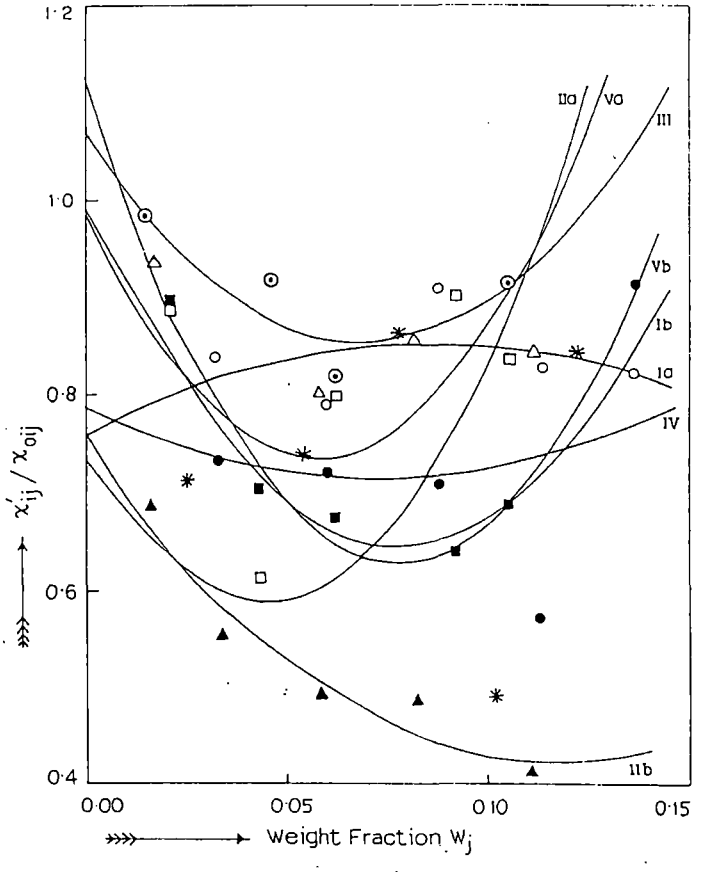

Figure 5 : Plot of χ'_{ij} / χ_{oij} against weight fraction w_j of monosubstituted anilines in benzene at 35°C under GHz electric field.

(Ia) o-anisidine at 3.86 GHz (-○-), (Ib) o-anisidine at 22.06 GHz (-●-), (IIa) m-anisidine at 3.86 GHz (-△-), (IIb) m-anisidine at 22.06 GHz (-▲-), (III) O-toluidine at 2.02 GHz (-⊙-), (IV) m-toluidine at 3.86 GHz (-*-), (Va) p-toluidine at 3.86 GHz (-□-) and (Vb) p-toluidine at 22.06 (GHz (-■-) respectively.

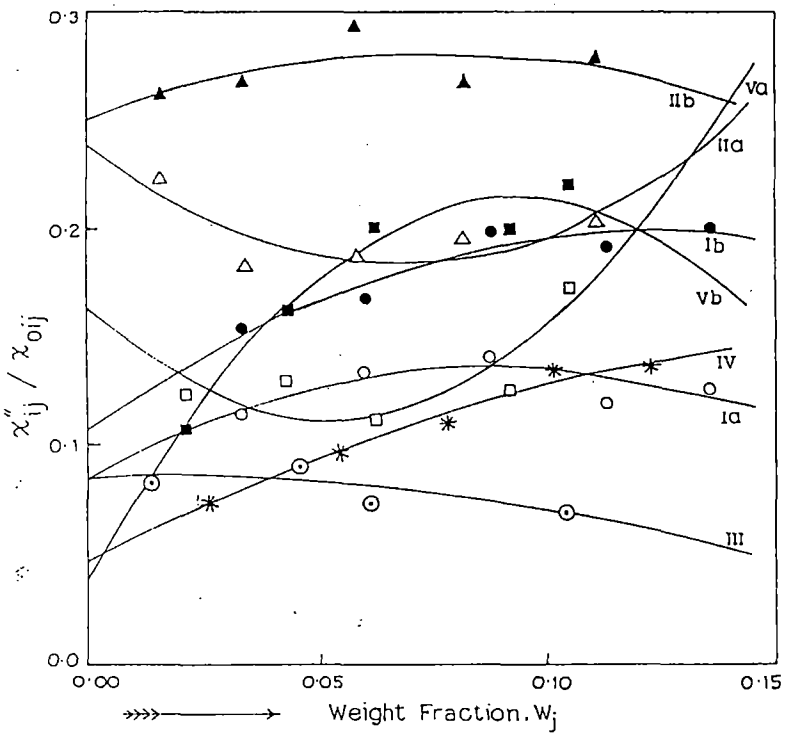

Figure 6 : Plot of χ''_{ij} / χ_{oij} against weight fraction w_j of monosubstituted anilines in benzene at 35°C under GHz electric field.

(Ia) o-anisidine at 3.86 GHz (–O–), (Ib) o-anisidine at 22.06 GHz (–●–), (IIa) m-anisidine at 3.86 GHz (–Δ–), (IIb) m-anisidine at 22.06 GHz (–▲–), (III) o-toluidine at 2.02 GHz (–⊙–), (IV) m-toluidine at 3.86 GHz (–*–), (Va) p-toluidine at 3.86 GHz (–□–) and (Vb) p-toluidine at 22.06 (GHz (–■–) respectively.

The theoretical weighted contributions of c_1 and c_2 towards dielectric relaxations were obtained from equations (4) and (5) by the measured τ_1 and τ_2 of equation (3) and χ'_{ij} / χ_{oij} and χ''_{ij} / χ_{oij} of Frohlich's equations (6) and (7). The 6th and 7th columns of Table 3 contain c_1 and c_2. The experimental c_1 and c_2 values were also obtained from $(\chi'_{ij} / \chi_{oij})\, w_j \to 0$ and $(\chi''_{ij} / \chi_{oij})\, w_j \to 0$ of the concentration variations of χ'_{ij} / χ_{oij} an χ''_{ij} / χ_{oij} of Figures 5 and 6 by using equations (4) and (5). They are presented in Table 3 for comparison with the theoretical ones. Fröhlich's equations (6) and (7) are related to Fröhlich parameter A, where $A = \ln (\tau_2 / \tau_1)$. Both the theoretical and experimental c_1 and c_2 as seen in Table 3 showed that $|c_1 + c_2| \simeq 1$ establishing the validity of equation (3). It is interesting to note that experimental c_2's are negative in case of o-anisidine and p-toluidine at 22.06 GHz and m-toluidine for the inertia of the flexible parts [23]. In Figures 5 and 6 it is also seen that the experimental points often do not lie on the smooth fitted curves probably due to solute - solute or solute - solvent molecular associations.

The dipole moments μ_1 and μ_2 of the flexible parts and the whole molecules were estimated from the linear coefficients β's in the 3rd column of Table 4 of both χ'_{ij} - w_j and σ_{ij} - w_j curves of Figures 3 and 7 and dimensionless parameters b_1 and b_2 involved with measured τ_1 and τ_2 from equation (3). The μ_1 and μ_2 thus obtained from equations (20) and (25) are placed in the 8th and 9th columns of Table 4 for comparison. Correlation coefficients r's and % of errors involved in the regression analysis in the 4th and 5th columns of Table 4 were made only to show how far χ'_{ij}'s and σ_{ij}'s are correlated with w_j's. Both the χ'_{ij}'s and σ_{ij}'s with w_j in Figures 3 and 7 give reliable β to yield accurate μ_1 and μ_2. It is seen in Figures 3 and 7 that almost all the curves show a tendency to be closer within the region $0.00 \leq w_j \leq 0.03$ indicating the same polarity of the molecules, in addition to solute - solvent (monomer) or solute - solute (dimer) molecular associations [6,22]. μ_1 and μ_2 in Table 4 from χ'_{ij}- w_j curves of Figure 3 are always smaller in magnitude than σ_{ij} - w_j curves of Figure 7, as χ_{ij}'s are associated with orientational polarisation while σ_{ij} is linked with bound molecular charges. Theoretical dipole moments μ_{theo}'s of monosubstituted anilines as estimated elsewhere [17] in terms of available bond angles and

bond moments of polar groups $C \rightarrow NH_2$, $C \rightarrow OCH_3$, $C \rightarrow CH_3$ are entered in the 10th column of Table 4 to compare with experimental μ_j's. The contribution of inductive, mesomeric and electromeric moments of the substituent polar groups of the molecules towards the hf μ_j's are, however, explained by the factor $\mu_{j(expt)} / \mu_{theo}$ of values 1.49, 1.68, 0.93, 0.92, 0.89, 0.75, 0.46 and 0.07 of Ia, Ib, IIa, IIb, III, IV, Va and Vb respectively. The amount of bound molecular charge is judged from the difference $\Delta\mu_j$ between μ_j's of hf σ_{ij} and χ'_{ij} respectively to contribute to hf σ_{ij} [8].

In absence of reliable μ_j's Gopalakrishna's method [15] were reemployed. The close agreement between reported μ_j's, (Gopalakrishna) μ_j and μ_{theo}'s confirms the basic soundness of the methods prescribed in getting hf μ_j, in addition to the fact that a part of the molecule is rotating under GHz electric field.

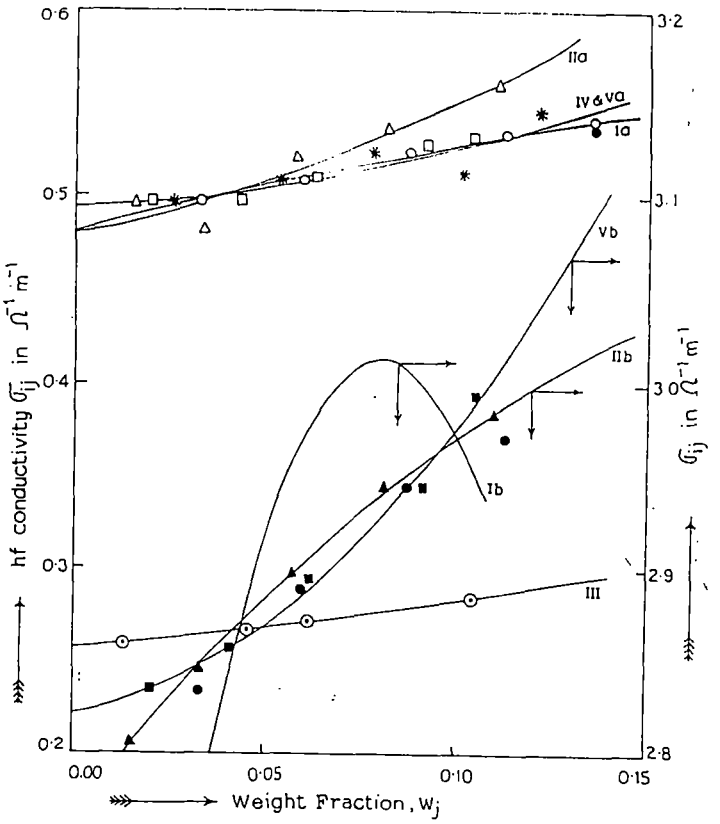

Figure 7 : Plot of σ_{ij} against weight fraction w_j of monosubstituted anilines in benzene at 35°C under GHz electric field.

(Ia) o-anisidine at 3.86 GHz (–O–), (Ib) o-anisidine at 22.06 GHz (–●–), (IIa) m-anisidine at 3.86 GHz (–Δ–), (IIb) m-anisidine at 22.06 GHz (–▲–), (III) o-toluidine at 2.02 GHz (–O–), (IV) m-toluidine at 3.86 GHz (–*–), (Va) p-toluidine at 3.86 GHz (–□–) and (Vb) p-toluidine at 22.06 (GHz (–■–) respectively.

6. CONCLUSION

The methodology so far presented in SI units with internationally accepted symbols of dielectric terminologies and parameters appears to be more topical, simple, straightforward and significant contribution to predict relaxation parameters as χ_{ij}'s are directly linked with molecular orientational polarisation. The interesting equations to evaluate τ_j's and μ_j's in terms of χ_{ij}'s helps one to shed more light on the relaxation phenomena of complicated molecules. The simple straight line equation (3) provides with microscopic τ_1 and macroscopic τ_2 respectively. The method to evaluate τ_j from the ratio of slopes of individual variations of χ''_{ij} and χ'_{ij} with w_j is a better representation of the earlier one of Murthy et al as it eliminates polar - polar interactions in a given solution. The relative weight factors c_1 and c_2 towards dielectric dispersions by Fröhlich and graphical methods show $|c_1 + c_2| \simeq 1$ confirming the applicability of the linear equation (3) to estimate τ_1 and τ_2 respectively for such dipolar liquids,. The close agreement of τ_j, τ_1 and τ_s confirms the nonrigid character of the molecules under hf electric field in C_6H_6. μ_1 and μ_2 by hf susceptibility and conductivity methods establish the fact that different types of polarisations are associated with χ_{ij}'s and σ_{ij}'s. The theoretical reasons of evaluating τ_1's and μ_1's in agreement

of τ_j's and μ_j's from freshly calculated Gopalakrishna's method is really sound. Various types of molecular associations are inferred from usual departure of graphically fitted plots of χ'_{ij} / χ_{oij} and χ''_{ij} / χ_{oij} with w_j's and conformational structure of the molecules in which the effects of inductive, mesomeric and electromeric moments of the polar groups of the molecule play the prominent role.

REFERENCES

[1] A. Sharma, D.R Sharma and M.S Chauhan Indian J Pure & Appl Phys **31** (1993) 841.

[2] K. Higasi, Y. Koga and M. Nakamura Bull Chem Soc. Japan **44** (1971) 988.

[3] K.S. Cole and R.H. Cole J Chem Phys **9** (1941) 341.

[4] E.A. Guggenheim Trans Faradey Soc **45** (1949) 714.

[5] S.K. Sit, N.Ghosh, U.Saha and S. Acharyya Indian J Phys **71B** (1997) 533.

[6] N.Ghosh, A. Karmakar, S.K. Sit and S. Acharyya Indian J Pure & Appl. Phys **38** (2000) 574.

[7] S.C. Srivastava and S Chandra Indian J Pure & Appl. Phys **13** (1975) 101.

[8] A. K. Jonscher Physics of Dielectric Solids, invited papers ed C H L Goodman Canterbury (1980).

[9] A. Budo Phys Z **39** (1938) 706.

[10] K. Bergmann, D.M. Roberti and C.P. Smyth J Phys Chem **64** (1960) 665.

[11] J. Bhattacharyya, A. Hasan, S.B. Roy and G.S. Kastha J Phys Soc Japan **28** (1970) 204.

[12] U. Saha, S.K. Sit, R.C. Basak and S. Acharyya J Phys D : Appl. Phys **27** (1994) 596.

[13] S. K. Sit, R. C. Basak, U. Saha and S. Acharyya J Phys D : Appl. Phys **27** (1994) 2194.

[14] M.B.R. Murthy, R.L. Patil and D.K. Deshpande Indian J Phys **63B** (1989) 491.

[15] K. V. Gopalakrishna Trans Faradey Soc **53** (1957) 767.

[16] H. Fröhlich *"Theory of Dielectrics"* (Oxford University Press: Oxford 1949).

[17] N.Ghosh, S. K. Sit, A.K. Bothra and S. Acharyya J Phys D : Appl. Phys (UK) **34** (2001) 379.

[18] C.P. Smyth *"Dieclectric Behaviour and Structure"* (New York : Mc Graw Hill 1955)

[19] K. Dutta, S.K. Sit and S. Acharyya, Pramana J Phys (2001) Accepted for Publication.

[20] F. J. Murphy and S.O. Morgan Bell Syst Tech J **18** (1939) 502.

[21] D.W. Davidson and R.H. Cole J Chem Phys **19** (1951) 1484.

[22] N. Ghosh, R.C. Basak, S.K. Sit and S. Acharyya J. Mol. Liquids **85** (2000) 375.

[23] S. K. Sit, N. Ghosh and S. Acharyya Indian J Pure & Appl. Phys **35** (1997) 329.